Reflectivity Measurement System Development and Calibration

A thesis
submitted in partial fulfilment
of the requirements of the degree
of
Master of Engineering
at the
University of Waikato

by
Tao Peng

University of Waikato
2007

Abstract

Accurate assessment of road luminance provided by overhead streetlights helps to optimize the visibility of objects on the road and therefore promotes driver safety, while minimizing energy consumption. To calculate road luminance, the road surface reflectivity has to be known. Odyssey Energy Limited has developed a prototype system that has the potential to determine the road reflectivity properties at high speed.

In this thesis, an investigation into the prototype system has been conducted and further enhancement and redesign has been done. A portable on-site road surface reflectivity measurement system that complies with the Commission Internationale de I' Eclairage (CIE) standard was developed. The road test of this new system has been carried out on a series of Hamilton city roads. It proved that the new system is capable of measuring the road surface reflectivity and classifying the road into its appropriate R class according to the CIE standards specified in street lighting design criteria. Later the OEL prototype system was calibrated against the new system to find out the correlation between the two systems.

Acknowledgements

I would like to express my thanks to all the staff at Odyssey Energy Limited, especially Roger Loveless and Michael Walker. They have provided enormous help and support during the project.

My thanks also go to my academic supervisor, Dr. Howell Round. He has provided many good suggestions throughout the project.

Thanks also go to my friend Daryl Budd for helping me immeasurably in the writing and printing of this thesis.

Finally great thanks go to my partner Tiantian Jia, for providing tremendous support and assistance for my project throughout the year.

Contents

Abstract iii
Acknowledgements v
Contents vii
List of Figures ix
List of Tables xi
1 Introduction 1
1.1 Project Motivation 1
1.2 Overview of Previous Systems 2
1.2.1 High-Speed Street Lighting Illuminance Collection System 2
1.2.2 High Road Reflectivity Measurement System 3
1.3 Project Objective 5
1.4 Thesis Structure 6
2 Background Theory 7
2.1 Light Theory 7
2.1.1 Visible Light 7
2.1.2 Solid Angles 7
2.1.3 Luminous Flux 9
2.1.4 Illuminance 9
2.1.5 Luminance 10
2.1.6 The Inverse Square Law 10
2.1.7 Luminous Intensity 11
2.1.8 Lambert's Cosine Law 12
2.1.9 Lambertian Surface 12
2.1.10 Reflection 14
2.2 Road Lighting Theory 14
2.2.1 Road Lighting Standard 14
2.2.2 Street Lighting Measurement Methodology 16
2.2.3 CIE Road Classification System 19
2.2.4 Measurement Method of Q_0 23
2.2.5 Measurement Method of Pavement r-Values 24
3 Hardware 29
3.1 Assessment of the OEL Road Reflectivity Measurement Prototype 29
3.1.1 OEL Specular Meter 30
3.1.2 OEL Q_0 Meter 33
3.2 New Developments 37
3.2.1 Improvement on the Q_0 Meter 37
3.2.2 Simplified Specular Meter 42
3.2.3 LDR Based Specular Meter Design 45
3.3 Standard Design 51
3.3.1 "Wellington" Reflectance Box 51
3.3.2 Design of Road Specularity Measurement Box 53
3.3.2.1 Validation of the CIE Box 55
4 Test Procedure and Results 63
4.1 System Setup 63
4.1.1 CIE Box Setup 63
4.1.2 OEL Specular Meter Setup 66

4.2 Road Specularity S1 Test 67
4.2.1 CIE Box Road Specularity S1 Measurement 68
4.2.2 CIE Box Repeatability 73
4.2.3 OEL Specular Meter and CIE Box Correlation Test 74
4.2.4 Road Specularity Consistency Test 77
4.3 Average Luminance Q_0 Measurement 78
4.4 Parameter S2 Analysis 82
5 Conclusion 87
5.1 Fulfilment of Project 87
5.2 Further Development 87
5.3 Summary 89

Appendix I Luminance Meter 91
Appendix II Circuitry Design 93
Appendix III Software 95
Appendix IV Datasheet 101
Appendix V Selected Raw Results 107
References 119

List of Figures

Figure 1.1 Example road brightness 1
Figure 1.2 High-speed street lighting illuminance collection system HISLAT® 2
Figure 1.3 Illuminance measurement setup 3
Figure 1.4 Example OEL illuminance system plot 3
Figure 1.5 OEL road reflectivity measurement system 4
Figure 1.6 Q_0 Versus distance 4
Figure 1.7 Average luminance vs distance 5
Figure 2.1 The optical portion of the electromagnetic spectrun 7
Figure 2.2 Steradian 8
Figure 2.3 Removed cone 8
Figure 2.4 Total flux output 9
Figure 2.5 Illuminance 9
Figure 2.6 Luminance 10
Figure 2.7 Inverse square law 11
Figure 2.8 Luminous intensity 11
Figure 2.9 Lambert's cosine law 12
Figure 2.10 Lambertian surface 13
Figure 2.11 Lambertian surface 13
Figure 2.12 Specular, diffuse and spread reflection from a surface 14
Figure 2.13 Pavement reflection profile for fixed observing angle 16
Figure 2.14 Geometry for luminance calculation. 17
Figure 2.15 Driver's view 19
Figure 2.16 Reflection contour 22
Figure 2.17 Reflection contour 23
Figure 2.18 integrating sphere 23
Figure 2.19 Road workers extracting pavement samples 25
Figure 2.20 Extracted pavement samples 25
Figure 2.21 Principle ofgonioreflector for measurement of the reflection properties of road surface 26
Figure 2.22 Gibbon's gonioreflectometer schematic 28
Figure 3.1 OEL's reflectometer prototype 29
Figure 3.2 OEL specular meter 30
Figure 3.3 Schematic of OEL specular meter 30
Figure 3.4 Schematic of CIE S1 meter 31
Figure 3.5 CIE 1° observation 32
Figure 3.6 OEL Q_0 meter 33
Figure 3.7 An integrating sphere 33
Figure 3.8 Schematic of OEL Q_0 meter 34
Figure 3.9 Luxmeter converted luminance meter 35
Figure 3.10 Grey Card 35
Figure 3.11 Reflectance test setup 36
Figure 3.12 Luminance meter with baffle 38
Figure 3.13 New Q_0 meter 39
Figure 3.14 Q_0 meter test 39
Figure 3.15 Road test one- Opioa Road 40
Figure 3.16 Road test two-parking lot 41

Figure 3.17 Hoop specular meter 42
Figure 3.18 Hoop specular meter operating 43
Figure 3.19 Hoop meter vs OEL specular meter 44
Figure 3.20 Hoop meter with attached leg 45
Figure 3.21 Pavement reflection profiles 46
Figure 3.22 New design conception 47
Figure 3.23 LDR based specular meter prototype 48
Figure 3.24 NORP12 photoconductive cell 48
Figure 3.25 Illuminance vs resistance 49
Figure 3.26 The replica of the "Wellington" reflectance measurement box 52
Figure 3.27 Bottom view 52
Figure 3.28 CIE box 54
Figure 3.29 CIE box schematic 54
Figure 3.30 experiment principle 56
Figure 3.31 CIE box validation test 58
Figure 3.32 Change in S1 with observation angle α for all R-Classes 60
Figure 4.1 CIE box upright view 63
Figure 4.2 CIE box horizontal view 64
Figure 4.3 OEL prototype setup 66
Figure 4.4 S1 values for 42 roads 70
Figure 4.5 S1 values for 41 roads with error bar 71
Figure 4.6 Fox street vehicle driving lane 71
Figure 4.7 Road classification histogram 72
Figure 4.8 CIE box repeatability test 74
Figure 4.9 OEL specular meter vs CIE box 76
Figure 4.10 OEL specular meter vs CIE box with Fox Street omitted 76
Figure 4.11 Q_0 meter testing procedure 79
Figure 4.12 Home yard and Naylor street 81
Figure 4.13 Q0 meter measurements results plot 81
Figure 4.14 Influence of alpha for all R classes 84
Figure 5.1 Specular meter with 10º observation angle 88

List of Tables

Table 1 Example of R table 20
Table 2 Road classification table 21
Table 3 CIE road surface classification 22
Table 4 OEL Q_0 meter Grey Card testing results 36
Table 5 Grey Card test 40
Table 6 Hoop and OEL specular meter measurement results 43
Table 7 LDR calibration results 49
Table 8 LDR vs Luxmeter 50
Table 9 Testing results 58
Table 10 Revised road classification table 61
Table 11 CIE box road measurement results 69
Table 12 Classification results 72
Table 13 CIE box repeatability results 73
Table 14 CIE and OEL specularity meter correlation test 75
Table 15 Revised road classification table for OEL specular meter 77
Table 16 Road consistency test 78
Table 17 Q meter measuring results 80
Table 18 S2 values 85

1 Introduction

1.1 Project Motivation

Accurate measurement of the road luminance provided by streetlights helps optimise the driver's visibility and therefore driving safety while minimising the energy consumption of street lighting[1].

Research has shown driving conditions are far safer when road luminance is considered. This is because luminance is a measure of the light reflected from the road surface and the amount of light that actually enters into a vehicle driver's eye[2].

Each year approximately 50% of a New Zealand city councils' total electricity expenditure is for street lighting. If a street lighting contractor is aware of the fact that the road luminance level depends not only upon the street light illuminance but also the road surface reflectivity then they may choose to have fewer lights or reduce the light intensity and still achieve the required luminance level. This would lead to a reduction in electricity consumption. Figure 1.1 shows two surfaces with different reflectivity.

FIGURE 1.1 EXAMPLE ROAD BRIGHTNESS

Concrete pavement reflects up to 27% of the light falling upon its surface. Black asphalt pavement reflects only 5%. In other words, to achieve the same luminance level, only one fifth of the lighting output power is needed for the concrete pavement. If the contractor is not aware of the difference in road surface reflectivity, it may apply the

same lighting to both roads. So it is very important to have a good knowledge of the reflectivity properties of a road when installing and maintaining the streetlights.

However the road surface reflectivity assessment method has so far not been made aware to most contractors, so there is a market for a reflectivity collection and reporting tool[2].

1.2 Overview of Previous Systems

Odyssey Energy Limited (OEL) is a Hamilton based electrical-engineering consultancy company; it offers services to power industries. With many years of experience in street lighting design, the company strongly felt obliged to design an efficient and reliable system to assess road lighting and road luminance properties. With cooperation from the University of Waikato, a high-speed street lighting illuminance assessment system and a road reflectivity measurement prototype was developed.

1.2.1 High-Speed Street Lighting Illuminance Collection System

FIGURE 1.2 HIGH-SPEED STREET LIGHTING ILLUMINANCE COLLECTION SYSTEM HISLAT®[3]

A high-speed street light illuminance measurement system, HISLAT® (Figure 1.2), was developed in OEL in the year of 2000. It has been successfully used in New Zealand for street lighting performance assessment for many years.

FIGURE 1.3 ILLUMINANCE MEASUREMENT SETUP[3]

A luxmeter is used to measure the streetlight illuminance, its photodetector is mounted on the survey vehicle's roof as shown in Figure 1.3, and the measured results are logged into the laptop in the survey vehicle. The vehicle's distance travelled is recorded by a tripmeter and then recorded into the same program. Then a travel distance versus lighting illuminance graph can be calculated and plotted (Figure 1.4). As the device can measure accurately when travelling up to speeds of 80 km/h it offers a very efficient way to assess road lighting performance.

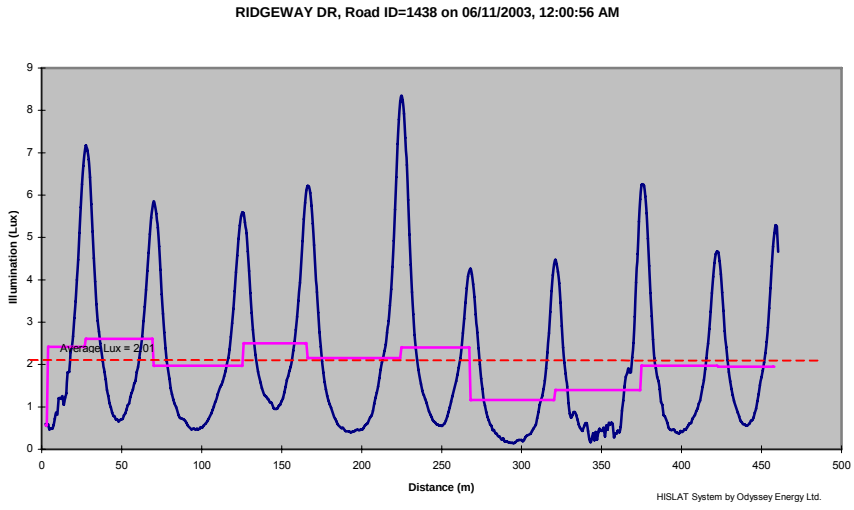

FIGURE 1.4 EXAMPLE OEL ILLUMINANCE SYSTEM PLOT[3]

1.2.2 High Road Reflectivity Measurement System

After the success of the high-speed street lighting illuminance meter, OEL has developed a high-speed pavement luminance measurement system as in Figure 1.5.

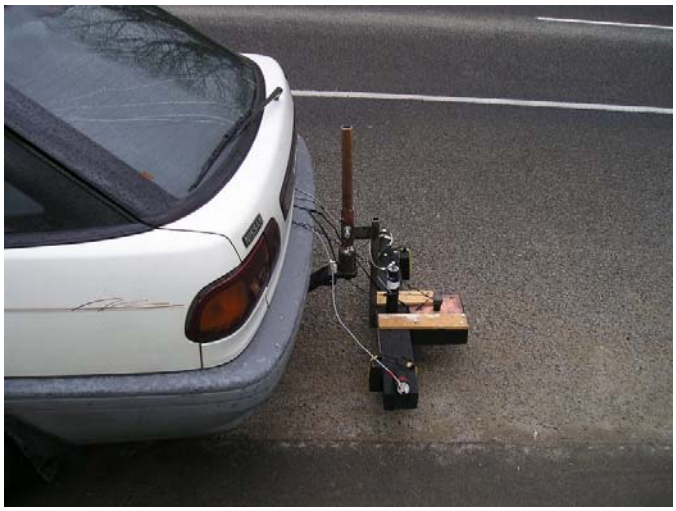

FIGURE 1.5 OEL ROAD REFLECTIVITY MEASUREMENT SYSTEM[4]

This system consists of a specular meter and average luminance meter. The specular meter was designed to measure road surface specularity, and average luminance meter was designed to measure road brightness.

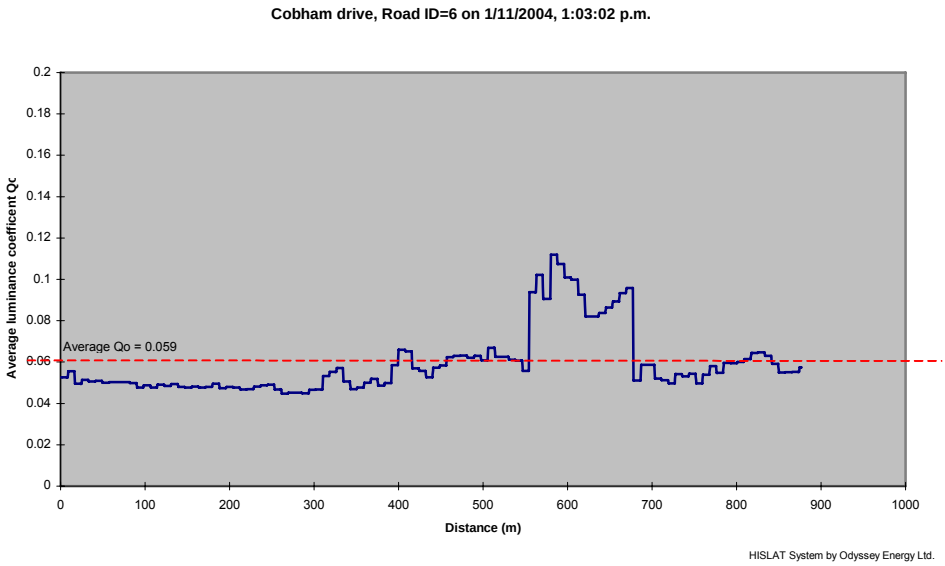

FIGURE 1.6 Q_0 VERSUS DISTANCE[4]

Figure 1.6 shows a typical graph of the distance versus road surface average luminance coefficient Q_0

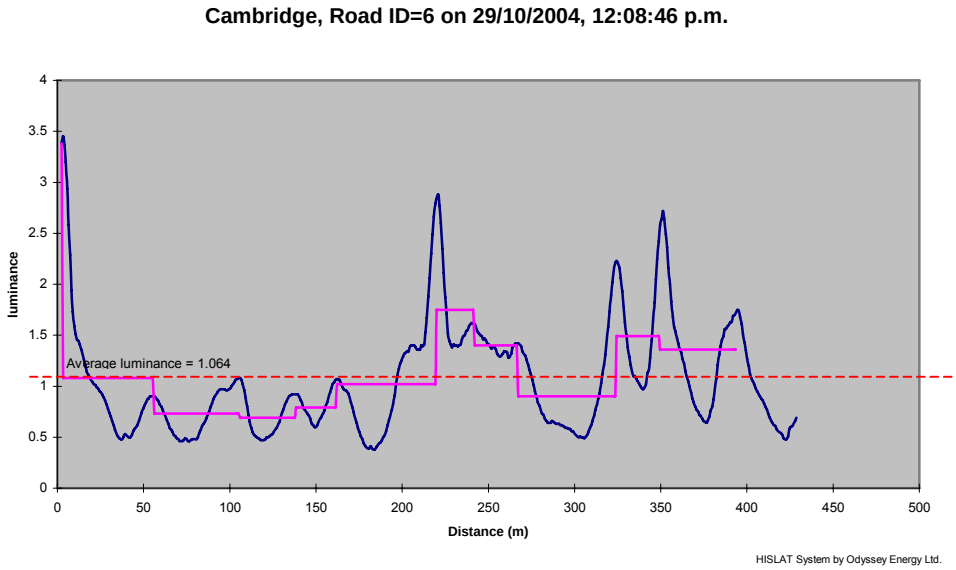

FIGURE 1.7 AVERAGE LUMINANCE VS DISTANCE[4]

Figure 1.7 shows a typical graph of distance versus the product of street light illuminance and brightness Q_0. Road tests proved that the dynamic unit was operational during street surveys. But the system is far from perfect since the design concept has not been verified and calibrated.

1.3 Project Objective

Test showed that the existing high-speed luminance measurement system performs adequately. But it has several major limiting factors when being used as a reliable tool by organizations. The system does give certain indications when testing different road surfaces, but its feasibility, certainty and reliability had to be investigated and verified.

Therefore, the objectives of this project were as follows:

- Research existing techniques for road luminance measurement
- Review the existing road reflectivity measurement prototype
- Improve the system and further development
- Verify design and calibrate
- Road test it
- Draw conclusions

1.4 Thesis Structure

The background information on light and street lighting design is discussed in Chapter 2. Luminance measurement techniques and existing research is reviewed in this chapter as well.

In Chapter 3, existing prototype assessment and new concept developments are described. In Chapter 4, road testing of the old system and new system are intensively carried out, and conclusions were drawn.

Chapter 0, conclusions and recommendations are made.

2 Background Theory

2.1 Light Theory

This section explains the fundamental light theory that is relevant to this research.

2.1.1 Visible Light

Visible light is defined as electromagnetic radiation, which is detectable by the human eye. It is just one portion of the various electromagnetic waves flying through space, shown in Figure 2.1. The electromagnetic spectrum covers an extremely broad range, from radio waves with wavelengths of a meter or more, down to x-rays with wavelengths of less than a billionth of a meter [5].

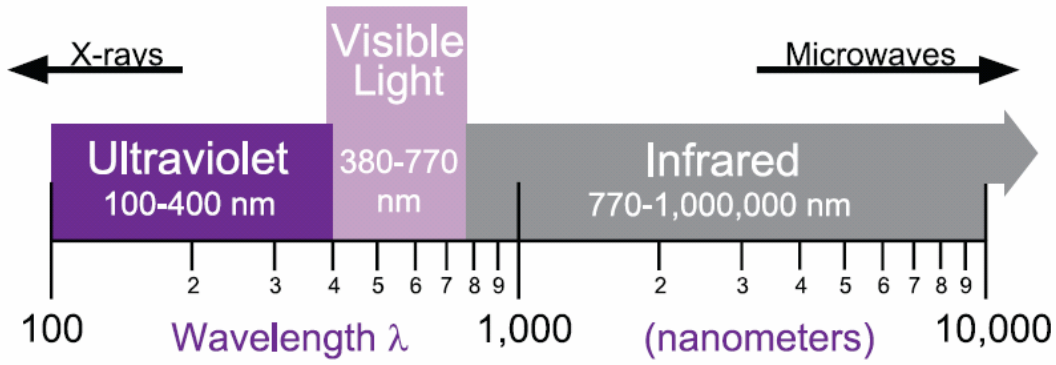

FIGURE 2.1 THE OPTICAL PORTION OF THE ELECTROMAGNETIC SPECTRUN[5]

The human eye is not equally sensitive to all wavelengths of light. Photometry attempts to account for this by weighting the measured power at each wavelength with a factor that represents how sensitive the eye is at that wavelength[6]. Most light measurement tools on the market are designed to mimic the spectral response of the eye.

All the research in this project is related to photometry.

2.1.2 Solid Angles

One of the key concepts to understanding the relationships between measurement geometries is that of the solid angle, and its unit the steradian. A sphere contains 4π steradians. A steradian is defined as the solid angle which, having its vertex at the

centre of the sphere, cuts off a spherical surface area equal to the square of the radius of the sphere. For example, a one-steradian section of a one-meter radius sphere subtends a spherical surface area of one square meter.

The sphere shown in Figure 2.2 illustrates the concept. A cone with a solid angle of one steradian has been removed from the sphere. This removed cone is shown in Figure 2.3. The solid angle, Ω, in steradians, is equal to the spherical surface area, *A*, divided by the square of the radius, *r* [5].

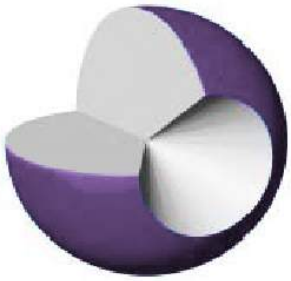

FIGURE 2.2 STERADIAN [5]

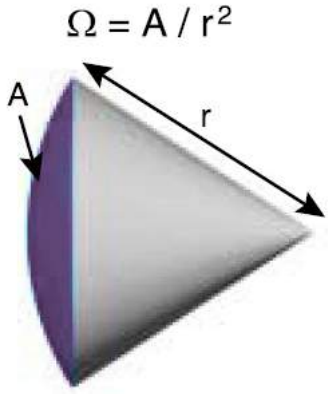

FIGURE 2.3 REMOVED CONE [5]

2.1.3 Luminous Flux

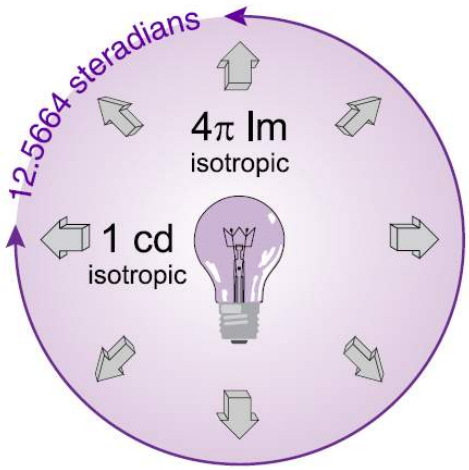

FIGURE 2.4 TOTAL FLUX OUTPUT [5]

Luminous flux is a measure of the power of visible light. Photopic flux, expressed in lumens, is a measure of the rate of energy flow, and is weighted to match the responsivity of the human eye, which is most sensitive to yellow-green[5].

2.1.4 Illuminance

Illuminance is a measure of photometric flux per unit area, or visible flux density. Illuminance is typically expressed in lux (lumens per square meter).

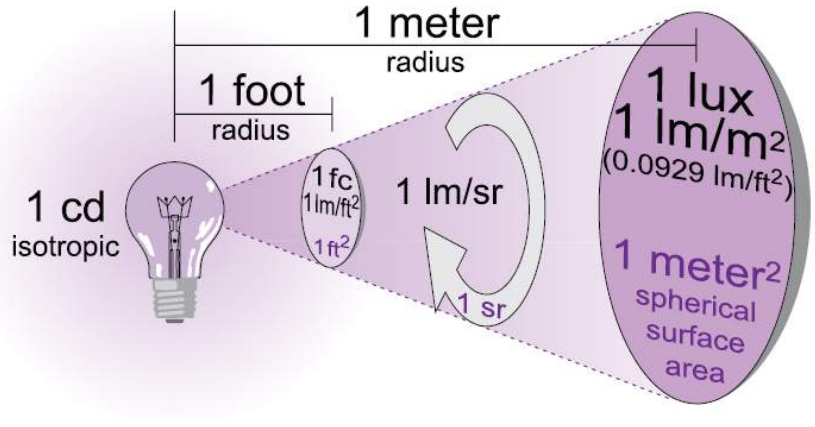

FIGURE 2.5 ILLUMINANCE [5]

In Figure 2.5, above, the light bulb is producing 1 candela. The candela is the base unit in light measurement, and is defined as follows: a 1 candela light source emits 1 lumen

per steradian in all directions (isotropically). The number of steradians in a beam is equal to the projected area divided by the square of the distance.

So, 1 steradian has a projected area of 1 square meter at a distance of 1 meter. Therefore, 1 lm/sr light source will similarly produce 1 lumen per square meter at 1 meter. Note that as the beam of light projects farther from the source, it expands, becoming less dense, for example, the light expanded from 1 lm/ m² (lux) at 1 meter to 0.25 lm/m² (lux) at 2 meter[5].

2.1.5 Luminance

Luminance is a measure of the flux density per unit solid viewing angle, expressed in lm/m²/sr or cd/m². Luminance is independent of distance for an extended area source, because the sampled area increases with distance, cancelling inverse square losses.

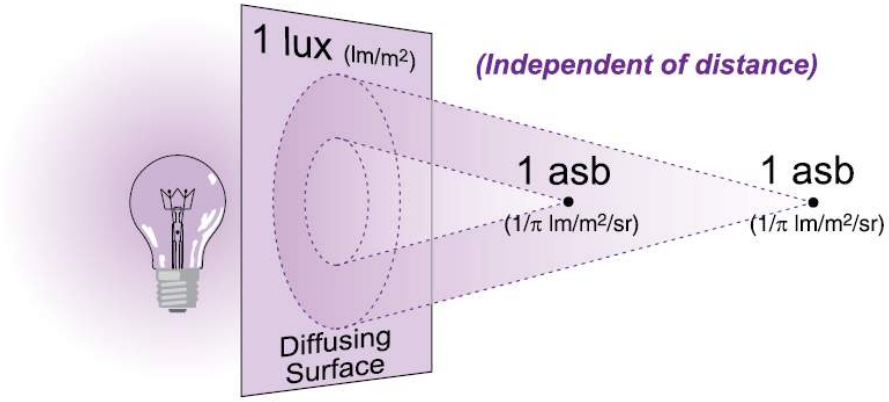

FIGURE 2.6 LUMINANCE [5]

The luminance, *L*, of a diffuse (Lambertian) surface is related to the luminance exitance (flux density), *M*, of a surface by the relationship[5]:

$$L = \frac{M}{\pi}$$

2.1.6 The Inverse Square Law

The inverse square law defines the relationship between the illuminance from a point source and distance. It states that the intensity per unit area varies in inverse proportion to the square of the distance.

$$E = \frac{I}{d^2}$$

In other words, if you measure 16 W/cm² at 1 meter, you will measure 4 W/cm² at 2 meter, and can calculate the illuminance at any distance. An alternate form is often more convenient.

$$E_1 d_1^{\,2} = E_2 d_2^{\,2}$$

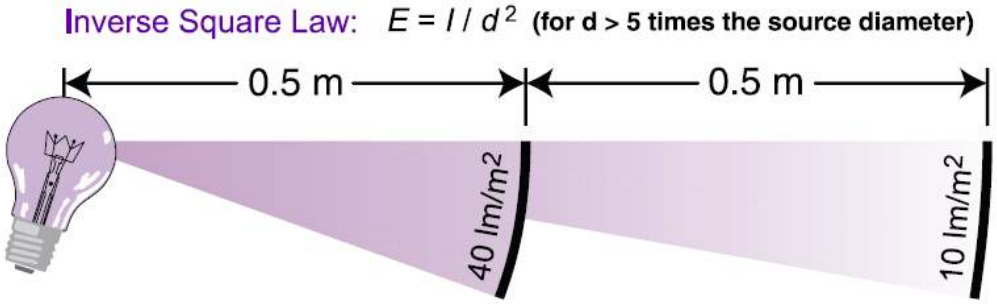

FIGURE 2.7 INVERSE SQUARE LAW [5]

The inverse square law can only be used in cases where the light source approximates a point source. A general rule of thumb to use for illuminance measurements is the "five times rules": the distance to a light source should be greater than five times the largest dimension of the source [5].

2.1.7 Luminous Intensity

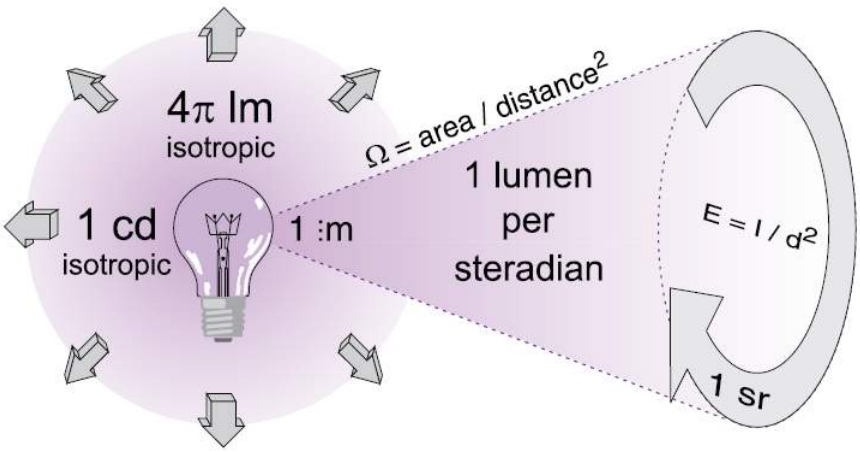

FIGURE 2.8 LUMINOUS INTENSITY [5]

Luminous intensity is a measure of visible power per solid angle, expressed in candela (lumens per steradian). Intensity is related to illuminance by the inverse square law, shown below in an alternate form:

$$I = Ed^2$$

Note that the units cancel to get flux/sr from flux/area times distance squared, remembering that steradians are a dimensionless quantity. Since the solid angle equals the area divided by the square of the radius, $d^2 = A/\Omega$, and substitution yields[5]:

$$I = \frac{EA}{\Omega}$$

2.1.8 Lambert's Cosine Law

The illuminance falling on any surface varies as the cosine of the incident angle, θ. The perceived measurement area orthogonal to the incident flux is reduced at oblique angles, causing light to spread out over a wider area than it would if perpendicular to the measurement plane[5] (Figure 2.9).

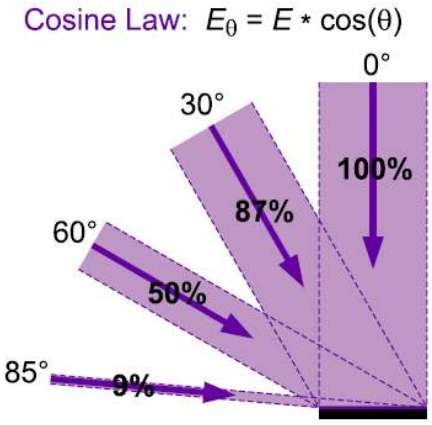

FIGURE 2.9 LAMBERT'S COSINE LAW [5]

2.1.9 Lambertian Surface

A Lambertian surface provides uniform diffusion of the incident radiation such that its luminance is the same in all directions from which it can be measured. Many diffuse

surfaces are, in fact, Lambertian. The human eye, with its restricted solid viewing angle, is an ideal luminance, or brightness, detector.

Figure 2.10 shows a surface radiating equally at 0° and at 60°. Since, by the cosine law, a luminance detector sees twice as much surface area in the same solid angle for the 60° case, the average incremental reflection must be half the magnitude of the reflection in the 0° case.

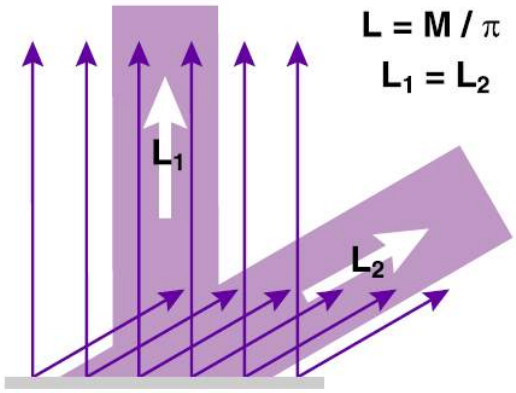

FIGURE 2.10 LAMBERTIAN SURFACE [5]

Figure 2.11 shows that a reflection from a diffuse Lambertian surface obeys the cosine law by distributing reflected energy in proportion to the cosine of the reflected angle.

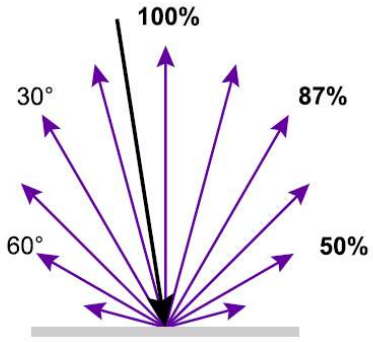

FIGURE 2.11 LAMBERTIAN SURFACE [5]

A Lambertian surface that has a luminance of 1.0 cd/cm² will radiate a total of $\pi * A$ watts, where A is the area of the surface, into a hemisphere of 2π steradians[5]

2.1.10 Reflection

Light reflecting off a polished surface or mirrored surface obeys the law of reflection: the angle between the incident ray and the normal to the surface is equal to the angle between the reflected ray and the normal. When the light obeys the law of reflection, it is termed a specular reflection (Figure 2.12). Most hard polished (shiny) surfaces are primarily specular in nature.

Diffusion reflection is typical of particulate substances like powders. If you shine a light on baking flour, for example, you will not see a directionally shiny component. The powder will appear uniformly bright from every direction.

Many surfaces are a combination of both diffuse and specular components. One manifestation of this is a spread reflection, which has a dominant directional component that is partially diffused by surface irregularities [5].

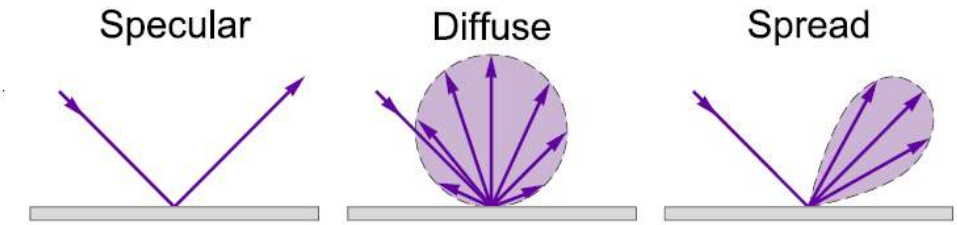

FIGURE 2.12 SPECULAR, DIFFUSE AND SPREAD REFLECTION FROM A SURFACE [5]

2.2 Road Lighting Theory

In this section street lighting background knowledge will be introduced, covering the street lighting design standard used in New Zealand, the street lighting calculation terminology and the Commission Internationale de I' Eclairage (CIE) road classification system.

2.2.1 Road Lighting Standard

In New Zealand and Australia, street lighting design must conform to part 3 of AS/NZS1158 *Lighting for Roads and Public Spaces* [7]. According to the purpose of usage, two categories were defined. They are:

Category P lighting

Lighting that is applicable to roads and other outdoor public areas on which the visual requirements of pedestrians are dominant, e.g. local roads, outdoor shopping areas. The illuminance level at the pavement surface is the main concern in Category P standard. The following definition is taken from the streetlight standard and is the main parameter concerning Category P lighting:

> **1.4.1 Horizontal Illuminance (E_h) –** the value of illuminance on a designated horizontal plane at ground level. Unit: lux (lx).

Category V lighting

Lighting that is applicable to roads on which the visual requirements of motorists are dominant, e.g. traffic route. In Category V lighting standard *luminance* is the main concerning parameter. The luminance definition is shown below:

> **3.3.1 Luminance (L) –** the physical quantity corresponding to the brightness of a surface (e.g. a lamp, luminare sky or reflecting material) in a specified direction. It is the luminous intensity of an area of the surface divided by that area. Unit: candela per square metre (cd/m^2) .

Illuminance is the measure of the amount of light flux falling on a surface (measured in lux). It is independent of the direction from which the light comes, the type of light source and the type of surface upon which it falls.

Luminance is the measure of the amount and concentration of light flux leaving a surface and towards an observer (measured in cd/m^2). The luminance of a surface depends on the direction from which the light strikes the surface, the direction from which the surface is viewed and the reflective properties of the surface. The source of radiation is not an issue and it is the luminance the producer of light intensity and reflectivity that controls the magnitude of the sensation that is received by the brain [8].

2.2.2 Street Lighting Measurement Methodology

Streetlight illuminance can be measured directly by placing a lux meter parallel to the ground level. In order to measure luminance the pavement reflectance has to be known. Road surface reflection properties are mixture of specular and diffuse reflection. A concept called Bidirectional Reflectance Distribution Function (BRDF) is used to describe such reflection characteristic. In road lighting design, luminance coefficient or reflection coefficient $q(\alpha,\beta,\gamma)$ is used to describe the road surface reflection characteristic.

$$BRDF = q(\alpha,\beta,\gamma)$$

The luminance coefficient $q(\alpha,\beta,\gamma)$ is a function of α, β and γ (explained in Figure 2.14), which depends on the position of the observer and the light source relatives to the point on the road surface under consideration

For a good understanding of luminance coefficient or reflection coefficient, a pavement reflection profile is shown in Figure 2.13.

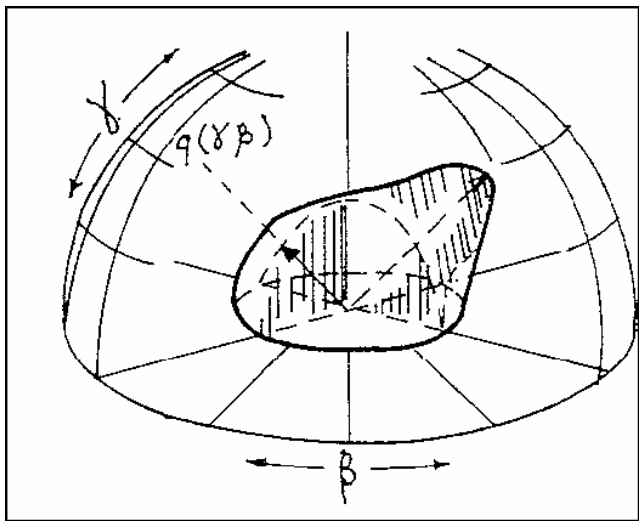

FIGURE 2.13 PAVEMENT REFLECTION PROFILE FOR FIXED OBSERVING ANGLE [9]

This reflection profile was plotted for a fixed viewing angle α (thus q is only a function of β and γ). The length of the arrow drawn in a certain β and γ direction gives the value of the luminance coefficient $q(\beta,\gamma)$ that corresponds to the direction of light incident.

Figure 2.14 is used to explain the road surface luminance calculation in streetlight measurement.

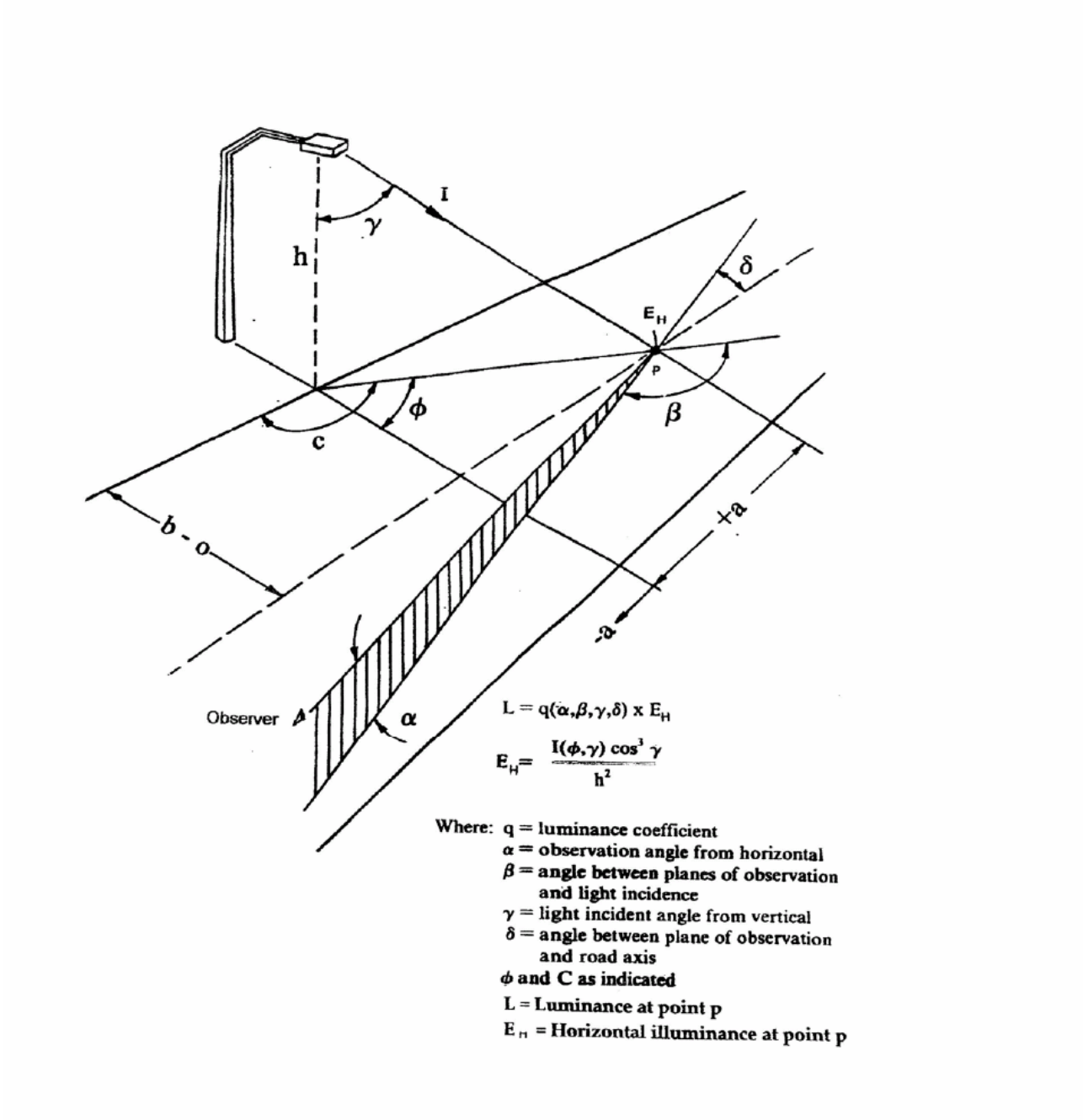

FIGURE 2.14 GEOMETRY FOR LUMINANCE CALCULATION.[10]

P is the point of interest. The luminance L_p measured for point P from observer can be calculated from luminance coefficient q and the horizontal E_H at point P:

$$L_p = q(\alpha, \beta, \gamma)E_p$$

The horizontal illuminance E_H at the point is:

$$E_H = \frac{I(c,\gamma)}{D^2}\cos(\gamma)$$

where $I(c,\gamma)$ is the luminous intensity of the light source in the direction defined by the c and γ, and D is the distance from the point P to the light source.

D follows from:

$$D = \frac{h}{\cos(\gamma)}$$

where h is the mounting height of luminaire or streetlight. With the substitution of D into the above equation for E_H:

$$E_H = \frac{I(c,\gamma)\cos^3(\gamma)}{h^2}$$

And the first equation then becomes:

$$L_p = \frac{I(c,\gamma)}{h^2} q(\alpha,\beta,\gamma)\cos^3(\gamma)$$

Under CIE standard for road luminance measurement, the observation angle α is fixed at 1° representing the average driver's line of sight. The reason for this is that the luminance is measured from a driver's point of view. With a driver's vision height of 1.5 meters, and a driving focus distance between 60 to 100 meters ahead from the driver's position in a vehicle, an observation angle range from 0.5° to 1.5° results as shown in Figure 2.15. A midpoint 1° therefore used. With this default, luminance coefficient is reduced to a function of β and γ, written as $q(\beta,\gamma)$.

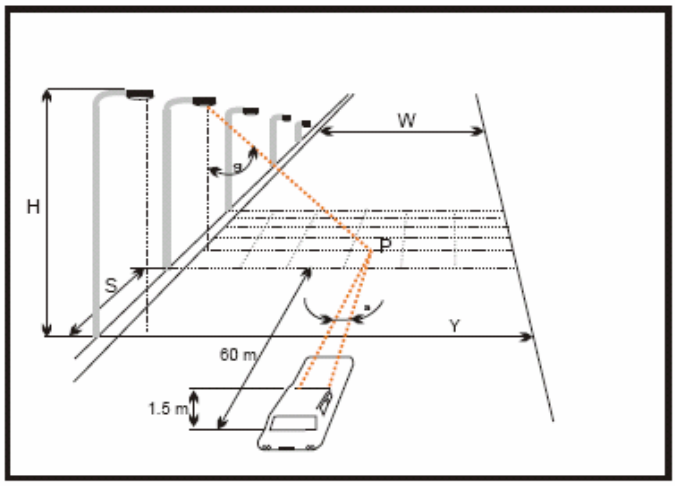

FIGURE 2.15 DRIVER'S VIEW [11]

For the purpose of road luminance calculation it is more convenient to use the reduced luminance coefficient $r(\beta,\gamma)$ defined as:

$$r(\beta,\gamma) = q(\beta,\gamma)\cos^3(\gamma)$$

It was introduced to reduce the magnitude of the values of $q(\beta,\gamma)$ and to ease the measurement methodology.

2.2.3 CIE Road Classification System

Research has shown that the road reflective properties depend not only on the colour, materials and texture, but also the method of structure and the wear of the road. Therefore every road surface has a unique reflection coefficient $r(\beta,\gamma)$ table. Due to this complication, a road classification system was developed by the Commission Internationale de I' Eclairage (CIE).

CIE is the recognised international organisation in the field of roadway lighting. It has successfully introduced a road surface classification method to classify the road surfaces into four standard reflectivity R-tables. Those tables are R1, R2, R3 and R4, which provide a close model of most existing roads.

Shown below in Table 1 is an example R1 table. $r(\beta,\tan(\gamma))$ values were measured for a standard R1 road at various β and γ angles.

TABLE 1 EXAMPLE OF R TABLE

	β																			
tan(γ)	0	2	5	10	15	20	25	30	35	40	45	60	75	90	105	120	135	150	165	180
0.00	655	655	655	655	655	655	655	655	655	655	655	655	655	655	655	655	655	655	655	655
0.25	619	619	619	619	610	610	610	610	610	610	610	610	610	601	601	601	601	601	601	601
0.50	539	539	539	539	539	539	521	521	521	521	521	503	503	503	503	503	503	503	503	503
0.75	431	431	431	431	431	431	431	431	431	431	395	386	371	371	371	371	371	386	395	395
1.00	341	341	341	341	323	323	305	296	287	287	278	269	269	269	269	269	269	278	278	278
1.25	224	224	224	215	198	180	171	162	153	148	144	144	139	139	139	144	148	153	162	180
1.75	189	189	189	171	153	139	130	121	117	112	108	103	99	99	103	108	112	121	130	139
2.00	162	162	157	135	117	108	99	94	90	85	85	83	84	84	86	90	94	99	103	111
2.50	121	121	117	95	79	66	60	57	54	52	51	50	51	52	54	58	61	65	69	75
3.00	94	94	86	66	49	41	38	36	34	33	32	31	31	33	35	38	40	43	47	51
3.50	81	80	66	46	33	28	25	23	22	22	21	21	22	22	24	27	29	31	34	38
4.00	71	69	55	32	23	20	18	16	15	14	14	14	15	17	19	20	22	23	25	27
4.5	63	59	43	24	17	14	13	12	12	11	11	11	12	13	14	14	16	17	19	21
5.00	57	52	36	19	14	12	10	9.0	9.0	8.8	8.7	8.7	9.0	10	11	13	14	15	16	16
5.50	51	47	31	15	11	9.0	8.1	7.8	7.7	7.7										
6.00	47	42	25	12	8.5	7.2	6.5	6.3	6.2											
6.50	43	38	22	10	6.7	5.8	5.2	5.0												
7.00	40	34	18	8.1	5.6	4.8	4.4	4.2												
7.50	37	31	15	6.9	4.7	4.0	3.8													
8.00	35	28	14	5.7	4.0	3.6	3.2				Q0 = 0.10: S1 = 0.25: S2 = 1.53									
8.50	33	25	12	4.8	3.6	3.1	2.9													
9.00	31	23	10	4.1	3.2	2.8														
9.50	30	22	9.0	3.7	2.8	2.5														
10.0	29	20	8.2	3.2	2.4	2.2														
10.5	28	18	7.3	3.0	2.2	1.9														
11.0	27	16	6.6	2.7	1.9	1.7														
11.5	26	15	6.1	2.4	1.7															
12.0	25	14	5.6	2.2	1,6															

In the CIE road classification system, instead of measuring the full set of $r(\beta, \tan(\gamma))$ values for a pavement surface as shown above, only a few measurement should be sufficient to classify the road into the appropriate standard R-tables. There are three parameters used for the classification.

They are:

- S1 and S2 specularity or shininess of the road surface
- Q_0 average luminance coefficient

S1 is used to define the road class. S1 is the ratio of an r-value that is generally large for specular reflection to another r-value that is generally large for diffuse reflection.

$$S1 = \frac{r(\beta = 0°, \tan(63°) = 2)}{r(\beta = 0°, \tan(0°) = 0)} = \frac{r(0,2)}{r(0,0)}$$

Thus S1 is a measure of the degree of specular reflection.

Similarly, S2 is the ratio of the average luminance coefficient to a r-value which is large for diffuse reflection[12].

$$S2 = \frac{Q_o}{r(0,0)}$$

Q_o, the average luminance coefficient, determines the brightness of a surface. It is calculated as the integral of the product of the luminance coefficient $q(\beta,\gamma)$ and the solid angle represented by q divided by the solid angle of all of the measurements

$$Q_0 = \frac{\oint q(\beta,\gamma) \cdot d\Omega}{\oint d\Omega}$$

where Ω is the solid angle of the integration area. The integration limits for the Q_0 calculation are $\beta = 0°$ to 180° and $\tan(\gamma) = -4$ to 12[12].

The range of the S1 values determines the class in which road surface is assigned, R1 through R4, as shown in Table 2. Table 3 gives a better appreciation of the different classification R1 to R4.

TABLE 2 ROAD CLASSIFICATION TABLE

Pavement Class	Standard S1	S1 Range
R1	0.25	< 0.42
R2	0.58	0.42 to 0.85
R3	1.11	0.85 to 1.35
R4	1.55	> 1.35

TABLE 3 CIE ROAD SURFACE CLASSIFICATION

Class	Q^0	Description	Mode of Reflectance
R1	0.10	Portland cement concrete roadway surface. Asphalt road surface with a minimum of 15 percent aggregates composed of artificial brightener (e.g., Synopal) aggregates (e.g., abradprote. quartzite)	Mostly diffuse
R2	0.07	Asphalt road surface with an aggregate composed of a minimum 60 percent gravel (size greater than 10 millimeters.)	Mixed (diffuse and specular)
		Asphalt road surface with 10 to 15 percent artificial brightener in aggregate mix (Not normally used in North America.)	
R3	0.07	Asphalt road surface (regular and carpet seal) with dark aggregates (e.g., trap rock, blast furnace slag); rough texture after some months use (typical highways.)	Slightly specular
R4	0.08	Asphalt road surface with very smooth texture.	Mostly Specular

The average luminance coefficient Q_0 is just a scaling factor of the overall pavement brightness and does not change the overall shape of the reflection characteristics.

Below are two examples to explain the application of Q_0. When only the Q_0 value changes, the reflection coefficient contour remains the same shape, but the volume changes, and it means that the specularity S1 stays the same as shown in Figure 2.16 below.

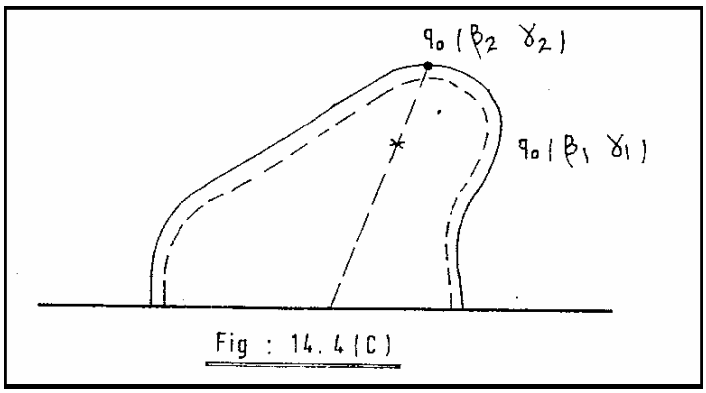

FIGURE 2.16 REFLECTION CONTOUR[9]

For the same Q_0 value, when the contour changes, so does the specularity S1, and the volume remains the same. Refer to Figure 2.17.

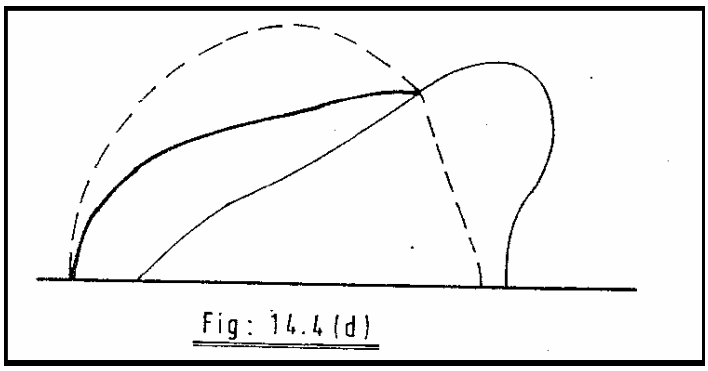

FIGURE 2.17 REFLECTION CONTOUR[9]

2.2.4 Measurement Method of Q_0

Measurement of pavement average luminance Q_0 can be done:

a) by numerical integration of an r-table, derived from equation

$$Q_0 = \frac{\oint q(\alpha,\beta,\gamma) \cdot d\Omega}{\oint d\Omega}$$

b) by direct measurement employing a reflectometer.

For option a), full set of q has to be known. For option b), an integrating sphere would be the perfect tool.

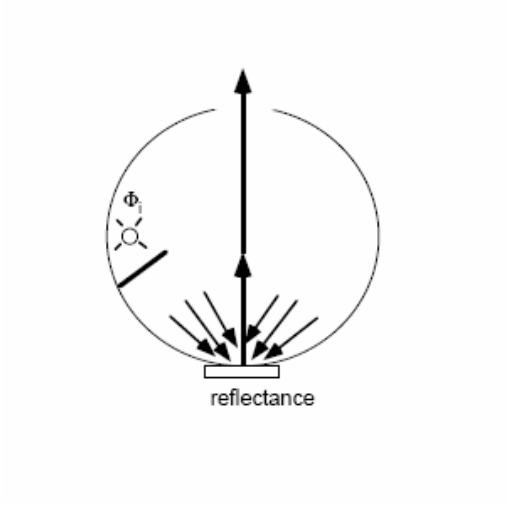

FIGURE 2.18 INTEGRATING SPHERE [13]

An integrating sphere can be used to measure the total average reflection from a surface. The inside of the sphere is coated with highly diffuse material, very similar to a Lambertian surface. The light is reflected off the surface evenly in all direction and hits the sample from all angles. A luminance meter measures the sample from the opening on the top and the result is compared with a reference material.

However, the problem is that the integrating sphere is very expensive to produce. So in the previous project, an average luminance meter was developed at Odyssey Energy Limited (OEL), and it proved capable of measuring the average reflectivity from a surface. The OEL Q_0 meter will be introduced later.

2.2.5 Measurement Method of Pavement r-Values

As mentioned in the previous section, the reflection properties of pavement surfaces possess the BRDF characteristic. BRDF measurement proved difficult to measure. It is a function of four degrees of freedom. The measurement procedure is quite complex since for each incident ray direction the reflected rays for all directions need to be measured.

A complete measurement of the r-table for a given road surface requires complex equipment in a laboratory.

The device for measuring the reflection properties of surface is called a gonioreflectometer. The measurements are done in a laboratory on road samples extracted from roadways.

FIGURE 2.19 ROAD WORKERS EXTRACTING PAVEMENT SAMPLES[14]

FIGURE 2.20 EXTRACTED PAVEMENT SAMPLES[14]

Figure 2.19 shows road workers extracting payments samples, and Figure 2.20 shows the extracted pavement samples.

The use of gonioreflectometers in past road reflection research is described below. A specially designed gonioreflectometer for measuring surface reflectance matrices was developed and automated at University of Toronto in 1986 by W. Jung, A. Kazakov and A.I. Titishov. The laboratory measurements were carried out on the pavement samples to determine the feasibility of classifying the pavement accordance with CIE practice [15]. The laboratory set up is detailed in Figure 2.21.

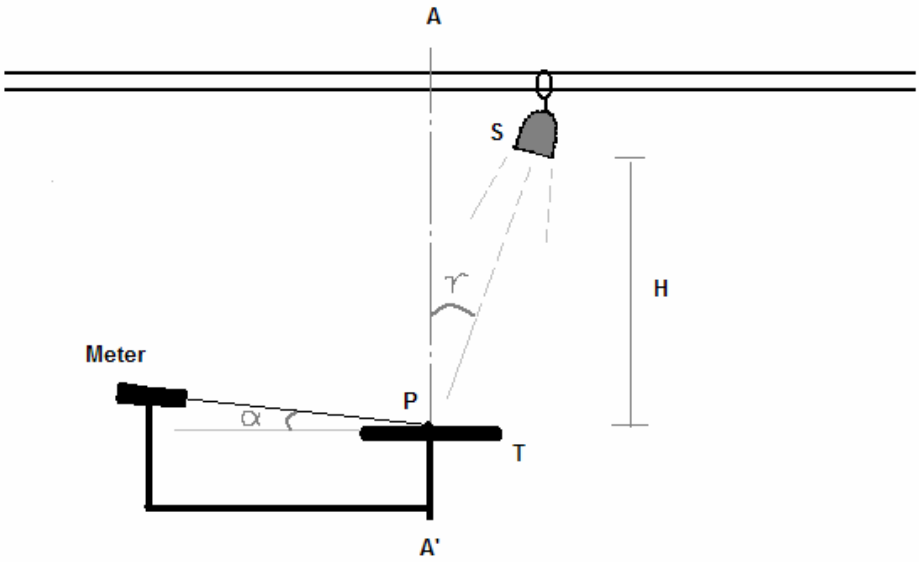

FIGURE 2.21 PRINCIPLE OFGONIOREFLECTOR FOR MEASUREMENT OF THE REFLECTION PROPERTIES OF ROAD SURFACE [15]

The extracted pavement sample is placed horizontally on a rotating table T, centered at P, and illuminated from the light source S. A luminance meter is aimed at point P to measure the reflected light or luminance from the sample at an angle of α. The meter support and the table P are rigidly fixed, and can rotate around the axis AA', so that the light projections plane S-P-A and the viewing plane M-P-A form successive increments of a rotating angle β varying from 0° to 180°. The luminous intensity I of the lamp, S, pointing towards P is kept constant. The lamp moves along a rail with constant height, H, above the table, which produces various projection angles γ relative to point P.

The above configuration is built accordance with a CIE proposal. It enabled this device to directly to measure the reduced luminance coefficient r(β, tan(γ)). The relation of the measured luminance value and r is calculate by the following relationship:

$$r = \frac{LH^2}{I}$$

where

L = luminance measured at P, in cd/m²

H = height of lamp above the sample surface.

I = luminous intensity of the lamp, in lumens.

In this report it states that the four R classes can be regarded as sufficiently accurate for design purposes. It concluded that the pavement reflection properties can be measured with fair accuracy and confidence, but that significant fluctuation of the reflection properties can occur on a given pavement. The CIE proposal for four specularity classifications under dry conditions can be recommended[15]. In this report the situation with the viewing angle α ranging from 1° to 3° was investigated. It was found that all parameters tend to decrease with increasing of viewing angle α.

Another useful reference is R. B. Gibbons's doctoral report *Influence of the Pavement Reflection on Target Visibility*[12]. In his report he made extensive research about pavement reflection properties. A laboratory gonioreflectometer was used to measure pavement reflection was developed and automated, it is illuminated in Figure 2.22. The test was also carried on the extracted pavement samples. In this report, a lot of useful information can be referred. The research topic emphasised on the visibility more, it studied how the specularity values were affected by a wide range of viewing angles up to 60°. Although this is never a case in the road luminance design (usually 0.5° to 3°), it gives very useful information later for my master research.

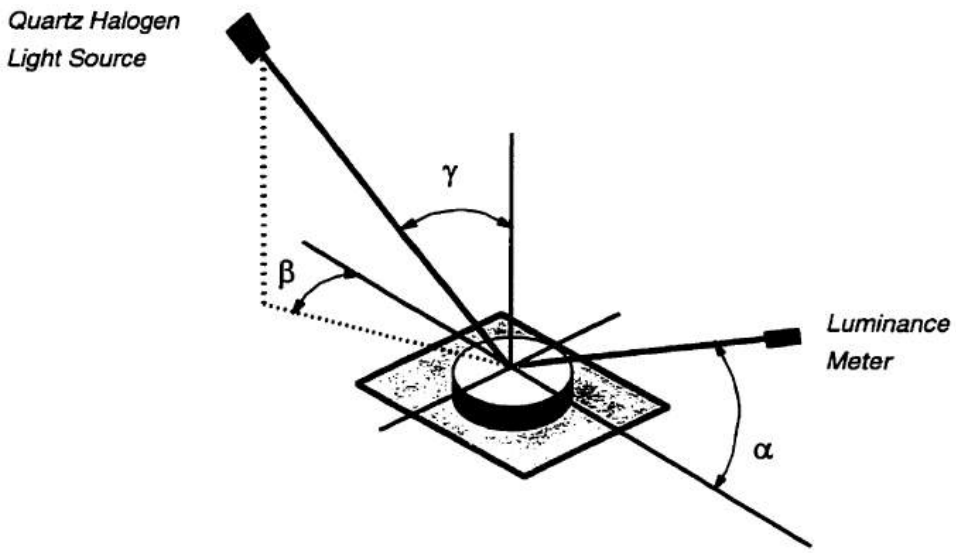

FIGURE 2.22 GIBBON'S GONIOREFLECTOMETER SCHEMATIC [12]

The research of Jung et al. and of Gibbons required the use of a complex device and data logging to measure the r-values for the interested specimens. The results produced are reliable and accurate, however, these results come at a monetary and time cost. Furthermore the samples are not always representative of the entire surface.

3 Hardware

This chapter starts with previous system assessments, followed by some new concepts developed that were not proved to be successful. Later conservative approaches were trialed and a CIE standard pavement S1 measurement system was developed.

3.1 Assessment of the OEL Road Reflectivity Measurement Prototype

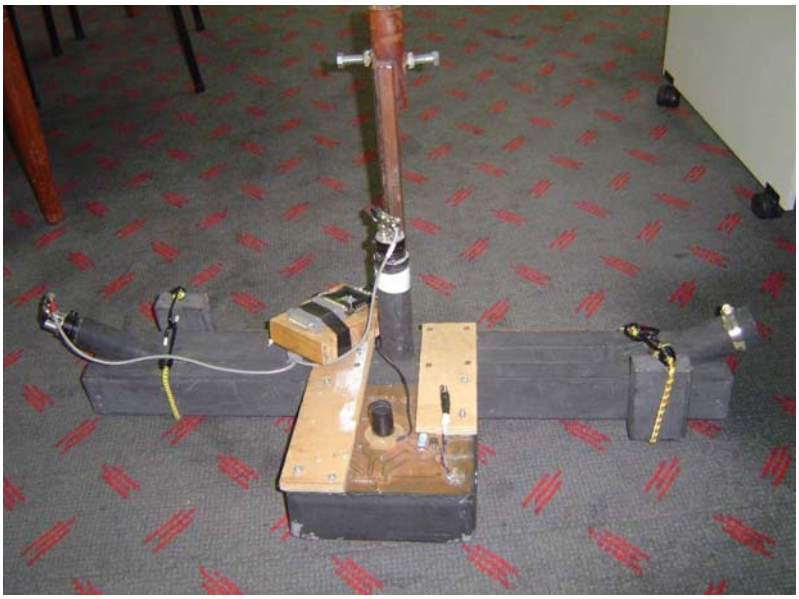

FIGURE 3.1 OEL'S REFLECTOMETER PROTOTYPE

The system in Figure 3.1 was designed to measure road surface reflectance by a Waikato University student, Jackson Hill, for OEL in 2004. When used with the OEL street light illuminance measuring system introduced in Section 1.2.1, the system can provide a means of street lighting luminance assessment.

The system consists of two parts, a specular meter and an average luminance coefficient meter. The specular meter measures the road surface specularity S1 value. The luminance coefficient meter measures the overall brightness of the pavement Q_0 value.

3.1.1 OEL Specular Meter

FIGURE 3.2 OEL SPECULAR METER[4]

OEL specular meter (Figure 3.2) is used to determine the specularity parameter S1 of pavements. The working principle for this meter is explained below:

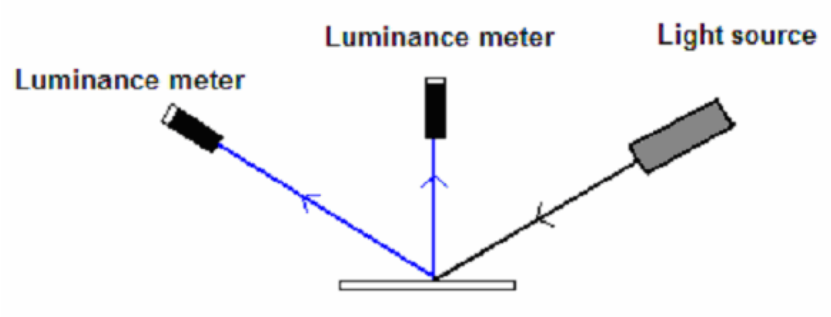

FIGURE 3.3 SCHEMATIC OF OEL SPECULAR METER

As shown in Figure 3.3 a collimated light is shone onto to a sample area of road surface from a 63° angle relative to the normal of the surface. The reflected light is measured by two luminance meters at observation angles 0° and 63°. The two measurement results are referred as r′ (0°) and r′ (63°) in this report.

In Hill's thesis it is stated that the road specularity factor S1 can be calculated as:

$$S1 = \frac{r'(63°)}{r'(0°)} = \frac{V_{S63°}}{V_{S0°}}$$

where $V_{S63°}$ and $V_{S0°}$ are the voltage outputs from luminance meter at 63° and 0° respectively when measuring the sample surface. This S1 value was used to classify road into one of four standard R-classes according to CIE road classification criteria.

His report states that the specular meter's S1 reading varied as expected over different surfaces; chip seal surfaces (typical of NZR2) gave an S1 rating of 0.8 while tarseal surfaces (typical NZR4) gave an S1 rating of about 1.45[4]. Those results nicely agreed with the CIE road surface classification criteria table (Table 2), but there were no details about how the test was done in his report.

Later in my project, static road testing was done with this meter (refer to Section 4.2.3). The measured S1 values ranged from 1.2 to 3. If according to the CIE classification criteria, there would be no roads in R1 and R2 class, and nearly all of the roads are in R4 class (mostly specular). This is not true since R2 and R4 class roads commonly exist in New Zealand.

In the CIE road classification system, road surface specularity S1 should be measured with the following configuration:

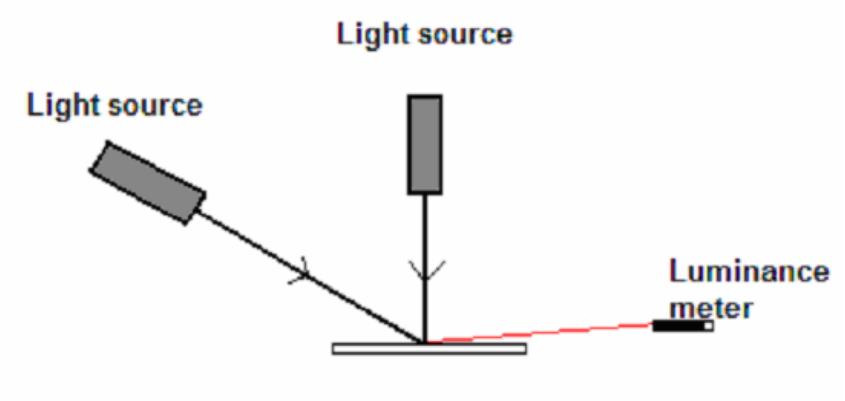

FIGURE 3.4 SCHEMATIC OF CIE S1 METER

In the CIE S1 measurement configuration (Figure 3.4) there are two incident light sources (63° and 0°) relative to the normal of surface. The luminance meter is aimed at the sample area with a fixed 1° observation angle, relative to the ground plane. Where specularity S1 is calculated as :

$$S1 = \frac{r(\alpha = 1°, \beta = 0°, \gamma = 63°)}{r(\alpha = 1°, \beta = 0°, \gamma = 0°)}$$

Obviously the two configurations demonstrated in Figure 3.3 and Figure 3.4 are quite different in operating principles. The S1 value measured by the OEL prototype specular

meter is not the one used in CIE road classification system. To distinguish between the prototype S1 and CIE standard S1, the prototype S1 is referred to as S1'. Strictly to say, the r′ (0°) and r′ (63°) measured by the prototype is $r(\alpha = 90°, \beta = 0°, \gamma = 63°)$ and $r(\alpha = 27°, \beta = 0°, \gamma = 63°)$ in CIE road lighting calculation terminology. So it is incorrect to use S1' directly to classify the road surfaces based on the CIE classification criteria.

The reason for why the prototype module uses a modified configuration instead of the CIE standard configuration is that it was designed for dynamic purposes. A 1° viewing angle is technically difficult to achieve under dynamic measurement scenarios where the device is installed on a vehicle. As moving vehicles do not maintain a static clearance from ground surfaces due to road surfaces not being uniformly flat, the unit needs to be attached to the vehicle with a sufficient height clearance from the ground so as to avoid collisions with the sample ground.

For example, if using the CIE proposed 1° observation angle, and the whole module is 10 cm above the ground to avoid collision with the ground, the luminance meter has to be installed 573 cm away from the light source as show in Figure 3.5. Obviously this is impractical in the real design.

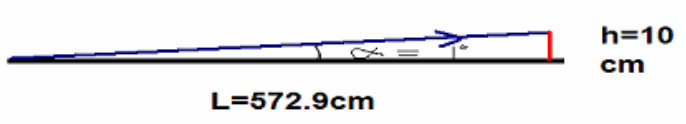

FIGURE 3.5 CIE 1° OBSERVATION

As a result, the CIE road classification criteria are no longer applicable to this prototype specular meter due to the modification; however, the meter can't yet be considered to be not useful. From the road testing for this meter, the S1' values measured by the prototype specular meter did vary over different surfaces. The meter still has the potential to be used a tool to assess the road surface reflectance properties; even the S1' value it produced is not a standard specularity value of the road surface. It was believed that there might be some correlation between the prototype S1' and the standard CIE S1. This was tested as is reported later in this thesis.

3.1.2 OEL Q_0 Meter

FIGURE 3.6 OEL Q_0 METER[4]

An average luminance coefficient Q_0 meter (Figure 3.6) was designed separately in the reflectivity prototype to determine the level of total reflection or degree of relative brightness of the pavement surface.

When measuring surface average reflectance, an integrating sphere as demonstrated in Figure 3.7 would be a proper tool to do this job, since reflectivity from all incident angles could be considered:

FIGURE 3.7 AN INTEGRATING SPHERE[13]

But it costs too much. A Q_0 meter was designed in OEL, the design principle is shown in Figure 3.8:

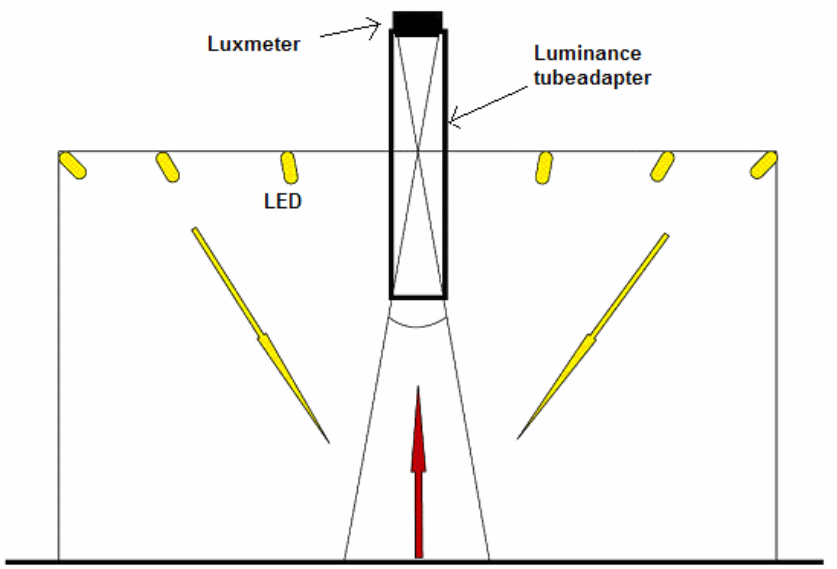

FIGURE 3.8 SCHEMATIC OF OEL Q_0 METER [4]

This Q_0 meter is built based on a luminance meter; an arrangement of LEDs is positioned around the luminance tube adapter and used as light source to light up the sample area.

Luminance meters on the market are very expensive, normally over ten thousand dollars. Instead of purchasing one, a luxmeter TECPEL DLM-530 (refer to datasheet in Appendix IV) was converted to a luminance meter. This luxmeter has good spectral response and closely matches the sensitivity of the human eye for photopic vision, as represented by the CIE spectral luminous efficiency V(λ). The luxmeter was converted to a luminance meter by attaching a black tube to the luxmeter's photodetector to limit the detector's field of view (Figure 3.9). For details of this conversion refer to Appendix I.

FIGURE 3.9 LUXMETER CONVERTED LUMINANCE METER

OEL prototype Q_0 meter works reasonably well. An experiment was setup to test the Q_0 meter in this project.

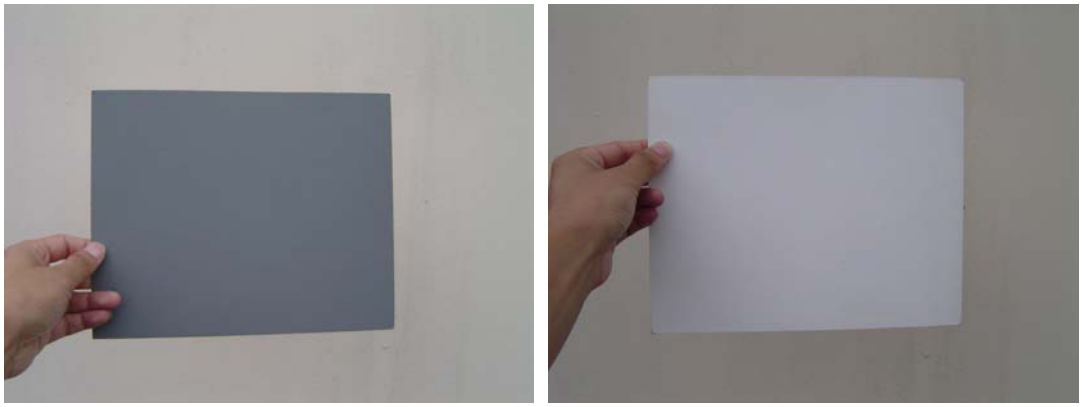

FIGURE 3.10 GREY CARD

A Grey Card (Figure 3.10) was used as a reference in this experiment – Grey Cards can be purchased from a photography shop. The card is used to help to determine photo exposure time, lighting ratios, colour balance and density. The purpose of using this card in this experiment is that it has two known reflectance surfaces in two sides that are used for calibration. One side is in grey, which reflects 18% of the light in all colours. The other side is in white and reflects 90% of all light. Theoretically under the same lighting condition, the quantity of reflected light will have a 5 times difference for the white side than the grey side.

FIGURE 3.11 REFLECTANCE TEST SETUP

The test was conducted in a dark environment in a static situation. Since the prototype Q_0 meter was designed for dynamic measurements a 10 cm clearance above the ground had to be created. This configuration forces the lower part of the unit open to air, therefore introducing any ambient light. Measurements were recorded for the white side and grey side of the Grey Card – results are listed in Table 4

TABLE 4 OEL Q_0 METER GREY CARD TESTING RESULTS

White side (90% reflection) Lux	Gray side (18% reflection) Lux	White /Gray
1165	288	4.05
1147	281	4.08
1161	285	4.09
1174	286	4.10
1164	286	4.07
1150	282	4.08
1143	278	4.11
1150	278	4.14
1129	277	4.08
1146	275	4.17
1126	274	4.11

In comparison to the theoretical ratio of 5, the measured results have an averaged reading of 4.1. Improvements to the design to make the ratio of the measurements closer to 5:1 are described later.

3.2 New Developments

Various new developments were tried to improve existing OEL prototype designs, and also to create a new method of measurement. Improvements were done to the Q_0 meter that allowed better results to be achieved. A simplified specular was made and can be considered to be used as a substitute for the OEL prototype specular meter. An LDR based specular meter was developed, and proven not successful.

3.2.1 Improvement on the Q_0 Meter

At the beginning of the projects work had been done to improve the accuracy of the average luminance Q_0 meter.

To minimise the stray light effect, the inside of the luminance tube was painted in matt black (blackboard paint). The black paint absorbs the unwanted light (the light rays that come from any angle other than the photodetector's field of view) and stops them from bouncing into the lux meter detector.

Theoretically only the light rays within the confined viewing angle can reach the photo detector without hitting the inside surface of the luminance tube adapter. Any light from different angles will inevitably hit the black surface twice or more. Each reflection off the black surface will attenuate the light intensity heavily. But due to imperfection of light absorption, some unwanted light could still reach the detector surface with sufficient photon energy to affect the measurement results.

One solution is that a baffle barrel was added onto the end of the luminance tube. The inside of the baffle was painted with the same black paint as luminance tube. The diameter of the barrel was larger than the tube adapter's, so there was a gap between those two cylinders.

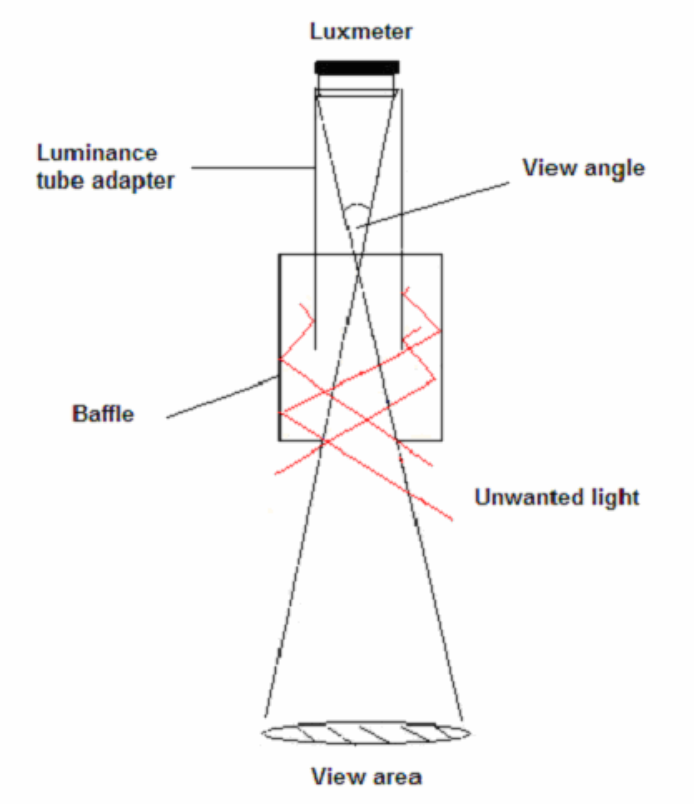

FIGURE 3.12 LUMINANCE METER WITH BAFFLE

From Figure 3.12 it can be seen, by adding the baffle, some of the unwanted light rays will be trapped in the gap between the luminance tube and the baffle barrel, so they never make their way to the photodetector. This modification cannot eliminate all of the unwanted light, but it helps.

Another solution for reducing the stray light is to use a longer luminance tube. The longer the tube, the more times the unwanted light bounces off the tube black surface and thus more intensity attenuation is achieved. But a longer tube decreases the luminance meter's view angle.

Based on the same principle as the prototype Q_0 meter, a new version of the Q_0 meter was made (Figure 3.13). Since the new version was used in a static situation, a light shielding case was used to block the external light from affecting measurement. In the new design 10 super bright white LEDs were used as light sources to illuminate the sample area. A PCB board (Appendix II) was designed to power and house them. The LEDs were arranged in a circle around the luminance tube. The projection angle of each LED is adjusted so that light intensity is maximised at the sampling spot. The circuit diagrams are included.

FIGURE 3.13 NEW Q_0 METER

A plastic case was used as the closure for the measurement device. There are two benefits of this case; firstly, it acts as a light shield. Secondly, the case had a white and glossy texture inside. When the LEDs are lit, the lights mirrored themselves onto the walls and behaved like many light sources shining from different positions, this helped to illuminate the sample area evenly, which kind of mimics the integrating sphere.

Once again the Grey Card was used to test the new Q_0 meter. The experiment is shown in Figure 3.14.

FIGURE 3.14 Q_0 METER TEST

Multiple readings have been taken for each side of the Grey Card (measurement positions on each side of the Grey Card varied randomly); results are shown in Table 5.

TABLE 5 GREY CARD TEST

White side (90% reflection) Lux	Gray side (18% reflection) Lux	White /Gray
3953	840	4.73
3923	833	4.71
3900	827	4.72
3902	826	4.72
3870	818	4.73
3862	817	4.73
3847	816	4.71
3823	816	4.69
3827	819	4.68
3821	812	4.70
3825	819	4.67

The average ratio for white/grey is approximately 4.7, which when compared to the previous meter's average ratio of 4.1 shows that improvement was achieved. This is sufficient close to 5 for our purpose.

To test the new Q_0 meter's feasibility, a field test was conducted on two real roads as shown in Figure 3.15 and Figure 3.16.

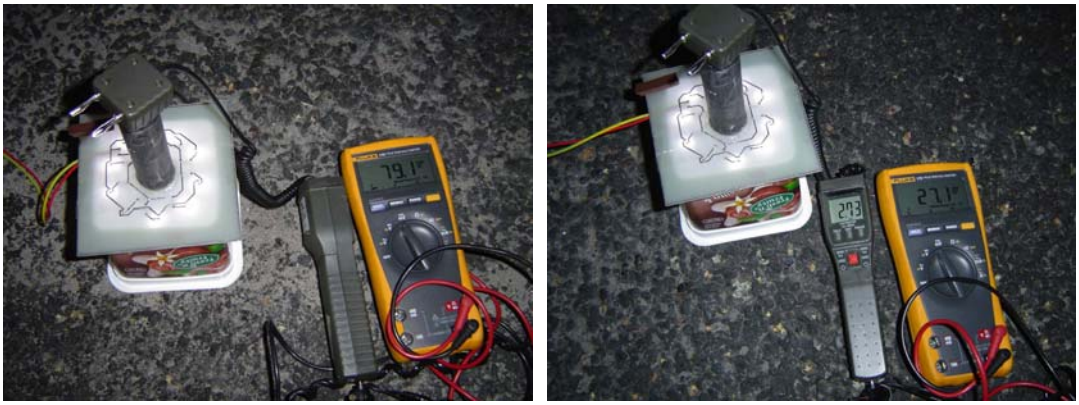

FIGURE 3.15 ROAD TEST ONE- OPIOA ROAD

The first test was conducted on Opoia Road, Hamilton. The whole street has the same road condition. A small section was chosen, with an area less than half a square meter. On the chosen section one spot was partially covered by sand and the remaining spots were relatively clean. The Q_0 reading for the sand spot is 79.1 lux and the clean part 27.1 lux. There was 3 times difference factor in the reading, the reason for this is that

the surface with sand on top appears much lighter than the pavement original colour, which increases pavement overall brightness.

FIGURE 3.16 ROAD TEST TWO-PARKING LOT

Here is another example. The measurement was done on the white stripe of the road and the unpainted part. Again the two spots have the same physical structure, the only difference is the colour of the road surface. The reading for the plain spot is 22.5 lux and the painted spot 172.1 lux.

The reading measured for the above roads was in lux, so to calculate the average luminance coefficient Q_0; the grey card is used as a reference. In the grey card experiment the grey side has an average reading of 82 lux under the same lighting condition, which corresponds to 18% reflectance. Therefore for Opia Street, 27.1 lux reading corresponds to 5.9% reflectance, and for the second road 22.5 lux corresponds to a 4.9% reflectance.

The above testing results are quite convincing. So later on in this research, it was decided to use this system as the standard tool to measure the brightness of the road surfaces. Later the work was concentrated on specular meter research and improvement.

3.2.2 Simplified Specular Meter

FIGURE 3.17 HOOP SPECULAR METER

A hoop shaped specular meter was made as in Figure 3.17. It was built based on the same principle as the OEL prototype specular meter. A steel semicircle was used as the light source and luminance meter holder. The benefit of the steel ring holder is that it can accurately locate 27° and 0° luminance tube and 63° light collimating tube positions with great ease. To find correct positions only a little math is needed. This device is referred to in this thesis as the ‘Hoop meter’.

Once the positions were found, the light collimating tube and luminance tubes were mounted perpendicular to the tangent of the hoop. This guarantees that the light sources and detectors are all aimed at the same sampling area, a task that is difficult to achieve accurately when working with flat sections of wood. The operating of the hoop meter is shown in Figure 3.18.

FIGURE 3.18 HOOP SPECULAR METER OPERATING

Static road tests were done with the hoop specular meter and the OEL specular meter on the same road section at the same time. The main objective is to check whether the new version produces similar results to the OEL specular meter. Table 6 shows the results.

TABLE 6 HOOP AND OEL SPECULAR METER MEASUREMENT RESULTS

Road No.	Location	S1 hoop	S1 OEL
1	Clarence St	1.256	1.247
2	House yard back	1.48	1.328
3	Hose yard front	1.593	1.471
4	Cook St	1.47	1.476
5	Wellington St	1.435	1.516
6	Pak'n'Save	1.896	1.524
7	Pharnacy carpark1	1.37	1.59
8	Pavement	1.721	1.605
9	Angleasea St	1.629	1.85
10	Pharmacy carpark2	1.64	2.133
11	New carpark	2.04	2.21
12	Power house	2.475	2.65

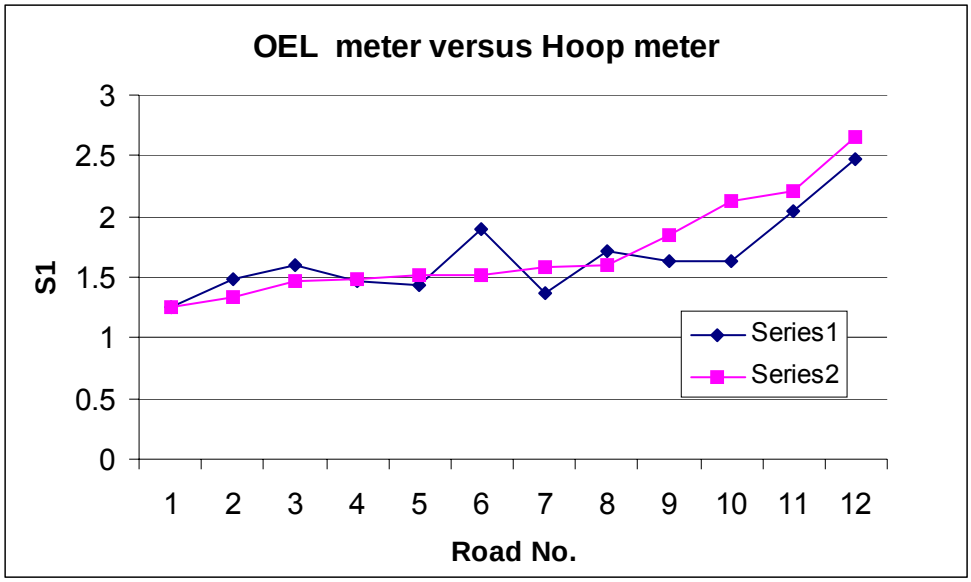

FIGURE 3.19 HOOP METER VS OEL SPECULAR METER

A graph (Figure 3.19) was plotted based on the above testing results. Series 1 is measured by the hoop meter, Series 2 by OEL unit and sorted in ascending order. Roughly it can be seen that the Series 1 follows with the trend of Series 2. There is a correlation factor of 0.838 between those two series. So the Hoop unit can be considered as a replacement for the OEL specular meter due to its simplicity. Again it can be seen that none of the S1' values measured by the hoop specular meter go below 1.2.

After the comparison test, a small modification was done to the hoop specular meter (Figure 3.20). Another 27° detector was introduced in, but this time it was installed on a rotating leg, and the leg can rotate about the vertical axis passing the 0° detector. By doing this, the angle between observation plane and light incident plane, that is angle β can range from 10° to 160° instead of the fixed $\beta = 0°$. It was hoped that this could give some more understanding on reflectivity of road surfaces.

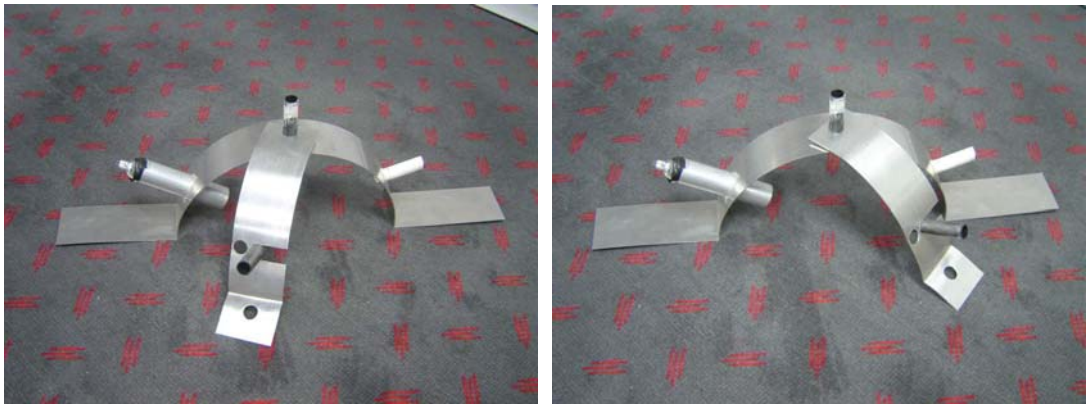

FIGURE 3.20 HOOP METER WITH ATTACHED LEG

A road test was done. The extra 27° detector did give some different readings in different β observation planes. Generally the reading is maximised at the two ends of approximately 10° and 160° and minimised at the middle, but it was not known how to relate this measurement to the standard classification, due to the lack of information of the road actual r-values. The new version still suffers the same problem as the OEL specular meter. There is not an effective tool to calibrate against to testify its feasibility.

3.2.3 LDR Based Specular Meter Design

As mentioned before each road surface has its unique reflection characteristics. In the CIE road classification system, the existing road surfaces are categorised into four standard classes, R1, R2, R3 and R4 according to their specularity. Class R1 is mostly diffuse, R2 is a kind of mixed with diffuse and specular, R3 is slightly specular and R4 is mostly specular. Figure 3.21 shows what the different R-class surface reflection profiles may look like.

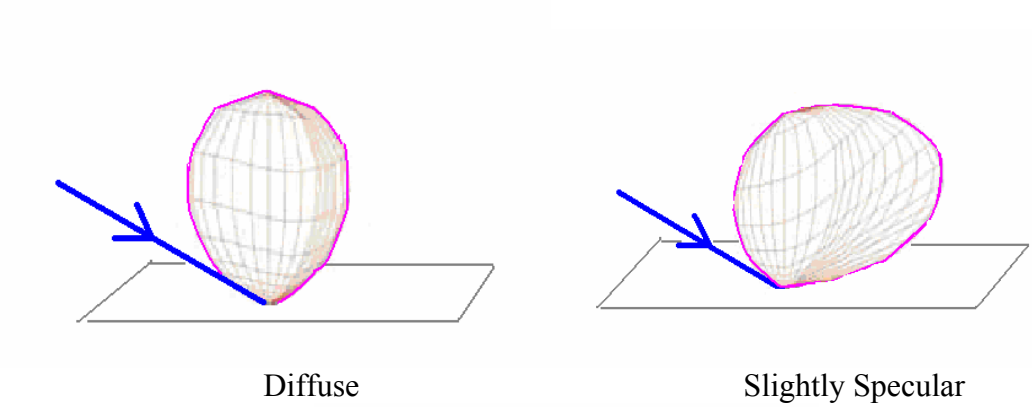

Specular

FIGURE 3.21 PAVEMENT REFLECTION PROFILES

Since the CIE road classification only provides an approximate method of categorising the road surfaces into four standard classes according to their specularity properties, there was no need to tell what exactly the r values was for each individual road. It was decided to make a device that could distinguish the road surfaces according to their reflection profile. This device should be able to tell which surface was diffuse, which surface was specular, and which was slightly diffuse or slightly specular.

It was assumed there might be a different approach to classify the road surfaces into the four standard R-classes instead of using the CIE proposed specularity parameter S1. The advantage of doing this is that it would simplify the design of the system as the low viewing angle issue can be solved and it would enable the system to be mobile.

The new design concept is demonstrated below in Figure 3.22:

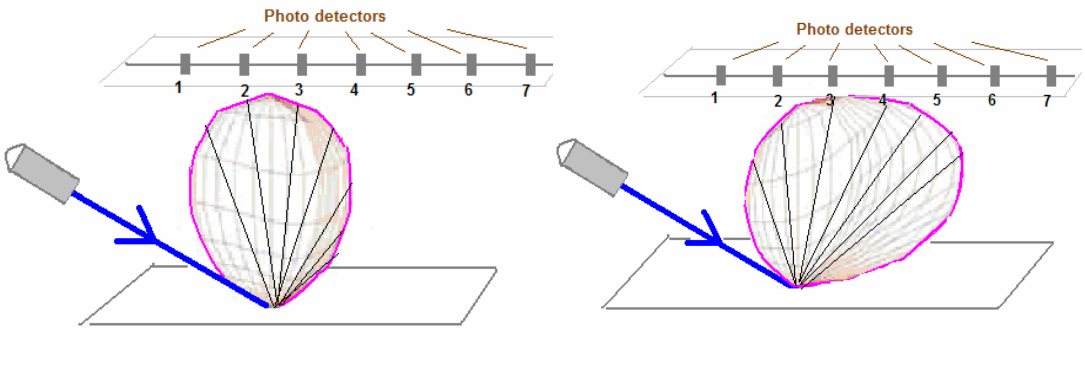

Diffuse Semi-diffuse

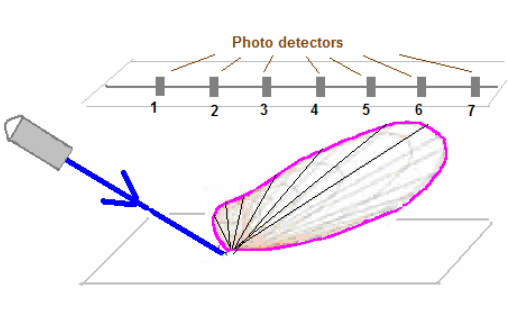

Specular

FIGURE 3.22 NEW DESIGN CONCEPTION

The new device has an array of photodetectors arranged in a line; each of them is capable of measuring light intensity individually. When light shines onto the road surface, the reflected light has its unique reflection contour according to the road reflection characteristic. During the measurement, the device was placed above the illuminated sample area. The photodetectors' readings were recorded. Through comparing the relative light intensities they each detected, the road surface reflection profile can be determined.

Here is the explanation on how the reflection contour can be determined. For a specular surface in Figure 3.22 the light intensities measured by detector 1 and 2 are the smallest, and from detector 3 onwards the measured values ascend. For a diffuse and specular mixed surface detector 3, 6 and 7 measure larger values. Overall all measurements are not too different. For a diffuse surface the measured results are maximised for detectors 2 and 3, and get lower on either side of those detectors.

A prototype was made as shown in Figure 3.23, for circuit schematic refer to Appendix II.

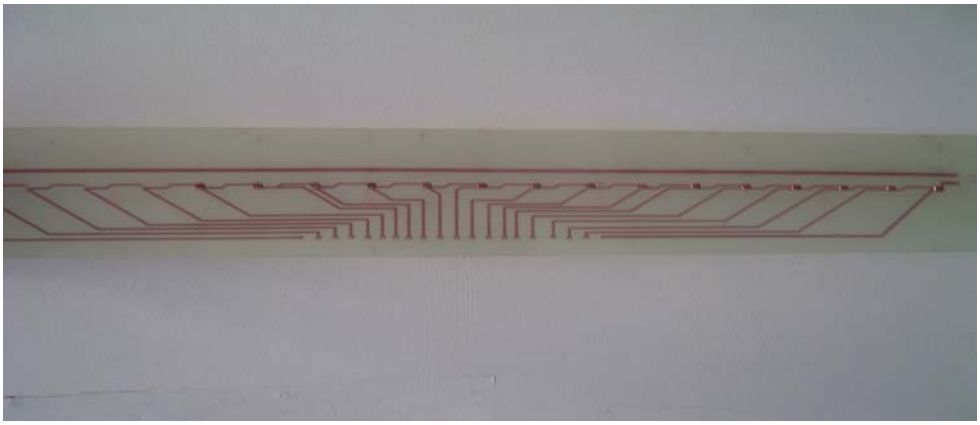

FIGURE 3.23 LDR BASED SPECULAR METER PROTOTYPE

In the prototype, light dependent resistors (LDR), NORP12 were used as the photodetectors because of ease of use and low cost. The datasheet is included in the Appendix IV. NORP12 (Figure 3.24) is a two cadmium sulphide (cdS) photoconductive cell with spectral response similar to that of the human eye. The cell resistance falls with increasing light intensity [16].

FIGURE 3.24 NORP12 PHOTOCONDUCTIVE CELL

16 such LDRs are evenly placed on PCB board in a line, 25mm apart. They are connected in serial. When doing the measurements, the light intensity received by each LDR can be calculated through the LDR's resistance. Or alternatively, a voltage can be applied to the two end of the whole serial; the resistance reading for each LDR will be converted to a voltage reading, which can be used by a data-logging device.

As mentioned in the NOR12 datasheet, the illuminance received by the LDR is a function of the resistance. An experiment has been set up to investigate this relationship.

The experiment was conducted against the commercial luxmeter TECPEL DLM-530; the luxmeter was used to accurately measure the light intensity. Under various light conditions the LDR's resistances were recorded, and also the illuminance readings measured by a luxmeter. The measurement results are listed in **Error! Reference source not found.** and illuminance vs resistance for the NORP12 is plotted in Figure 3.25.

TABLE 7 LDR CALIBRATION RESULTS

LDR (k ohm)	Luxmeter (lux)
0.608	381
2.768	52
0.703	311
0.787	267
0.863	227
6.74	18.1
16.62	5.12
36.3	1.62
0.611	443

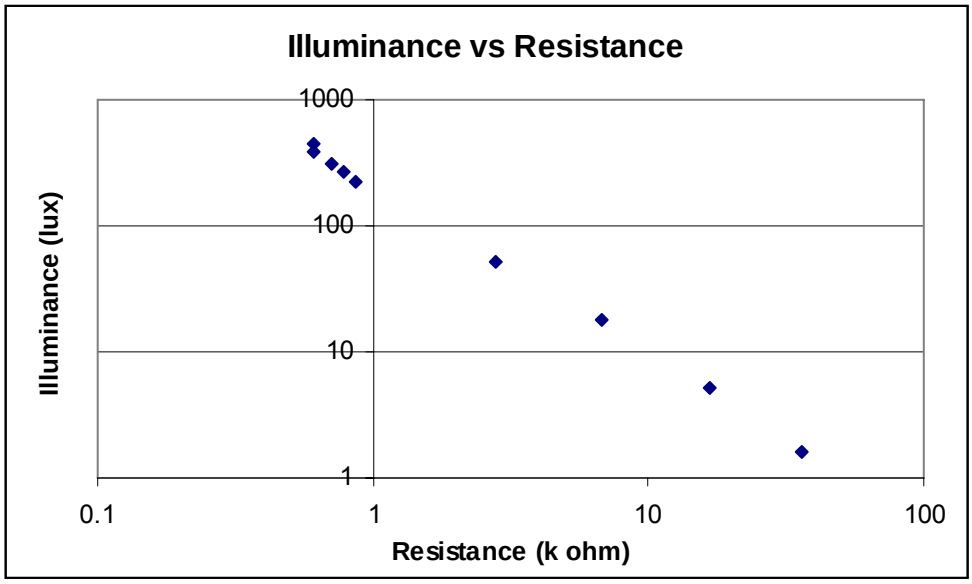

FIGURE 3.25 ILLUMINANCE VS RESISTANCE

Based on the measured LDR resistances and the luxmeter readings, a relationship was found between the resistance *R* and the illuminance *E* it represented:

$$E_{LDR} = \left(\frac{R_{LDR}}{53}\right)^{-1.333}$$

Applying this formula, a LDR's resistance reading can be converted to an illuminance value as it is shown in Table 8. Comparing the calculated LDR illuminance results with the luxmeter reading, LDR gives a very close match to the commercial luxmeter. The performance of the LDR is really impressive for such an economical device.

TABLE 8 LDR VS LUXMETER

LDR (lux)	Luxmeter reading (lux)
385	381
51	52
318	311
271	267
242	227
15.6	18.1
4.7	5.12
1.65	1.62
383	443

Once the illuminance was decided, certain correction factors needs to be applied to each measured value according to the rule of inverse square law and cosine law introduced in Section 2.1 to compensate for the geometry difference resulting from each photodetector's relative position to the sample spot. Hopefully from these results the detailed pavement characteristics can be determined.

Before the prototype build was completed a road test was carried out for its feasibility. With a light shone on the pavement surface at a certain angle, a multimeter was used to measure each LDR's resistance and the readings were converted into illuminance.

The results achieved from the on-site road test were rather disappointing. No obvious differences for the different pavement surfaces could be seen from the readings.

After referring to a document on the Internet, it is realised the failure was partially due to LDR's inaccuracy. Since the LDR was mass manufactured, the error for each one can be up to 50%. It is the wrong choice for them to be used in such subtle measurement, a fairly high quality photodiode should be used instead, and also with so many parameters to measure (there are 16 LDRs), the complexity is too overwhelming. Further development was abandoned due to above reasons.

3.3 Standard Design

As introduced in section 3.1.1, the OEL prototype specular meter was not designed according to the CIE road classification standard, and hence the road classification criteria was not applicable. It means we cannot directly use the S1' value produced by the prototype to classify the road into the appropriate R classes. If we have the information on which road belongs to which R class then the calibration procedure could be simply done by observing how the specular prototype behaves on different classes of roads. So we can get ideas on how to relate S1' to the standard S1, in another words, what range of S1' represents R1, and what range represents R2 and so on. Road companies were consulted. Unfortunately, none of them seemed to have the information on which roads belong to which R classes.

Due to this lack of information, more researches have been done in an effort to find a reliable tool that is capable of determining road R-class; nearly all of the search results related to this topic were conducted in the laboratory condition with extracted road samples. Finally, one road reflectance measurement system was found, which was relatively simple to make and capable of the in site road test.

3.3.1 "Wellington" Reflectance Box

A report *Road Reflection Properties, Wellington Area* by J. V. Nicolas and R. J. Stevens [17] published in 1981 was found. In this report a static in situ road surface reflectivity measurement system was designed and used to measure the road reflection properties and classify the road surfaces into the standard R-classes according to the CIE proposal. 20 roads were tested and analysed, and it concluded that the CIE road classification is applicable to the New Zealand road surfaces.

FIGURE 3.26 THE REPLICA OF THE "WELLINGTON" REFLECTANCE MEASUREMENT BOX

FIGURE 3.27 BOTTOM VIEW

Referring to the report, a replica of the "Wellington" reflectance measuring system was built (Figure 3.26 and Figure 3.27). The system used four independent light sources and one luminance meter to detect the reflected light. The four light sources are situated at four different positions with projection angles of (β= 0°, γ = 0°), (β = 90°, γ = 45°), (β = 0°, γ = 63°) and (β = 5°, γ = 79°), and are operated separately. For each measurement location, the luminance meter reads the four light sources in turn.

In J. V. Nicolas and R. J. Stevens' report, a procedure was used for the purpose of calibration. In the procedure the intensity of four light sources were adjusted by series resistors so that the luminance meter reading for each light source was approximately

the same on a standard surface. The standard surface is a grade 00 glass paper and has a high diffuse reflectance property. It is used as a substitute for the perfect diffuser [17].

The same calibration procedure was also done to the replica box, but a problem was encountered. During the calibration, the light source at (90°, 45°) gave the lowest luminance reading, which is over 10 times lower in magnitude than the reading for the rest of the light sources. To achieve the same reading for all light sources as instructed, the intensity of the three other light sources has to be reduced. This caused problems however, as once the readings were adjusted to the same, the remaining of the light sources were becoming too dim for the luxmeter converted luminance meter to detect reliably at the 1° viewing angle. The reading was falling well below 1 lux, which is the lowest measurement range on the luxmeter used. The measurement accuracy cannot be guaranteed by this self-made luminance meter at this measurement range. In the original reflectance box, a professional luminance meter was used, which was capable of picking up even a sensitive change.

Another factor of this design is that the box had large dimensions of $50 \times 50 \times 100$ cm³, and was quite heavy in weight. It was too bulky for the operation on the road reflection properties assessment in this project. Eventually this approach was given up due to the technical and practical difficulties.

3.3.2 Design of Road Specularity Measurement Box

Eventually it was decided to design a new system accordance to the CIE standard that is capable of measuring the specularity parameter S1. A conservative design approach was used. A road classification system (Figure 3.28) was designed to measure the road surface specularity as recommended by the CIE proposal. This system is now to be referred to in this report as the 'CIE box'. The design concept was partially borrowed from the gonioreflectometer used at Ontario University as described in Section 2.2.5. Instead of making a complex gonioreflectometer to measure the whole set of r values for a road sample, the new design only measures two values being r($\beta = 0°, \gamma = 63°$) and r($\beta = 0°, \gamma = 0°$) to determine the S1 value for a given road.

FIGURE 3.28 CIE BOX

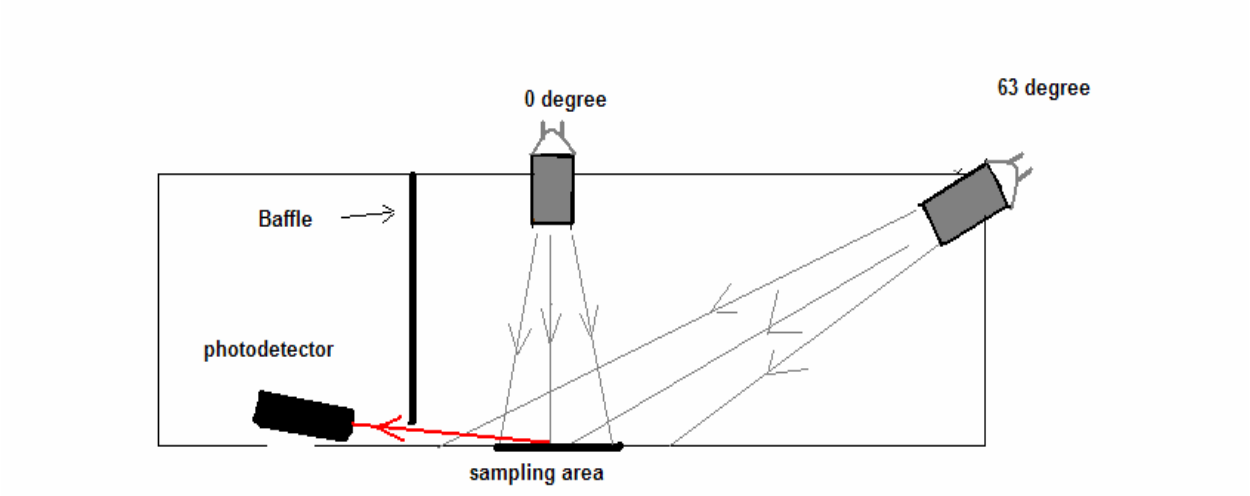

FIGURE 3.29 CIE BOX SCHEMATIC

A wooden box was constructed to accommodate two independent light sources as shown in Figure 3.29. The light collimating tubes were installed with fixed angles of 0° and 63° relative to the normal of the surface. The two halogen lights at the end of the collimating tubes sat at the same height of 250 mm to the ground, and 490.7 mm apart. This configuration would guarantee the same test surface could be illuminated either by the 0° light source or by the 63° light source. The luxmeter-converted luminance meter is fixed at a 6° viewing angle and is aimed at the same test surface. To reduce unwanted light, a black wooden board is used as a baffle to only allow certain reflected light to reach the luminance meter.

The benefit of this design is that the pavement luminance L_p can be measured by this reflectance measurement box, therefore the reduced reflection coefficient r can be calculated. The following explains how this can be done:

Using the equation from Section 2.2.2,

$$L_p = \frac{I(c,\gamma)}{h^2} q(\beta,\gamma) \cos^3(\gamma)$$

$$= \frac{I(c,\gamma)}{h^2} r(\beta,\gamma)$$

I(c, γ) is the luminous intensity of the light source in the direction of c and γ. Since in this application, the two light sources are using the same configuration (identical light bulbs and light collimating tubes are being used), so c and γ values for both light sources are the same. Therefore I(c, γ) values are the same for both the 63º and 0º incident light sources. Let h be the height of the halogen lights above the ground, a constant value of 250mm. Then the term I(c, γ)/h² in the above equation is a constant value, and L_p (β,γ) is proportional to the r(β,γ).

$$L_p \propto r(\beta,\gamma)$$

This reflectance box is specially designed so that the luminance L_p of the 63º or 0º light source can be directly measured, and then r(0º,0º) and r(0º, 63º) can be derived from above equation. With a knowledge of r(0º,0º) and r(0º,63º), the road surface specularity S1 can be determined.

3.3.2.1 Validation of the CIE Box

As a new tool designed from concept, its working theories have to be verified by the means of experiment. A set of experiments has been devised and performed to validate the CIE box's design concept. The experimental method and their associated results are detailed, along with the discussion of the results.

Inverse square and Cosine law

The main objective of this experiment is to test whether the light follows the Inverse Square and the Cosine laws in the CIE box. The experiment theory is explained below (Figure 3.30).

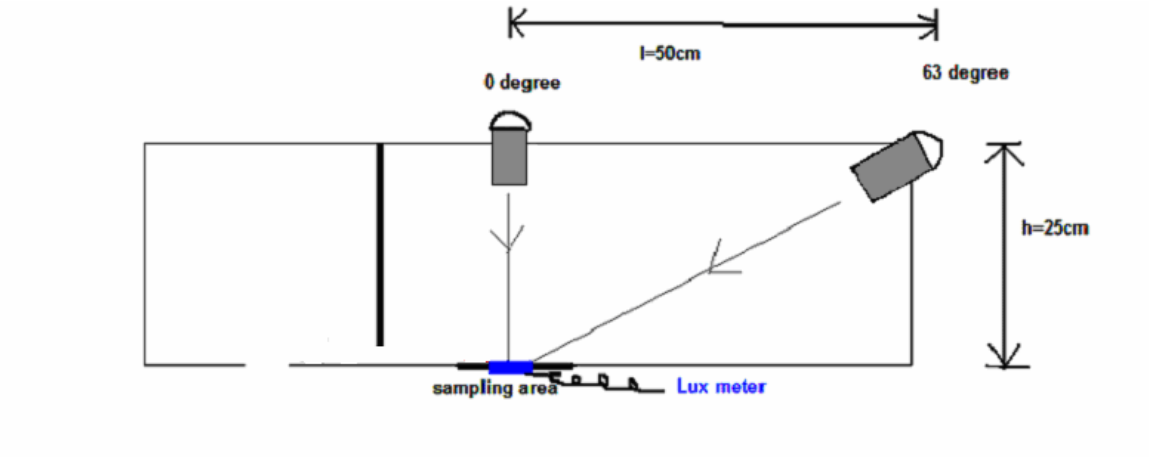

FIGURE 3.30 EXPERIMENT PRINCIPLE

According to Inverse square law, illuminance E at sampling area is calculated as:

$$E = \frac{I}{D^2}$$

where D is the distance from the light source to the sampling area and I is the light intensity. It is noteworthy that E calculated above is on a plane perpendicular to the incident light ray. To get the horizontal illuminance E_H (illuminance at road surface), Cosine law is applied.

$$E_H = \frac{I}{D^2}\cos(\gamma)$$

where D is calculated as:

$$D = \frac{h}{\cos(\gamma)}$$

then substituting,

$$E_H = \frac{I}{h^2}\cos^3(\gamma)$$

Here we got the same formula as introduced in section 2.2, where term I/h^2 is constant as introduced previously. The ratio is computed for the illuminance provided by the 63º and 0º light source:

$$\frac{E_{H63^\circ}}{E_{H0^\circ}} = \frac{\frac{I}{h^2}\cos^3(63^\circ)}{\frac{I}{h^2}\cos^3(0^\circ)} = \frac{\cos^3(63^\circ)}{\cos^3(0^\circ)} = 0.09357$$

It means at the sampling spot, the illuminance provided by the 63° light source is 0.09357 times the one produced by 0°. To test if this relation was held for the CIE box, the experiment setup is shown in Figure 3.31. A hole was drilled on the bottom board of the CIE box, which was right underneath the 0º light collimating tube. The luxmeter's detector could just be fitted in face upwards, and the board was reinstalled back onto the bottom of the calibration box. Then illuminance readings for the 63º and 0º light sources were recorded and ratios calculated.

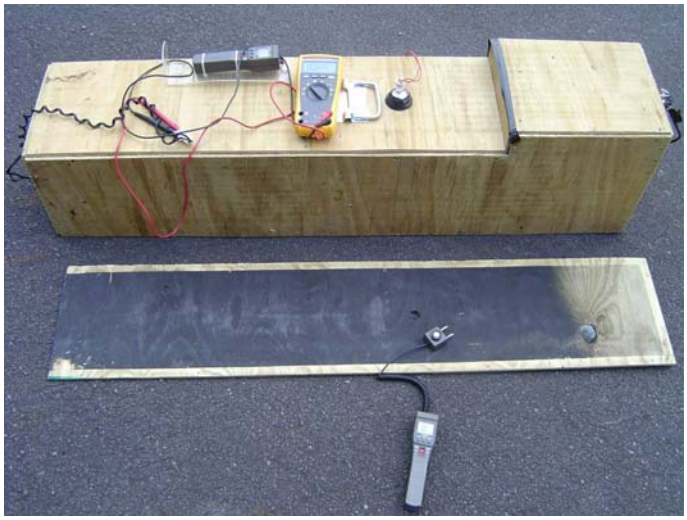

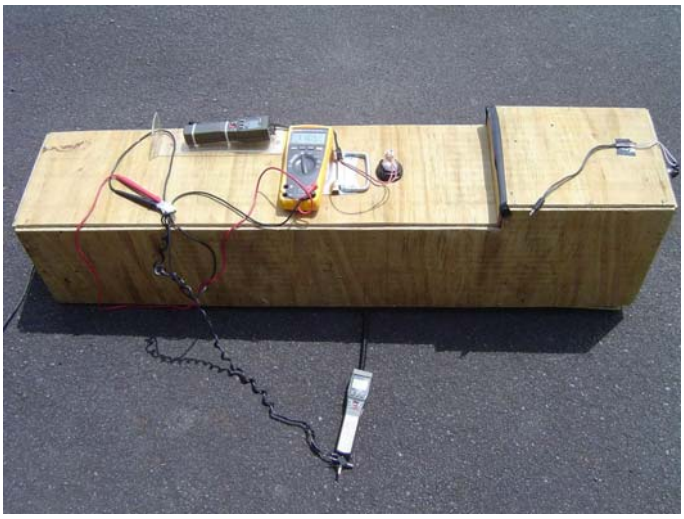

FIGURE 3.31 CIE BOX VALIDATION TEST

The testing results are (Table 9):

TABLE 9 TESTING RESULTS

E_{63^o} (lux)	E_{0^o} (lux)	E_{63^o}/E_{0^o}
1020	10620	0.09604
1010	10360	0.09749
1030	10370	0.09932
1020	10380	0.09926

Comparing to the calculated results 0.09357, the test results indicates the rules are closely followed. The difference was caused by minute instrument errors such as the light collimating tube alignment angle not being perfect, the imperfection of halogen lights, the fluctuation of power supply and reading errors. For a better result, calibration can be easily done by slightly adjusting the height of either light collimating tube. The higher the tube sits, the lower the E_H value gets.

The Luminous intensity assumption verification

Previously, we assumed two light sources have the same $I(c, \gamma)$. Referring to the definitions written in section 2.1, luminous intensity $I(c, \gamma)$ is a measure of visible power per solid angle, expressed in lumens per steradian. The 0º and 63º light sources in the CIE box used the same halogen lights and identical collimating tubes. It is supposed to have the same output power and confined output solid angle, in other words, the same luminous intensity.

To prove this is true, $I(c, \gamma)_{0^o}$ and $I(c, \gamma)_{63^o}$ need to be measured. Recall that luminous intensity is related to illuminance by the inverse square law, expressed as:

$$I = Ed^2$$

For a fixed distance *d*, luminance intensity *I* is proportional to illuminance *E*. Therefore we only need to measure the illuminance *E* provided by either of the two light sources from the same distance. Still using the same setup as Figure 3.31 except this time the two light collimating tubes were both measured at the 0º position of the CIE box. The testing results were 10450 lux and 11060 lux. The results were fairly close. It proved that the assumption stands, $I(c, \gamma)_{0^o}$ and $I(c, \gamma)_{63^o}$ have the same value.

The slight differences were caused by the manufacturing errors of the halogen lights and slight setup differences. This difference was not critical either, as it can be easily fixed by adding a resistor in series to regulate the current.

The viewing angle issue

The luminance meter installed in the CIE box actually measures the reflected light or road luminance from a viewing angle of 6° instead of the CIE recommended angle of 1°. This modification is due to practical difficulties. To achieve a viewing angle of 1° the luminance tube adapter has to be placed nearly parallel to the ground. For example assuming that the tube length is 100 mm, to get a 1° tilt the detector's end is only needed to be lifted 1.75 mm. This is very prone to error and difficult to guarantee. In the actual design the detector end is lifted 10 mm from the ground, which creates a 6° viewing angle.

The new question is how this difference in observation angle influences the measurement results. Luckily some valuable information was found in R. B. Gibbons' report *Influence of Pavement Reflection on Target Visibility*[12]. With the gonioreflectometer introduced in Section 2.2.5, R. B. Gibbons has done some research to find the relationship of how specularity S1 is affected by various observation angles α up to 60°. This is really an uncommon study since all the research found on the Internet only consider α less than 3°.

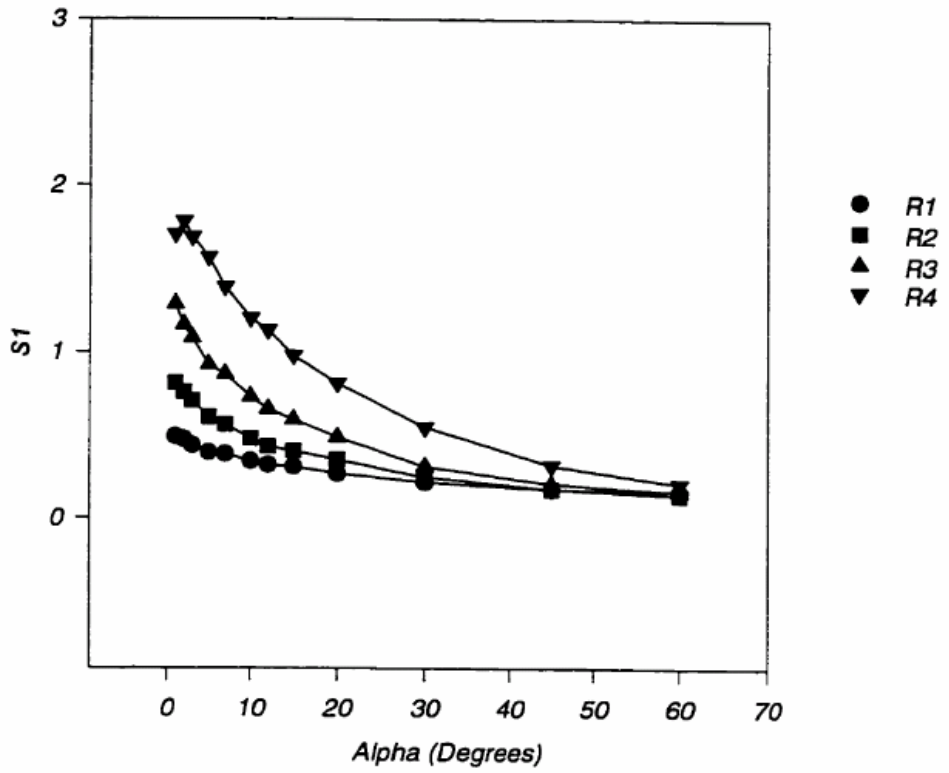

FIGURE 3.32 CHANGE IN S1 WITH OBSERVATION ANGLE α FOR ALL R-CLASSES [12]

Figure 3.32 was taken from Gibbons' thesis. The plot shows, the larger the observation angle α, the less the S1 value for all four R-classes roads. And also the S1 boundaries for each R-class becomes less distinguish and eventually merge together at 60°.

At CIE proposed $\alpha = 1°$, the R-classes can be uniquely separated by the S1 value. At 6°, the R-classes can still be clearly separated by S1. But at 20°, R1 and R2 classes are starting to have very close S1 values, which means that the road classification based on S1 is becoming ineffective. With the increment of α, the S1 values increasingly converge and at 60° all four classes of road will have the same S1 value.

The CIE box used an observation angle of 6°, which was proved to be feasible. But one thing should be taken notice, that for all four classes, the road classification criteria S1 values measured at 6° are smaller than the actual standard S1 values measured at 1°.

So a modified road classification criteria was created for the CIE box as shown in Table 10. From now on the S1 measured by the CIE box would use the new defined S1 values to classify the road surfaces into the appropriate class.

TABLE 10 REVISED ROAD CLASSIFICATION TABLE

Pavement Class	CIE box S1 Range (6º viewing angle)	Standard S1 Range (1º viewing angle)
R1	<0.33	< 0.42
R2	0.33 to 0.68	0.42 to 0.85
R3	0.68 to 0.95	0.85 to 1.35
R4	>0.95	> 1.35

As a conclusion, the CIE reflectance box has proven valid and feasible in the indoor experimental situation. It was confident to use it as a reliable tool to classify the road surfaces into appropriate standard R-tables.

4 Test Procedure and Results

Finally at this stage a tool was developed, which was verified and ready to do the road surfaces classification task with confidence. At the beginning of the road test, the CIE box was tested alone to assess its performance. Afterwards the CIE box and the OEL specular meter were tested together for the purpose of calibration. Then the road average luminance measurements were done.

4.1 System Setup

This section introduces the setup of the CIE box and OEL specular meter.

4.1.1 CIE Box Setup

FIGURE 4.1 CIE BOX UPRIGHT VIEW

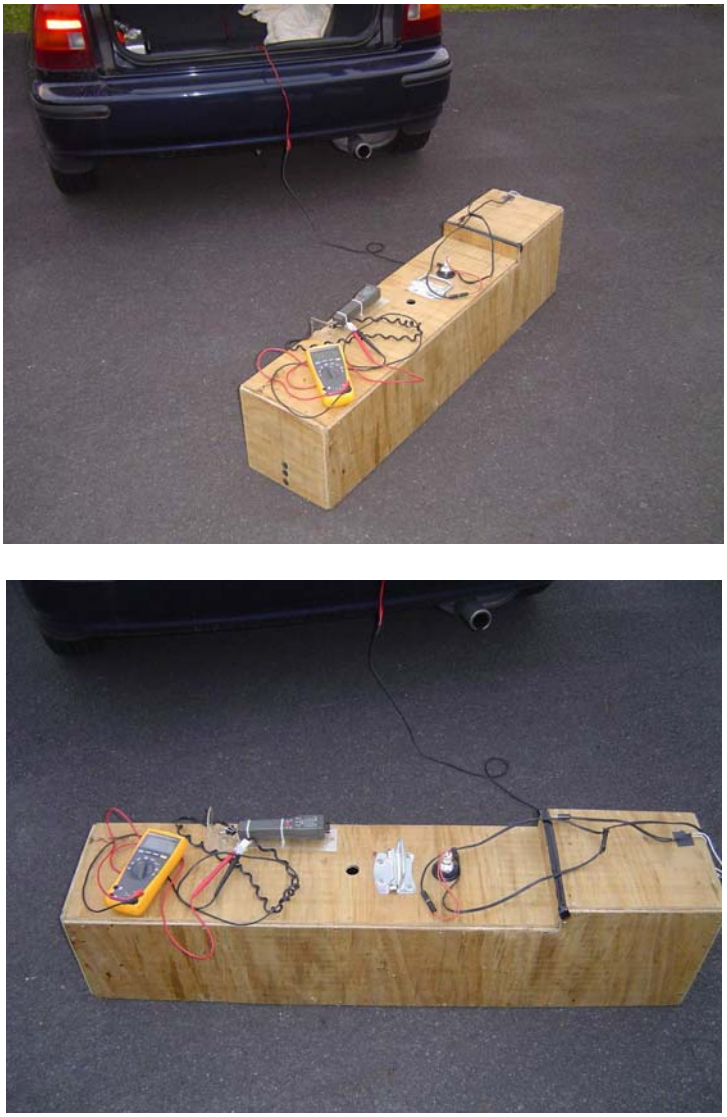

FIGURE 4.2 CIE BOX HORIZONTAL VIEW

Figure 4.2 is used to show how the test is done with the CIE road specularity measurement box. The bottom edges of the box have rubber seals glued to them so as to block the ambient light from affecting measurement results; this enables accurate daytime measurements.

The 0° and 63 ° light sources are 12V, 50W halogen bulbs. They are powered up through the cigarette port on the testing vehicle. The luxmeter converted luminance meter has an analogue output; the measured reading is output as a voltage that is linear to the measured illuminance value. At the lowest measurement scale, the conversion factor is 10 mV/lux. In the test, the analogue output is read with a multimeter since the luxmeter's LCD display refresh rate is much slower than the multimeter's.

The following equations explain how road classification can be done with CIE box:

$$L_p = \frac{I(c,\gamma)}{h^2} r(\beta,\gamma) \quad \Rightarrow \quad r(\beta,\gamma) = \frac{h^2}{I(c,\gamma)} L_p$$

$$S1 = \frac{r(\beta = 0°, \gamma = 63°)}{r(\beta = 0°, \gamma = 0°)}$$

where h is a constant value and $I(c, \gamma)/h^2$ are the same for both light sources as proved , we got:

$$S1 = \frac{L_{P63°}}{L_{P0°}}$$

$L_{P63°}$ and $L_{P0°}$ are the luminance readings for the 63° and 0° light source. In the real test the reading is in the unit of lux (since the luminance meter is basically a luxmeter), so to get the exactly luminance reading in the unit of cd/m² a conversion factor of 30.8 was needed to multiply to the lux reading as introduced in Appendix I.

Since S1 is a ratio of two luminance readings, the conversion factor used to calculate $L_{P63°}$ and $L_{P0°}$ will be cancelled out – we can directly take the ratio of the two luxmeter readings to get S1.

$$S1 = \frac{Lux_{P63°}}{Lux_{P0°}}$$

During the road test, the CIE box is placed stationary on the road surface. Firstly with only the 63° light source lit the meter reading is recorded. Then the light sources are swapped (only the 0° light is now lit) and this second meter reading is recorded. Based upon the two readings, the specularity parameter S1 for that sampling spot can be determined. Then the box is moved to a nearby spot to do the next measurement. For each sampling spot $Lux_{P63°}$ and $Lux_{P0°}$ are always measured as a pair.

4.1.2 OEL Specular Meter Setup

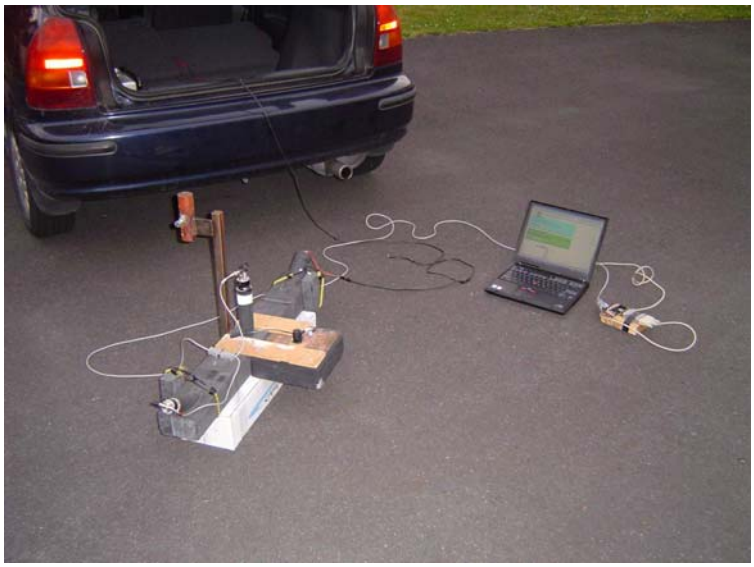

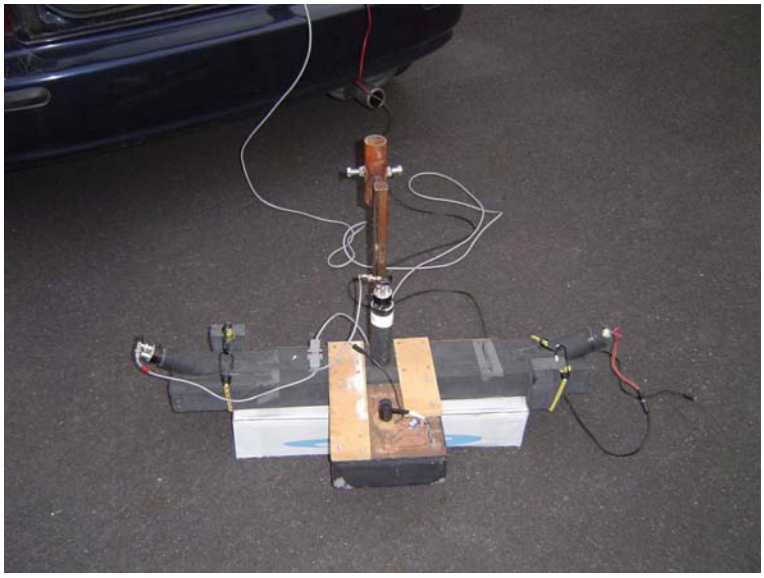

FIGURE 4.3 OEL PROTOTYPE SETUP

The OEL specular meter (Figure 4.3) was designed for night measuring only as there was no ambient light shield. To enable the daytime measurement a box was attached to the bottom of the prototype specular meter; and slots were created on the top of the box to allow measurements to be taken.

As introduced earlier, the OEL specular meter has one light source and two luminance meters. The light source is 12V, 50W halogen bulb, the same type as used by the CIE box, and powered up through the cigarette port on the vehicle. According to the Hill's report, the specularity S1' value was calculated as:

$$R(\beta = 0, \tan(\gamma)) = \frac{V_s}{V_P}$$

$$S1' = \frac{R(0,2)}{R(0,0)} \times S1_P$$

where, $R(\beta = 0, \tan(\gamma))$ is the reflectivity value measured under light source at angle γ, V_s is the detector voltage when measuring the sample surface, V_p is the voltage when measuring a perfect diffuser. V_p is the same for R(0,2) and R(0,0) and can be cancelled out when S1 is calculated. $S1_p$ is the S1 rating for the perfect diffuser and equals to 1. Therefore, S1' was calculated as**Error! Bookmark not defined.**:

$$S1' = \frac{V_s(63°)}{V_s(0°)}$$

It means that S1' is determined by taking the ratio of the 63° and 0° luminance meter output voltages.

During the static road test, the 63° light is turned on all the time, the readings for the 63° and 0° sensors are recorded at the same time for each testing spot. For the ease of measurements, a small computer program (refer to Appendix III) was written to assist with data collection. Since the output from the luminance meter is a voltage, which is proportional to the measured luminance, an ADC converter was used to convert this analogue signal into a digital signal before feeding them into a laptop. An Excel worksheet with a Macro records the measurements.

4.2 Road Specularity S1 Test

Approximately 40 roads within the Hamilton city limits were measured. For safety reasons tests were normally conducted on quiet residential roads and in car parks.

4.2.1 CIE Box Road Specularity S1 Measurement

In this part, the CIE box was tested alone for its feasibility. On each tested road a small section, normally of a couple of square meters in area, was randomly chosen for the investigation. This sampling method may however not give a true representative for the whole road, but this was still good enough to give some useful indication of the overall characteristics of the road. In Section 4.2.4 road surface reflectance consistency test was conducted to prove this.

During the measurement, the selected road section was measured in a random fashion, which means the sampling spots was taken in different positions and orientations. At each sampling spot, the 0° and 63° meter readings were recorded as a pair. About 30 pairs were taken on each section. A photograph of the road was also taken for reference. The raw data was later input into a Microsoft Excel worksheet. Below is an example of the raw data gathered.

Example

Angelsea St south end

3

0 degree	90degree	S1
206	416	0.495192
218	394	0.553299
220	380	0.578947
217	402	0.539801
207	397	0.521411
216	397	0.544081
210	400	0.525
205	372	0.551075
197	343	0.574344
233	410	0.568293
193	347	0.556196
203	353	0.575071
216	405	0.533333
210	397	0.528967
223	407	0.547912
225	417	0.539568
241	433	0.556582
216	392	0.55102
211	390	0.541026
203	389	0.521851
207	380	0.544737
210	397	0.528967

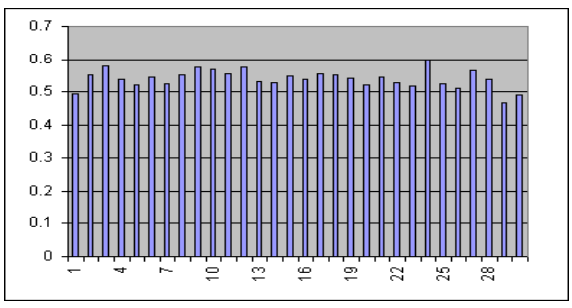

211	407	0.518428		
216	360	0.6		
203	387	0.524548		
183	357	0.512605		%
223	395	0.564557		
222	412	0.538835	0.539847	S1 avg
203	434	0.467742		
185	376	0.492021	0.027646	S1s.d
			5.1%	Covariance

Raw data was processed upon the completion of the road sampling. For each road, firstly the individual S1 value was calculated based on 0° and 63° reading pair, then the average and standard deviation ($S1_{avg}$ and $S1_{s.d}$) were calculated. The covariance (standard deviation to average ratio) was calculated based on $S1_{avg}$ and $S1_{s.d.}$ The bars plotted next to each road surface photo shows the S1 values for all measured spots on one selected road section. Those processed data give a fairly good indication to the specularity of each road.

A total of 42 roads were measured in the same manner as the above samples. Due to the number of measurements made for each road and the number of roads tested, only the processed results are listed in Table 11. All roads are sorted in ascending order based on S1 value (for a selected raw data listing, refer to Appendix V).

TABLE 11 CIE BOX ROAD MEASUREMENT RESULTS

Location	S1	Standard deviation	Covariance	Majority S1
Queens Ave	0.227	0.0492	21.7	(.16-.28)
Paterson St	0.244	0.0311	12.7	(.20-.28)
Liverpool Church	0.26	0.0323	12.6	(.22-.31)
Sillary St	0.268	0.041	15.3	(.21-.33)
Wiremu St	0.274	0.0234	8.6	(.27-.31)
Clarence St	0.29	0.0782	26.9	(.19-.39)
Garden Gate2 lot1	0.297	0.036	12.1	(.25-.37)
Onslow Ave	0.298	0.03	10.1	(.28-.34)
Pharmacy lot1	0.301	0.0269	8.9	(.27-.35)
Concrete	0.303	0.0374	12.3	(.25-.35)
Galway St	0.315	0.0616	19.5	(.23-.38)
Clinic	0.318	0.0645	20.3	(.28-.38)
Markrell	0.338	0.0314	9.3	(.30-.39)
French St	0.34	0.0315	9.3	(.29-.38)
Joffer St	0.343	0.0257	7.5	(.29-.37)
Wellington St	0.348	0.0611	17.6	(.26-.44)
Yard Front	0.352	0.0303	8.6	(.30-.38)
Brookfield Back	0.385	0.0613	15.8	(.34-.48)

Cliffton St	0.392	0.023	5.9	(.35-.42)
Upper Kent	0.413	0.0867	21	(.26-.52)
Yard	0.421	0.0302	7.2	(.38-.45)
Cook St	0.435	0.0729	16.7	(.32-.50)
Plunket	0.445	0.0568	12.8	(.36-52)
Blackburn	0.451	0.0748	16.6	(.36-.50)
PaknSave	0.471	0.0797	17	(.34-.56)
Blidisole	0.474	0.0688	14.5	(.38-.58)
Hamilton	0.488	0.07	14.3	(.36-.61)
Upper Clarence	0.489	0.0733	15	(.40-.58)
Clarence Pavement	0.498	0.0352	7.1	(.47-.54)
Garden Gate2 lot2	0.531	0.0426	8	(.46-.57)
New Carpark	0.531	0.0346	6.5	(.48-.57)
Anglesea Back	0.54	0.0276	5.6	(.52-.57)
Livepool	0.544	0.0321	5.9	(.49-.59)
Pharmacy lot1	0.548	0.0281	5.1	(.53-.59)
London St Back	0.55	0.0376	6.8	(.53-59)
Fox St	0.607	0.0449	7.4	(.58-.68)
Farton St	0.618	0.1552	19.8	(.46-.75)
Ramsay St	0.627	0.129	20.6	(.44-.75)
Power House	0.628	0.051	8.1	(.58-.68)
Naylor St	0.729	0.148	20.3	(.44-.90)
Firth St	0.852	0.1199	14.1	(.74-.95)
Fox St South	4.87	0.72	14.3	(4.18-4.95)

The standard deviation $S1_{s.d}$ was used as the uncertainty for each road:

$$S1 = S1_{avg} \pm S1_{s.d}$$

In Figure 4.4, $S1_{s.d}$ was plotted as error bar for each of the 42 $S1_{avg}$ values:

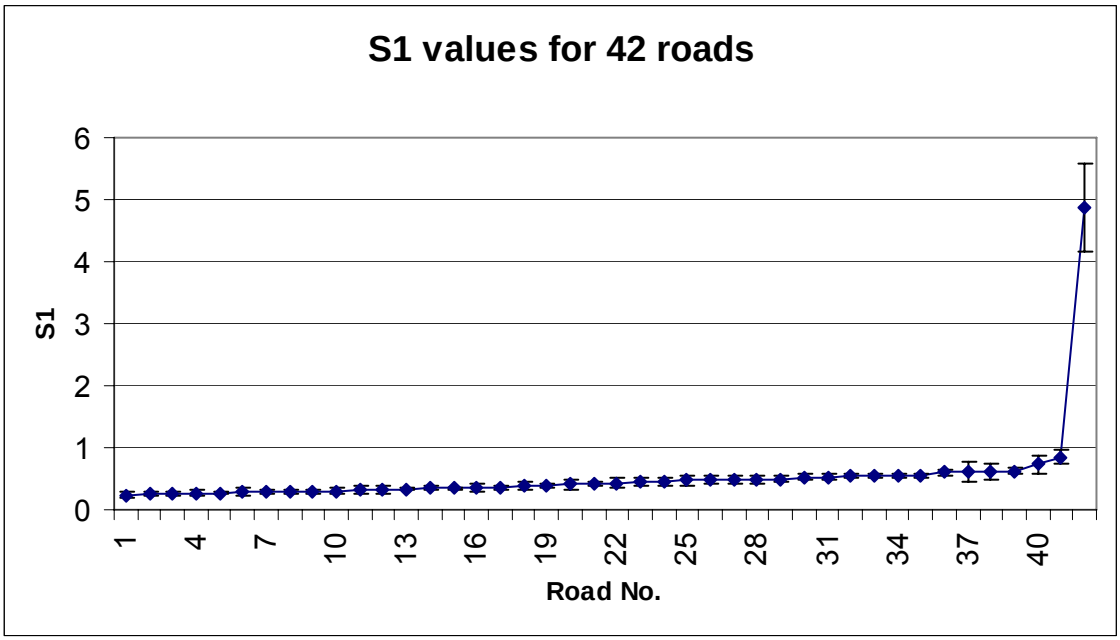

FIGURE 4.4 S1 VALUES FOR 42 ROADS

Since the first 41 roads have the $S1_{s.d}$ values less than 1, for a clear view, only the first 41 roads are plotted in Figure 4.5.

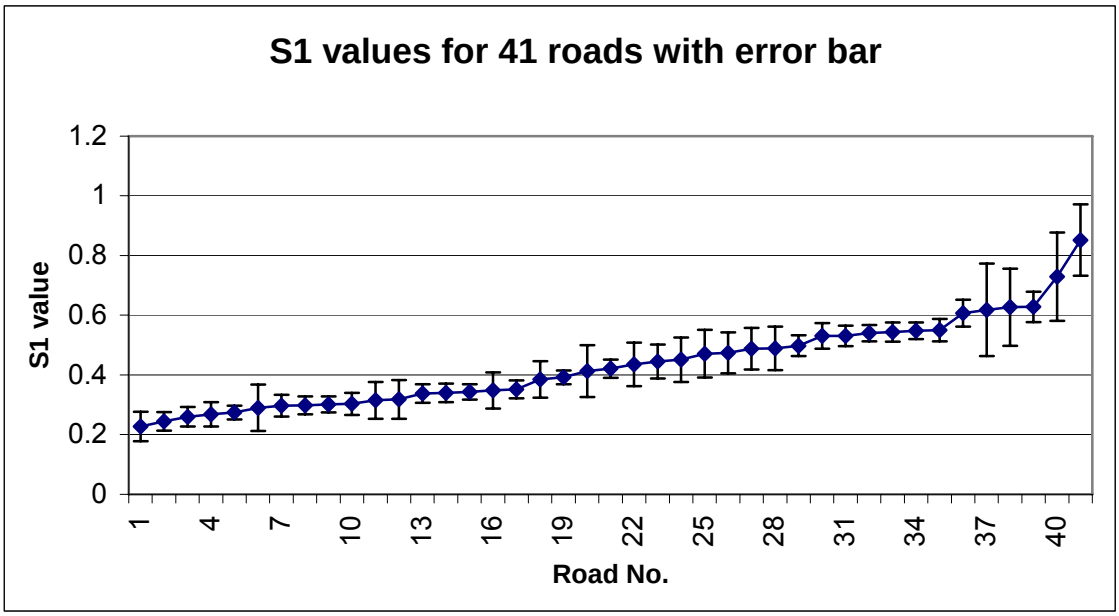

FIGURE 4.5 S1 VALUES FOR 41 ROADS WITH ERROR BAR

The plots show that nearly all roads tested have $S1_{avg}$ values range from 0.22 to 0.85 and have covariance values from 5% to 27%. In the results there is only one road section that has a much large $S1_{avg}$ value at 4.87, which does not mean a high $S1_{avg}$ road rarely exists. That high $S1_{avg}$ value was measured at the south section of the Fox St, the measurement was taken in the vehicle-driving lane. Figure 4.6 shows this section of the road.

FIGURE 4.6 FOX STREET VEHICLE DRIVING LANE

Actually such tracks commonly exist on many worn road surfaces. During night driving, they can be easily spotted due to its shiny appearance. Those tracks normally exist on the vehicle-driving path; and it is too dangerous to take more measurements from other roads with such features.

From the experience gained during road measurement, a relatively smooth and uniform looking road surface generally has quite consistent S1 values, which results in a low $S1_{s.d}$ value. In contrast, an old, rough or dirty looking road normally has a large $S1_{s.d}$ values.

Based on the calculated $S1_{avg}$ values, 42 roads can now be categorised into the corresponding R- class. As mentioned, the viewing angle for the CIE box is not the default 1°. So the modified classification criteria (Table 9) introduce in Section 3.3.2.1 is used. The classification results (
Table 12) are displayed in a histogram shown below (Figure 4.7).

TABLE 12 CLASSIFICATION RESULTS

S1 range	*Frequency*
< 0.33	8
0.33 - 0.68	28
0.68 - 0.95	5
More	1

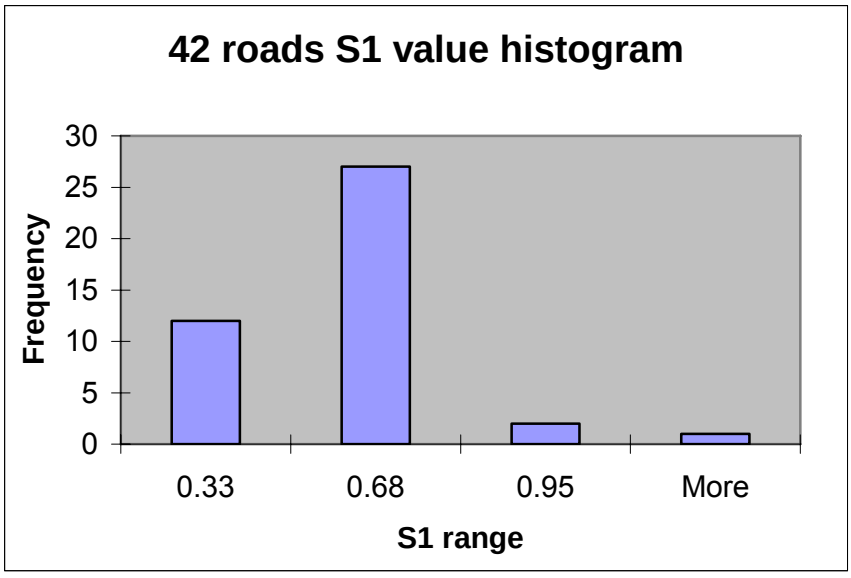

FIGURE 4.7 ROAD CLASSIFICATION HISTOGRAM

The histogram shows that 12 roads belong to R1 class, 28 roads to R2 and 5 roads to R3 and 1 road to R4. It means all four classes of road exist in New Zealand. From the sampled results, it can be seen that the majority of the roads measured are in R1 and R2 classes.

4.2.2 CIE Box Repeatability

Similar road tests were conducted to testify the CIE box's repeatability. These road tests were carried out at a different time from when the original test on that road was done. The processed results are listed in Table 13 and plotted in Figure 4.8.

TABLE 13 CIE BOX REPEATABILITY RESULTS

Test1	Test2	Delta	Location
0.232	0.227	0.005	Queens Ave
0.3494	0.274	0.0754	Wiremu St
0.2777	0.29	-0.0123	Clarence St
0.3521	0.298	0.0541	Onslow St
0.2943	0.301	-0.0067	Pharmacy lot 1
0.4065	0.315	0.0915	Galway Ave
0.336	0.34	-0.004	French St
0.356	0.343	0.013	Joffre St
0.3846	0.348	0.0366	Wellington St
0.4223	0.35	0.0723	House yard front
0.3717	0.385	-0.0133	Brookfield St
0.3992	0.413	-0.0138	Upper Kent St
0.3873	0.42	-0.0327	House Yard back
0.45	0.435	0.015	Cook St
0.4916	0.445	0.0466	Plunket Tce
0.5107	0.471	0.0397	Paksave carpark
0.4018	0.474	-0.0722	BledisloeTce
0.5165	0.498	0.0185	Clarence St pavement
0.508	0.54	-0.032	Anglesea St south end
0.481	0.548	-0.067	Pharmacy lot 2
0.5143	0.607	-0.0927	Fox St
0.603	0.626	-0.023	New carpark
0.6505	0.628	0.0225	Power house
0.7436	0.729	0.0146	Naylor St

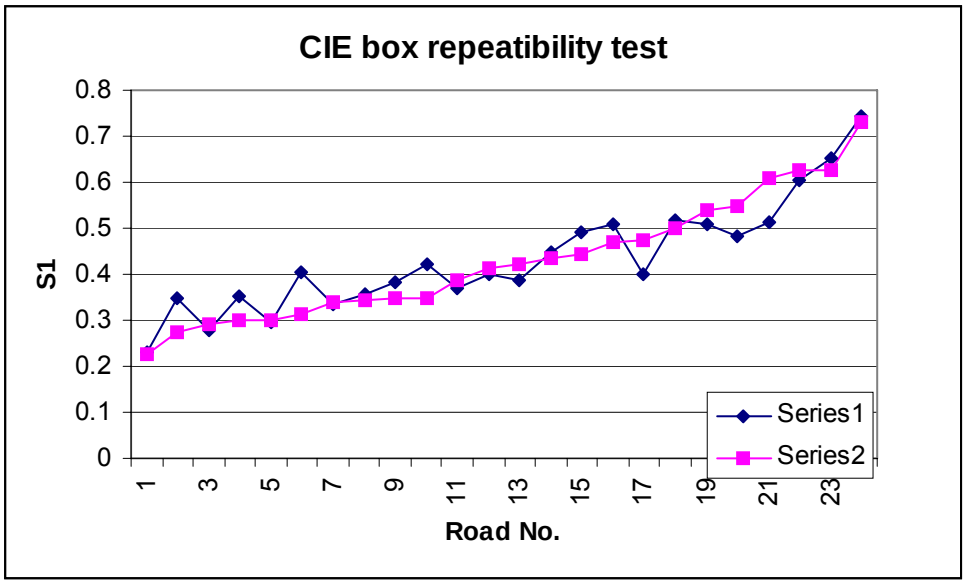

FIGURE 4.8 CIE BOX REPEATABILITY TEST

From the plot, it can be seen that the two separate tests agree to each other very well, overall the series 1 follows the same trend as series 2. The correlation factor between the two tests in Table 13 is 0.936. There is some relatively large variation between some of the measurement results, which were mainly due to the difference in choosing sampling spots. Overall the specularity measured on the two different occasions for each road was quite consistency. It is now certain that the CIE box performs satisfactorily in the repeatability test.

4.2.3 OEL Specular Meter and CIE Box Correlation Test

In order to investigate the correlation between the two specular meters, the OEL specular meter and CIE box were brought together in the testing routine. For a fair comparison, the measurements were conducted on the same selected road section for both units. Within the selected section both the CIE box and the OEL prototype randomly takes sets of measurements. The collected raw data for both units were processed the same way as it has been done to the CIE box detailed in the previous section. The $S1_{avg}$ and $S1_{s.d}$ were calculated for each device respectively.

The processed results are listed in Table 14.

TABLE 14 CIE AND OEL SPECULARITY METER CORRELATION TEST

Road No.	Location	CIE		OEL	
		S1	S1s.d	S1'	S1's.d
1	Queens Ave	0.227	0.0492	1.16	0.13
2	Sillary St	0.268	0.041	1.38	0.19
3	Wiremu St	0.274	0.0234	1.58	0.262
4	Clarence St	0.29	0.0782	1.237	0.222
5	Onslow St	0.298	0.03	1.348	0.05
6	Pharmacy lot 1	0.301	0.0269	1.59	0.061
7	Galway Ave	0.315	0.0616	1.423	0.197
8	French St	0.34	0.0315	1.545	0.21
9	Joffer St	0.343	0.0257	1.852	0.077
10	Wellington St	0.348	0.0611	1.516	0.296
11	House Yard Front	0.352	0.0303	1.47	0.0783
12	Brookfield St west end	0.385	0.0613	1.838	0.205
13	Upper Kent St	0.413	0.0867	1.581	0.192
14	House Yard Back	0.421	0.0302	1.328	0.227
15	Cook St	0.435	0.0729	1.476	0.169
16	Plunket Tce	0.445	0.0568	2.166	0.202
17	Fox St	0.446	0.07	1.56	0.2
18	PaknSave carpark	0.471	0.0797	1.524	0.192
19	Bledisloe Tce	0.474	0.0688	2.217	0.32
20	Riro St	0.477	0.036	1.78	0.17
21	Nixon St	0.487	0.116	1.65	0.143
22	Clarence St Pavement	0.498	0.0352	1.6	0.089
23	Opia Rd	0.503	0.055	1.92	0.162
24	New Carpark	0.531	0.0346	2.21	0.132
25	Anglesea St south end	0.54	0.0276	1.85	0.117
26	Pharmacy lot 2	0.548	0.0281	2.133	0.23
27	Fox St	0.607	0.0449	1.53	0.1
28	Powerhouse carpark	0.628	0.051	2.65	0.111
29	Wilson St	0.648	0.11	2.28	0.237
30	Naylor St	0.729	0.148	3.127	0.405
31	Fox St south	4.87	0.72	16.37	3.63

The S1 and S1' values measured by the CIE box and OEL specular meter were plotted on the same graph (Figure 4.9), where standard deviation $S1_{s.d}$ and $S1'_{s.d}$ are used as horizontal and vertical error bars.

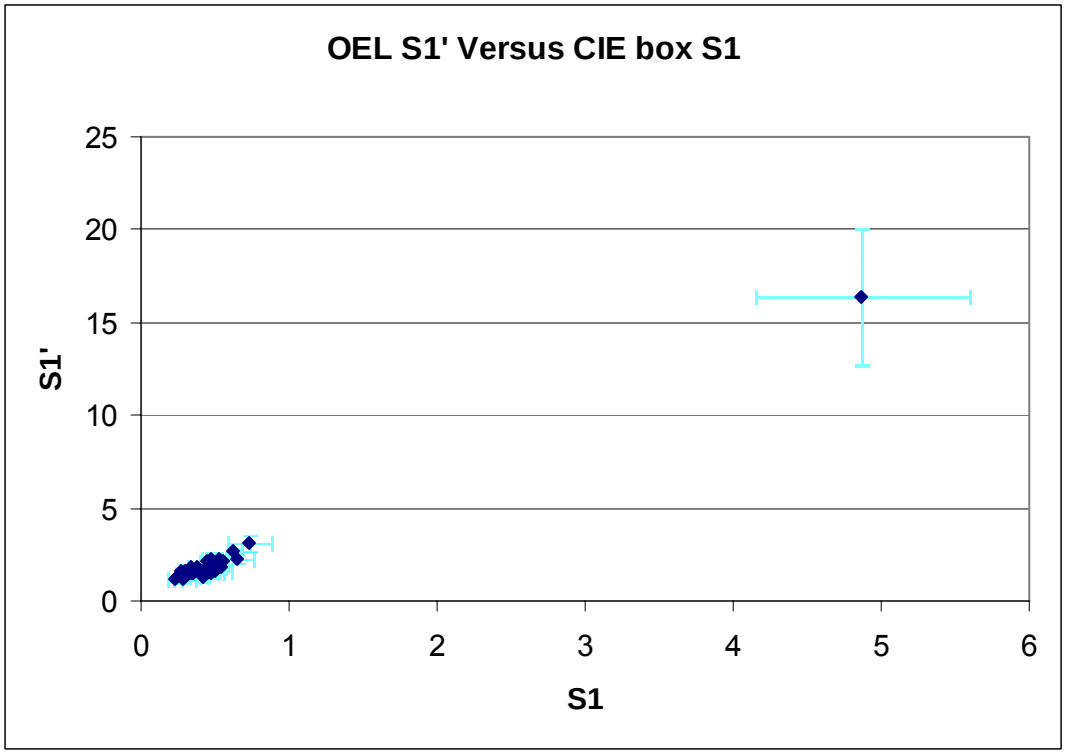

FIGURE 4.9 OEL SPECULAR METER VS CIE BOX

For a clearer view, the values measured for the Fox St south section is omitted in the next plot (Figure 4.10).

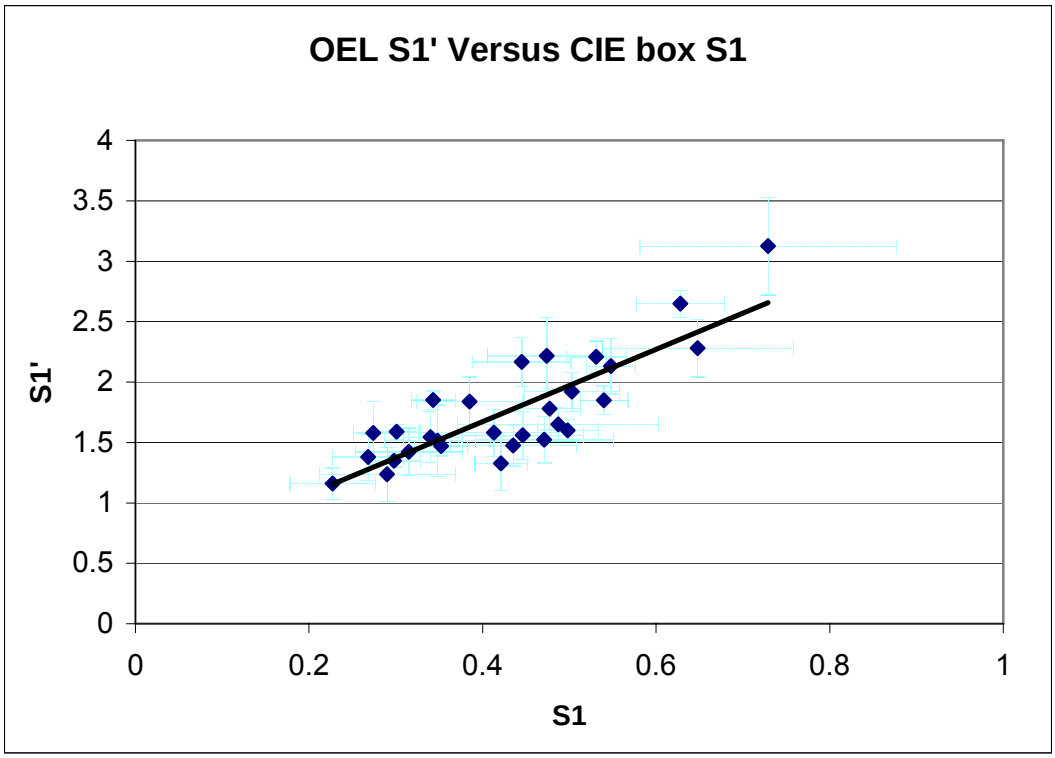

FIGURE 4.10 OEL SPECULAR METER VS CIE BOX WITH FOX STREET OMITTED

From Figure 4.10 it can be seen that there is certain correlation between those two sets of measurements. For both units high specular surfaces result in large S1 values, and low specular (more diffuse) surfaces result in low S1 values. Obviously the relationship between them is not linear, but the OEL unit proved to give some good indication about the road specularity properties. Based on the measured data, a correlation factor of 0.833 was found between the S1' and S1 values.

A road classification criteria table (Table 15) for the OEL meter was created based on the experimental results, which is just an approximation since clear classification boundaries are hard to draw.

TABLE 15 REVISED ROAD CLASSIFICATION TABLE FOR OEL SPECULAR METER

Pavement Class	CIE box S1 Range	OEL meter S1' Range
R1	<0.33	< 1.6
R2	>0.33 but <0.68	1.2 to 2.7
R3	>0.68 but <0.95	2.7 to 6
R4	>0.95	> 6

4.2.4 Road Specularity Consistency Test

Later road specularity consistency tests were carried out on three roads with OEL prototype and CIE box. On each road, 3 or 4 sections were tested, usually being a few hundred meters apart. The measurement procedure was the same as described in the previous section. This test will show if a few selected sections on a road can be a representative of the whole road. The results are shown in Table 16.

TABLE 16 ROAD CONSISTENCY TEST

	CIE			OEL	
	S1	S1sd		S1	S1sd
Clarence St 1	0.327	0.046		1.503	0.129
2	0.292	0.047		1.556	0.204
3	0.332	0.043		1.538	0.197
Albert St 1	0.467	0.075		1.311	0.112
2	0.482	0.044		1.353	0.134
3	0.529	0.079		1.373	0.156
4	0.497	0.067		1.37	0.136
Wellington St 1	0.324	0.055		1.788	0.273
2	0.295	0.033		1.687	0.133
3	0.346	0.02		1.938	0.328
4	0.371	0.036		1.764	0.55

The reason for choosing those roads was because they respectively have a consistent appearance, which means they have the same physical structure and condition. From the above results, it can be seen for an overall consistent road, the measurement results were very close. It proved that a small sampling section could give some useful information of the whole road.

4.3 Average Luminance Q_0 Measurement

The measurement for the road average luminance or brightness was done separately. During the measurements, the Grey Card was used as the reference for the road average luminance calculation. Right before starting to measure the road surface, the Q_0 meter readings for both sides of the grey card were recorded. Recall that in the Section 3.2.1 the experiment was done to validate the Q_0 meter. There is approximately 5 times difference in the Q_0 meter reading for the white side and grey side; they have a reflection of 90% and 18%. So for a given road, we only need to measure the Q_0 reading and then comparing with either the grey card or the white card to get its relative reflection. For example, if a Grey Card reading is 300 and the road surface reading is 100 this means that the road has one third of the Grey Card reflection, so road reflectivity is 6%.

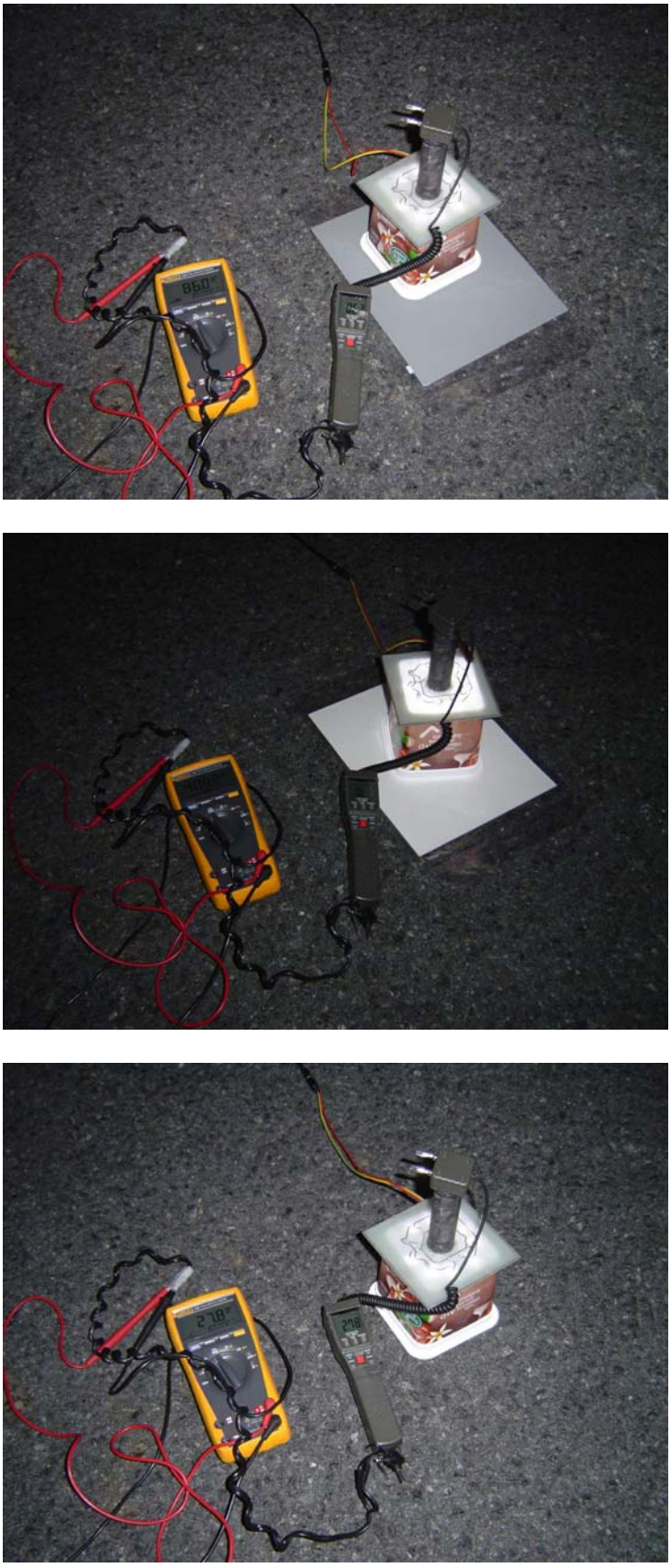

FIGURE 4.11 Q0 METER TESTING PROCEDURE

40 roads were measured for their overall luminance value, with only a small section of each road being investigated. One dozen readings were taken for each section; the processed results are shown below in Table 17.

TABLE 17 Q METER MEASURING RESULTS

Road No.	Location	Q0 (%)	Q0s.d
1	Naylor St	3.11	0.417
2	Upper Kent St	3.57	0.257
3	Brookfield St west endk	3.61	0.274
4	Wellington St	4.17	0.06
5	Blackburn	4.37	0.154
6	Hamilton	4.39	0.174
7	Clarence St Pavement	4.47	0.12
8	French St	4.49	0.141
9	Firth St	4.54	0.122
10	Fox St	4.68	0.16
11	Ramsay St	4.76	0.27
12	Plunket Tce	4.81	0.145
13	Cook St	4.91	0.234
14	Onslow St	4.96	0.218
15	Markrell carpark	5.02	0.169
16	Sillary St	5.03	0.097
17	Galway St	5.06	0.496
18	Liverpool St	5.12	0.182
19	Upper Clarence	5.23	0.21
20	Gardens Gate2 lot2	5.23	0.184
21	PaknSave Carpark	5.29	0.178
22	Bledisloe Tce	5.29	0.063
23	Anglesea Back	5.35	0.38
24	Clarence St	5.37	0.175
25	House Yard	5.45	0.996
26	Pharmacy Lot 2	5.63	0.088
27	Queens Ave	5.64	0.226
28	New Carpark	5.76	0.216
29	Paterson St	5.77	0.227
30	Yard Front	5.78	0.356
31	Joffre St	6	0.286
32	Power house carpark	6.07	0.085
33	Liverpool Church	6.11	0.197
34	London St Back	6.12	0.143
35	Clinic	6.21	0.321
36	Gardens Gate2 lot1	6.32	0.236
37	Clifton Rd	6.35	0.111
38	Wiremu St	6.77	0.093
39	Pharmacy Lot 1	7.01	0.084
40	Concrete	23.6	3.7

Two roads have been shaded in the list; the reason for this is that they have a quite high standard deviation for Q_0 values. This is caused by the uneven colour distribution on the road surface. From the photo (Figure 4.12) it can be seen the Yard has some whiter patches and Naylor Street has uneven tar stains. Those factors affected the measurement results as expected.

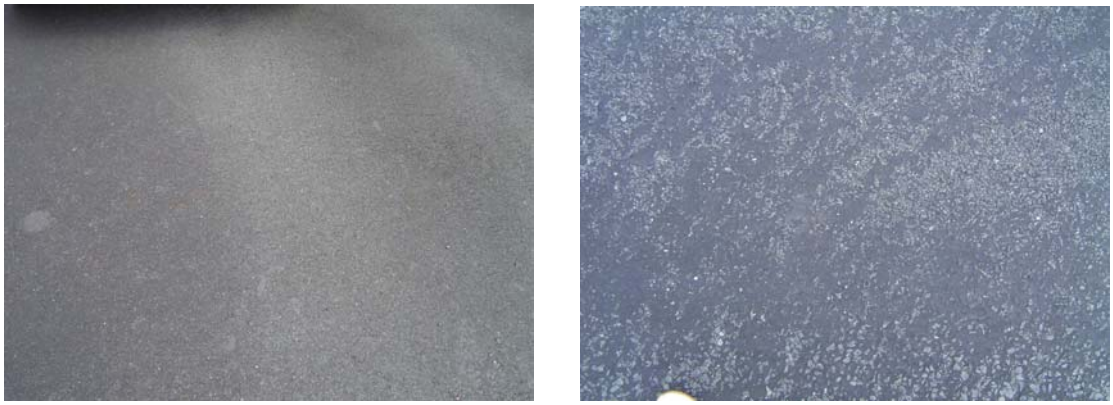

FIGURE 4.12 HOME YARD AND NAYLOR STREET

Based on the results in Table 17, the average luminance with the error bar is plotted in **Error! Reference source not found.**

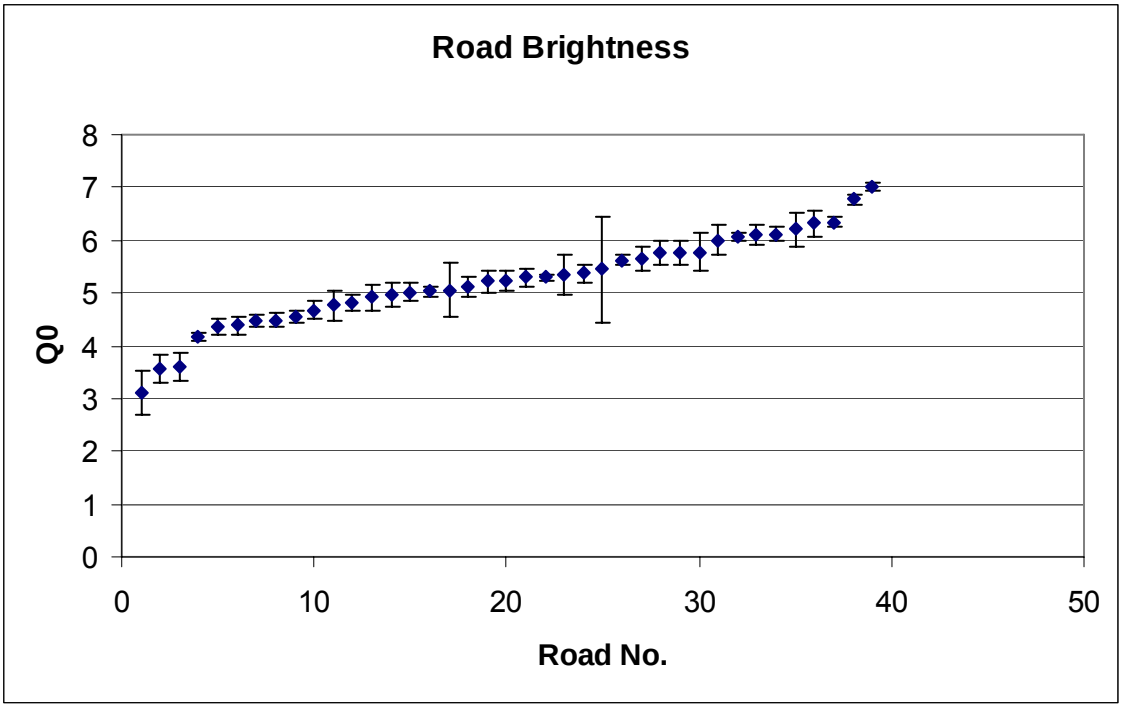

FIGURE 4.13 Q0 METER MEASUREMENTS RESULTS PLOT

The measured Q_0 values range from 3% to 7% and the majorities lie between 4% and 6%, which is slightly lower than the CIE standard road surfaces (7% -10%, see Table 3). In other words, the roads measured appear darker than the standard roads. .

4.4 Parameter S2 Analysis

Once parameter S1 and Q_0 were determined, the parameter S2 can be calculated. From the definition:

$$S2 = \frac{Q_0}{R(0,0)}$$

Q_0 can be measured. The r(0,0) can be calculated from the raw data measured in the road specularity test. Recall that:

$$L_p = q(\beta,\gamma)E_p$$

$$r(\beta,\gamma) = q(\beta,\gamma)\cos^3(\gamma)$$

when $\beta = 0$ and $\gamma=0$,

$$r(0,0) = q(0,0)$$

$$L_p = r(0,0)E_p$$

$$L_p = E_p \frac{r(\beta,\gamma)}{\cos^3(\gamma)}$$

where E_p is the illuminance measured at the sampling spot for 0° incident light source, which was experimentally measured in section 4.2, about 10000 lux.

Therefore,

$$r(0,0) = \frac{L_p}{10000}$$

L_p can be determined from the CIE box measurement results, as explained in Section 2.2.2 L_p is calculated by multiplying the luxmeter-converted luminance meter reading

(in the unit of lux) by the conversion factor 30.8 to get the actual luminance reading (in the unit of cd/m²). With the above knowledge, r(0,0) can be calculated.

Using Anglesea St back section as an example, referring to the specularity measurement example in Section 4.2.1. The average reading from the luxmeter-converted luminance meter with a 0° incident light source is 3.91 lux, and when multiplied by 30.8, we get the average L_p value 120 cd/m². r(0,0) was calculated as 0.012. Looking up the Q_0 table in Section 4.3, Q_0 is 5.35%.

$$S2 = \frac{Q_o}{r(0,0)} = \frac{5.35}{0.012} = 4.16$$

There is one factor has to be considered, since the formulas used here are for a standard CIE road luminance measurement configuration, that is for a 1° observation angle. The r(0,0) calculated above was measured at an α = 6° observation angle. This does cause a difference between the true value and the one calculated as the q reflection coefficient is affected by the change of the observation angle α as proven by R. B. Gibbons.

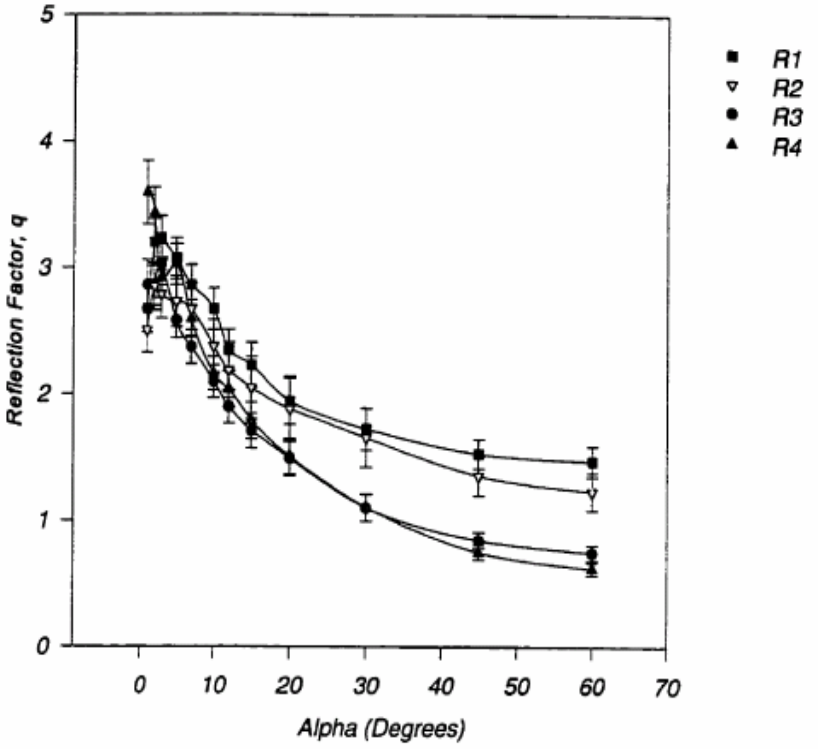

FIGURE 4.14 INFLUENCE OF ALPHA FOR ALL R CLASSES [12]

Figure 4.14 shows, the reflection coefficient q is reduced as the observation angle α increases. Therefore the measured reflectance coefficient q provided by the CIE box should be lower than the actual q value – in another words the r(0,0) value measured is lower than the actual r(0,0). By observing the graph, a correction factor of 1.4 is used, which means

$$r(0,0)_{actual} = 1.4 \times r(0,0)_{measured}$$

The adjusted S2 value for Anglesea St is

$$S2 = \frac{4.16}{1.4} = 2.97$$

The same calculation procedure was used on the measured S2 figure for all (Table 18).

TABLE 18 S2 VALUES

Road number	Location	Q_0%	r(0,0)	r(0,0) adjusted	S2
	Yard	5.45	0.0103796	0.01453144	3.750488596
	Anglesea Back	5.35	0.0120428	0.01685992	3.173206041
	Cook St	4.91	0.0102872	0.01440208	3.409229778
	Fox St	4.68	0.0110572	0.01548008	3.02324019
	Wellington St	4.17	0.0113652	0.01591128	2.620782238
	Firth St	4.54	0.0093632	0.01310848	3.463406894
	Clarence St	5.37	0.0097636	0.01366904	3.92858606
	Clarence Pavement	4.47	0.01078	0.015092	2.961834084
	Pharmacy Lot 1	7.01	0.0152768	0.02138752	3.277612365
	Pharmacy Lot 2	5.63	0.01232	0.017248	3.264146568
	PaknSave	5.29	0.0100716	0.01410024	3.751709191
	Powerhouse Carpark	6.07	0.0142604	0.01996456	3.040387567
	Queens Ave	5.64	0.0093016	0.01302224	4.331052108
	Upper Kent	3.57	0.0074844	0.01047816	3.40708674
	Joffer St	6	0.0158004	0.02212056	2.712408727
	French St	4.49	0.006776	0.0094864	4.733091584
	Ramsay St	4.76	0.0101024	0.01414336	3.365536902
	Blackburn ??	4.37	0.0079464	0.01112496	3.928104011
	Paterson St	5.77	0.0116424	0.01629936	3.540016295
	Plunket St	4.81	0.010164	0.0142296	3.380277731
	Galway St	5.06	0.008778	0.0122892	4.117436448
	Bledisloe St	5.29	0.0100408	0.01405712	3.763217501
	Onslow Ave	4.96	0.0088088	0.01233232	4.021952074
	Sillary St	5.03	0.0097328	0.01362592	3.691493859
	Naylor St	3.11	0.0078848	0.01103872	2.817355635
	Wiremu St	6.77	0.0155848	0.02181872	3.10284013
	Brookfield Back	3.61	0.00924	0.012936	2.790661719
	Liverpool St	5.12	0.010164	0.0142296	3.598133468
	Liverpool Church	6.11	0.0108724	0.01522136	4.014095981
	Markrell ??	5.02	0.0089628	0.01254792	4.000663058
	Cliffton St	6.35	0.0130592	0.01828288	3.473194595
	Hamilton	4.39	0.0094556	0.01323784	3.31625099
	London St Back	6.12	0.012166	0.0170324	3.593151875
	New Carpark	5.76	0.0107492	0.01504888	3.827527364
	Clinic		0.0163548	0.02289672	0
	Concret		0.043582	0.0610148	0
	Yard Front		0.01001	0.014014	0
	Garden Gate 2 Lot 1		0.0114576	0.01604064	0
	Garden Gate 2 Lot 2		0.0126896	0.01776544	0

5 Conclusion

5.1 Fulfilment of Project

This research originated with the objective of further developing the OEL high-speed pavement reflectivity measurement system prototype, and to calibrate the system for commercial usage. After studying the original prototype some improvement was done to the road brightness measurement system Q_0 meter and better accuracy was achieved. It was also realised the previous specular meter was not designed according to the CIE standard. So before doing any further development and calibration, this meter's feasibility had to be investigated. There are two ways the prototype feasibility can be tested; either by testing a series of roads with known r-values, or calibrating against a reliable pavement reflection measurement system. Unfortunately the first choice was not accessible due to lack of information of existing road reflection properties.

Research has switched to find and build a device which is relatively simple to build, and can produce standard measurement results which can be used under CIE road classification criteria. However this effort proved not so successful. Eventually a pavement specularity measurement system 'CIE box' was developed and verified.

Measurements of the reflective properties of various roads were conducted with the 'CIE box' and the improved Q_0 meter (based on the same principle as the Q_0 meter of OEL prototype) in the Hamilton area. The results were very satisfactory. Later the OEL prototype was calibrated against the 'CIE box' to test its feasibility. Certain correlation was found between those two specular meters and an approximate road classification criteria based on specularity for the OEL specular meter was defined.

5.2 Further Development

Despite the 'CIE box' being verified to conform to the CIE standard and to give reliable results in road measurement, there is still a lot work that can be done to the system. The data sampling process of the CIE box is manual, which is a trivial but time consuming task, so this process could be automated by applying a circuitry to automatically pilot

the light sources and take measurements when the system is placed on the sampling road. Process control and data logging could be done through a laptop or PDA device, so the operator only needs to move the device to enable data to be sampled automatically.

Another issue is device mobility. The OEL prototype was designed for dynamic measurement purpose, but the system designed in this project is only capable of measuring static situations, which seems to a backward step in terms of usefulness. But due to the lack of a standard tool (or road surface real reflectivity properties) to testify for the OEL high-speed reflection measurement system's feasibility, this basic procedure is inevitable. The immobility of the new system could be solved if R-classes still can be distinguished at a large observation angle. Refer to Figure 3.32 in section 3.3.2.1, and it shows the S1 boundaries for the four R-classes can still be distinguished at an observation angle of 10º. If this is proved true, the system (similar to 'CIE box') can be designed with a 10º observation angle as shown in Figure 5.1. The luminance meter is only needed to be installed 56.6 cm away from the sample spot to achieve a 10 cm clearance above the road surface. This clearance would enable mobility of the system and also keep the system physically compact at less than 1 metre long, which is much more practically applicable compared to a system of at least 573 cm of length that encompasses a 1º observation angle (see Figure 3.5).

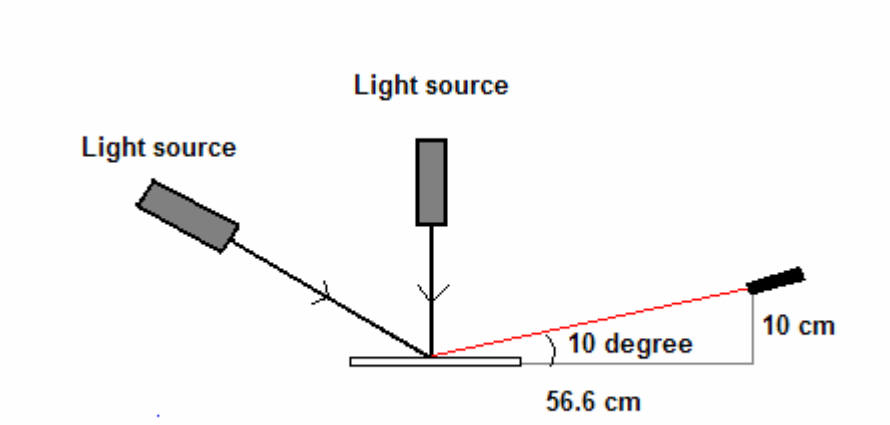

FIGURE 5.1 SPECULAR METER WITH 10º OBSERVATION ANGLE

Due the limitation of the time allocated to this project the above proposal cannot be done.

5.3 Summary

In this project an improved Q_0 meter was designed. This Q_0 meter proved to have better measurement accuracy. The measurement results from the new Q_0 meter shows that road surface brightness mostly lies between 4% and 6%. This is slightly lower than the CIE standard road surface brightness. In other words, the roads measured appear darker than CIE standard road surfaces.

A road specularity measurement meter was designed. Its feasibility was verified both in experimental and on-site situations, and it proved effective and fairly accurate. It can be used alone to classify a road surface according to its specularity base on the CIE road classification standard. The measurement results from this new meter shows that most of the tested roads are within the R1 and R2 classes. There is also large number of R4 class roads, but they normally only exist on a portion of a road, mostly being in the driving lane.

For both the Q_0 meter and the specular meter, significant fluctuation of measurements can occur on a given road surface. This is due to an uneven appearance of the same road.

Appendix I Luminance Meter

A luxmeter can be converted into a luminance meter by attaching a luminance tubeadapter at the luxmeter's photodector as shown in Figure 1. The tube is used to limit the field of view of the luxmeter meter. The conversion principle is introduced below.

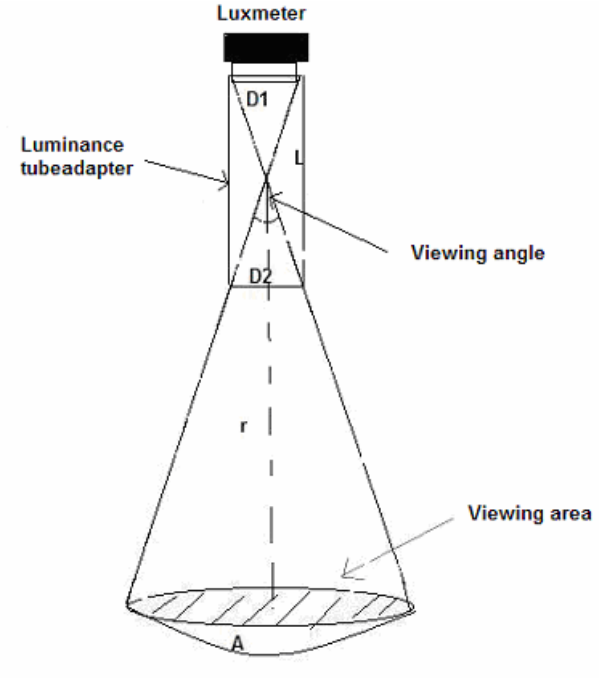

FIGURE 1 LUMINANCE METER WORKING PRINCIPLE

The viewing angle α of this converted luminance meter is decided by the length L of the adapter tube, the photodetector diameter D_1 and luminance tube adapter inner diameter D_2 through the following formula.

$$\tan(\frac{\alpha}{2}) = \frac{\frac{D_1}{2}}{\frac{D_1 L}{D_1 + D_2}}$$

cancel out D_1

$$\tan(\frac{\alpha}{2}) = \frac{D_1 + D_2}{2L}$$

where D_1 = 10 mm, D_2 = 22 mm and L = 110 mm. Substituted into the formula, we get α = 16.5°. With this angle, we can work out the solid angle it corresponds.

As mentioned in section 2.1.5

$$\Omega = \frac{A}{r^2}$$

where,

$$A = 2\pi r^2 (1 - \cos(\frac{\alpha}{2}))$$

where A is the spherical surface area, r is the distance from the sample to the intersection point in the luminance tube. Cancel out r^2, we get,

$$\Omega = 2\pi \bullet 0.01035$$

It can be seen the solid angle for this luminance meter is a constant, which is independent on the distance between the luminance meter and the sample. Imaging there is a flat perfect diffuse surface illuminated by 1 lux light. The light will be 100% reflected evenly in a 2π steradians hemisphere (recall a sphere contains 4π steradians). The luminance meter designed has a perception solid angle Ω =2π*0.01035. Therefore the proportion of the light detected by the luminance meter can be calculated.

$$Ratio = \frac{\Omega}{2\pi} = 0.01035$$

The reading on the modified luxmeter would be 0.01035 lux. And we know a perfect diffuser with 100% reflectance and 1 lux of light falling upon it; it will emit 1/ π cd/m². Therefore the conversion factor is:

$$CF = \frac{\frac{1}{\pi}}{0.01035} = 30.8$$

In another word, for a 1 lux reading on the luxmeter converted luminance meter, it actually measures a luminance of 30.8 cd/m².

It is noteworthy that all luminance meters used throughout this project were made based on this principle.

Appendix II Circuitry Design

Figure 1 and Figure 2 are the schematic and PCB diagrams for the new Q_0 meter.

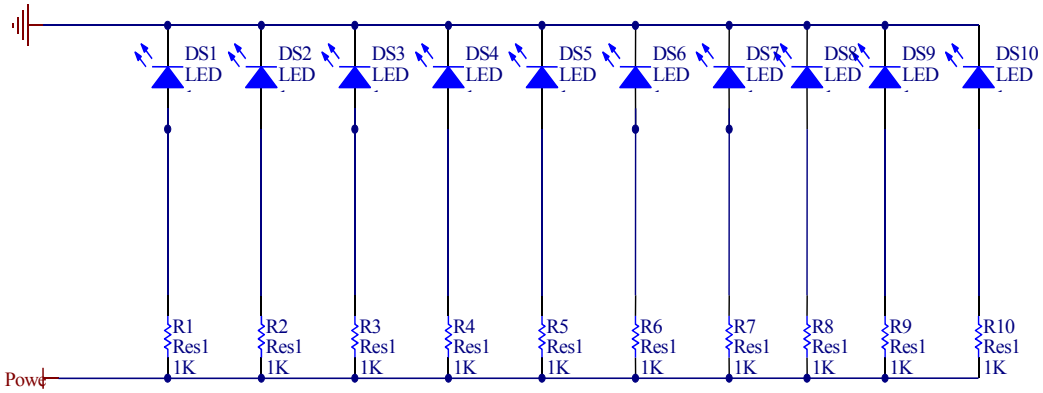

FIGURE 1 LED CIRCUIT

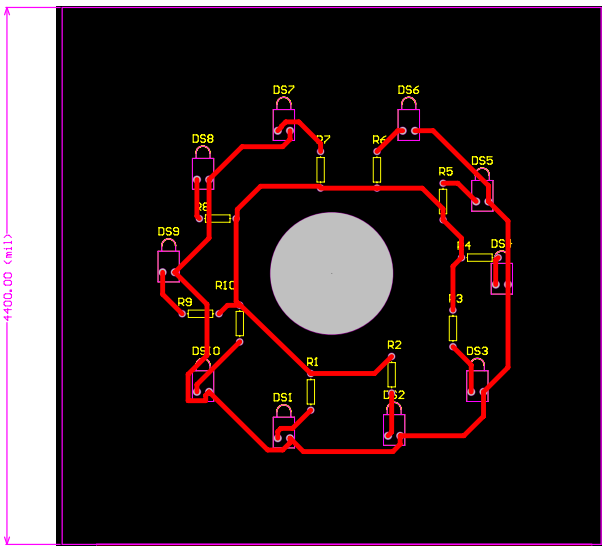

FIGURE 2 LED PCB CIRCUIT

Figure 3 is the PCB diagram for the LDR based specular meter.

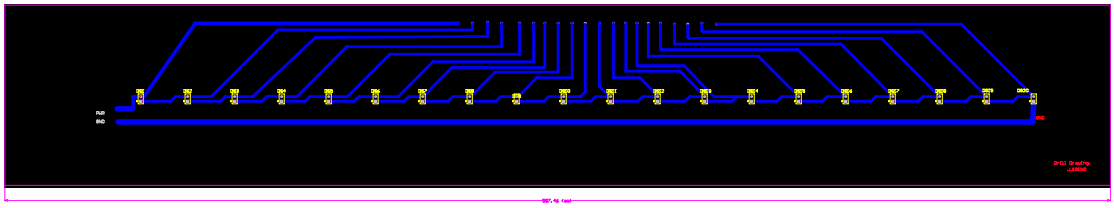

FIGURE 3 LDR BASED SPECULAR METER

Appendix III Software

Road measurements in this project involved a lot of data recording and processing. A small program was written to ease the procedure of collecting specularity readings from the OEL specular meter. The language used was Visual Basic running via Microsoft Excel's macro functionality. Since the same type of program was used in the previous project to log and process the street lighting illuminance readings and the vehicle travel distances as shown in Figure 1 it was very convenient to use the same type of program. The existing analogue to digital converter PicTech 11 channel ADC11/12 was used to convert the analogue signal from the sensors to the digital signal. The connection block diagram is shown below:

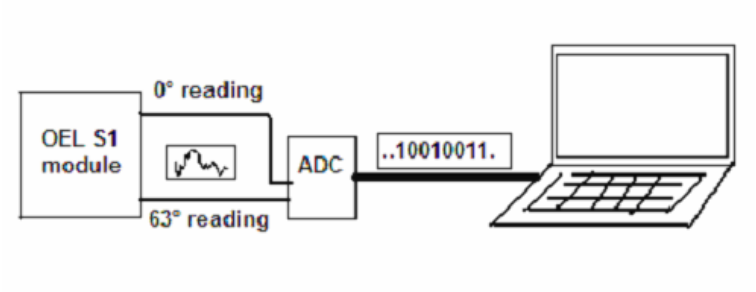

FIGURE 1 CONNECTION BLOCK DIAGRAM.

The 63° and 0° meters' output were connected to the ADC11/12 channel 1 and channel 2. The ADC was connected to the laptop through the LTP1 port.

A macro was written in Excel to read and record values produced from the 63° and 0° luminance meter at nearly the same time, then the S1' calculated. The readings from the luminance meters continue to be read and recorded every two seconds until the user terminates the macro.

Algorithm diagram is shown below:

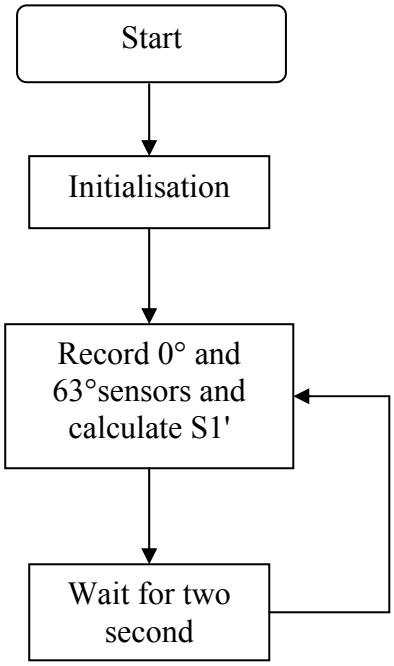

Start

The program is started by pressing **CTRL+SHIFT+S** in the Excel worksheet.

Initialisation

Initialisation includes the declaration of variables and opening of the ADC converter.

```
port = 1
product = 11
opened = adc11_open_unit(port, product) <> 0
```

The above code opens the ADC11/12 on the LPT1 port.

Recording

Once the initialisation is done, the program starts to read the values coming from ADC11/12 channel l and channel 2, which are connected to the 63° and 0° sensors. The values read are placed in spreadsheet cell(22+m,1) and cell(22+m,2), where m starts from 0. The ratio of those two values, S1', is calculated and saved to cell(22+m,3). Value m is then increased by 1, so the next set of measurements will be saved to cell(23,1),cell(23,2) and cell(23,3) . The code looks like:

```
While (True)
```

```
Cells(22 + m, 1) = Round(adc_to_mv(reflection_value(1)), 2)
Cells(22 + m, 2) = Round(adc_to_mv(reflection_value(2)), 2)
Cells(22 + m, 3) = Round(Cells(22 + m, 1) / Cells(22 + m, 5), 1)
 m = m + 1
Sleep 2000

Wend
```

Where *reflection_value(channel #)* and *adc_to_mv(value)* are two functions. Function *reflection_value(channel #)* is defined to take 20 measurements from the designated channel and return the average value. This roughly takes 4ms. Function *adc_to_mv(value)* is defined to convert the ADC reading into millivolts.

Wait

A 2 second delay is used before next recording cycle starts. The purpose of this is to give operator enough time to move the OEL specular module to the next measuring spot. Code *Sleep 2000* is used here for the 2 second delay. Once the 2 seconds has passed, the program jump back to the recording step. The program will keep returning to the recording step until the user presses the **Esc** button on the keyboard – the **Esc** button terminates program execution.

During road test, we only need to set the hardware up before starting sampling. Once sampling has finished, the spreadsheet is saved as the road name. The following (Figure 2) is an example of the spreadsheet produced from measuring Opia Street.

OEL specularity measurement Macro

Channel connections:
Channel 1: Spectral meter, 63 degree sensor
Channel 2: Spectral meter, 0 degree sensor

Measurement procudure:

1 Connect sensors to ADC and turn them on.
2 Connect 12 V DC to halogen light
3 Press Ctrl+Shift+S to start measurement
4 Press Esc to teminate the program

OEL specular system				CIE specular system		
63°	0°	S1		63°	0°	S1
49.94	25.09	1.990434		80	155	0.516129
49.33	24.97	1.975571		75	149	0.503356
48.69	24.79	1.964098		60	138	0.434783
45.57	23.69	1.923596		69	120	0.575
45.09	23.23	1.941025		63	127	0.496063
44.69	23.2	1.926293		80	141	0.567376
44.38	23.23	1.910461		65	160	0.40625
43.83	22.8	1.922368		56	116	0.482759
51.13	24.76	2.065024		60	125	0.48
50.55	24.48	2.064951		63	128	0.492188
3.11	12.18	0.255337		81	140	0.578571
40.84	20.21	2.020782				
40.75	19.99	2.038519				
35.32	20.76	1.701349				
34.89	20.76	1.680636				
34.58	20.73	1.668114			0.502952	
35.26	21.34	1.652296				
34.71	21.21	1.636492				
34.74	20.73	1.675832			0.055072	

FIGURE 2 OEL SPECULARITY MEASUREMENT MACRO

Examine cell(32,1) and cell(32,2) closely as it can be seen that the values are quite different from the rest. This is due to the situation that the measurement was interrupted when moving the device to a new test spot. During data processing erroneous data has to be filtered out. Through carefully studying of the raw data it was found that the good measurements from 0° sensor are quite consistent in value, they only vary in a small range. Later an extra code was added into the program in an effort to filter out the outliners. The codes are:

```
If Cells(22 + m, 2) > (Cells(22,2) * 0.7) And Cells(22 + m, 1.35) < (Cells(22,2) * 1.25) Then
m = m + 1
End If
```

It sets up a tolerance range for new means each new measurement from 0° sensor has to be compared with the first 0° measurement. If the new value is 1.25 greater or 0.7 lesser than the first value, that set of measurements will be discarded (overwrite by next set of measurement). Test proves that it works effectively. When lifting up the unit or

disconnecting the halogen light power during the measurement, the values just keep overwriting in the same column in the Excel worksheet until not the unit is placed down or power is reconnected will the recording continue. Since all the data collected were saved in Excel worksheet, analysis can be easily done.

Appendix IV Datasheet

Light Meter

MODEL: DLM 530

Features:

- CE-Mark approval
- Portability and simplicity one-hand operation
- Accurate visible compensation filter f'_1 is used
- CIE(λ): f'_1<2%, <3%, <5%, <8%, V(λ) match
- Cosine corrected: f'_2<2%
- Signal output function (output impedance 500Ω)
- With MAX/DATA HOLD function
- Valox housing to withstand accidental drops
- Attached carrying case

Applications:

- Indoor
- Office environment
- Labs
- Environment studies

Specifications:

Display: 3½digit liquid crystal display (LCD) with a maximum reading of 1999.
Low battery indication: The " ⊟ " is displayed when the battery voltage drops below the operating level.
Operating environment: 0°C to 50°C, <70% R.H..
Storage environment: -20°C to 60°C, 0 to 80% R.H. with battery removed from meter.
Accuracy: Stated accuracy at 23°C±5°C, <75% R.H..
Dimensions: 170mm(H) x 44mm(W) x 40mm(D).
Weight: Approx. 220g including battery (1.5Vx4pcs AAA size).

Lux:

Sensor: Silicon photodiode
Range: 20lux, 200lux, 2000lux, 20000Klux, 200000lux
Resolution: 0.01lux
Accuracy:

MODEL	630-2	630-3	630-5	630-8	630
Spectral Response	CIE Photopic	CIE Photopic	CIE Photopic	CIE Photopic	White Light
Spectral Accuracy	f'_1<2%	f'_1<3%	f'_1<5%	f'_1<8%	NO spec.
Cosine Response	f'_2<2%	f'_2<2%	f'_2<2%	f'_2<2%	f'_2<2%
Total Accuracy For All Common Light Source	±(5%+2)	±(6%+2)	±(8%+2)	±(11%+2)	NO spec.
Total Accuracy For Source A 2856K Standard Light Source	±(3%+10)	±(3%+10)	±(3%+10)	±(3%+10)	±(3%+10)

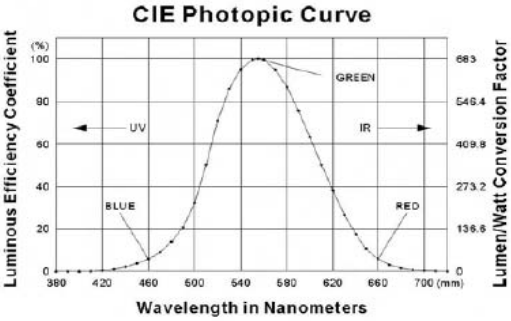

TECPEL CO., LTD.

Appendix V Selected Raw Results

The results are shown from the following page.

Anglesea St south end

0 degree	63 degree	S1
206	416	0.495192
218	394	0.553299
220	380	0.578947
217	402	0.539801
207	397	0.521411
216	397	0.544081
210	400	0.525
205	372	0.551075
197	343	0.574344
233	410	0.568293
193	347	0.556196
203	353	0.575071
216	405	0.533333
210	397	0.528967
223	407	0.547912
225	417	0.539568
241	433	0.556582
216	392	0.55102
211	390	0.541026
203	389	0.521851
207	380	0.544737
210	397	0.528967
211	407	0.518428
216	360	0.6
203	387	0.524548
183	357	0.512605
223	395	0.564557
222	412	0.538835
203	434	0.467742
185	376	0.492021

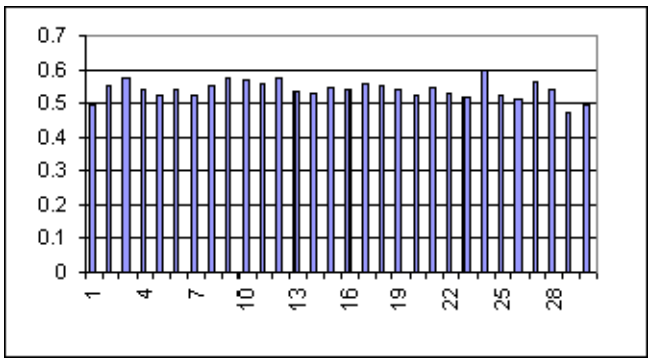

0.539847 S1 avg

0.027646 S1 s.d 5.1

Garden Gate 2 carpark 1

0 degree	63 degree	S1
115	380	0.302632
121	350	0.345714
122	342	0.356725
107	345	0.310145
111	356	0.311798
112	336	0.333333
101	359	0.281337
116	367	0.316076
100	370	0.27027
105	373	0.281501
111	442	0.251131
102	403	0.253102
143	352	0.40625

110	412	0.26699			
120	434	0.276498			
111	370	0.3			
106	383	0.276762			
109	380	0.286842			
115	359	0.320334			
109	392	0.278061			
108	381	0.283465			
113	373	0.302949			
107	391	0.273657			
100	352	0.284091			
91	347	0.262248			
101	383	0.263708			
101	346	0.291908			
126	345	0.365217	0.296616	S1 avg	
104	405	0.25679			
102	353	0.288952	0.03599	S1 s.d	12.1

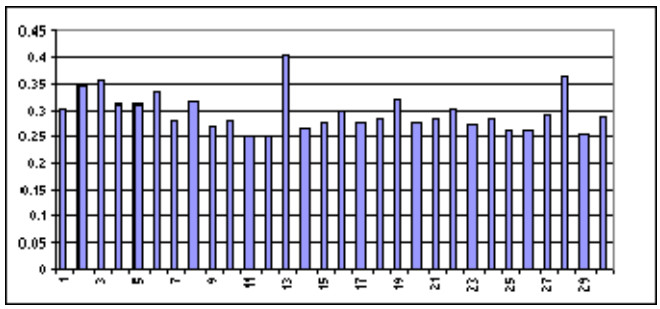

Garden Gate2 lot 2FRENCH ST
0 degree

251			
213	75	239	0.313808
203	77	246	0.313008
191	88	254	0.346457
204	86	250	0.344
206	73	231	0.316017
186	77	196	0.392857
228	76	206	0.368932
238	75	214	0.350467
272	86	222	0.387387
237	82	232	0.353448
250	74	220	0.336364
261	77	229	0.336245
264	70	204	0.343137
257	66	224	0.294643
186	70	213	0.328638
225	70	219	0.319635
250	62	193	0.321244
203	80	196	0.408163
227	81	215	0.376744
203	65	216	0.300926
210	76	188	0.404255
226	84	277	0.303249
187	69	206	0.334951
199	65	213	0.305164
185	90	247	0.364372
195	77	248	0.310484
185	83	229	0.362445
220	72	232	0.310345
215	48	151	0.317881

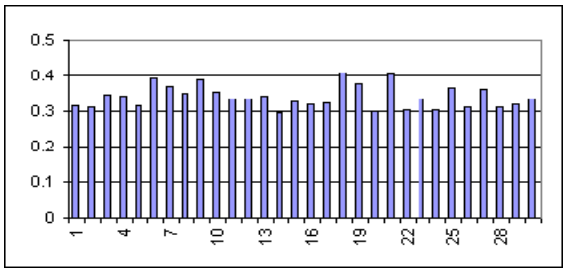

0.340005 AVG

	72	215	0.334884	0.031519	SD	9.3

Cook St

0 degree	63 degree	S1
163	338	0.482249
126	342	0.368421
128	301	0.425249
181	288	0.628472
167	353	0.473088
152	373	0.407507
148	382	0.387435
133	338	0.393491
172	406	0.423645
147	370	0.397297
135	329	0.410334
148	320	0.4625
148	277	0.534296
141	366	0.385246
149	333	0.447447
104	293	0.354949
172	353	0.487252
114	337	0.338279
117	347	0.337176
152	348	0.436782
133	372	0.357527
153	332	0.460843
120	310	0.387097
145	315	0.460317
124	386	0.321244
153	337	0.454006
161	274	0.587591
160	291	0.549828
128	296	0.432432
153	332	0.460843

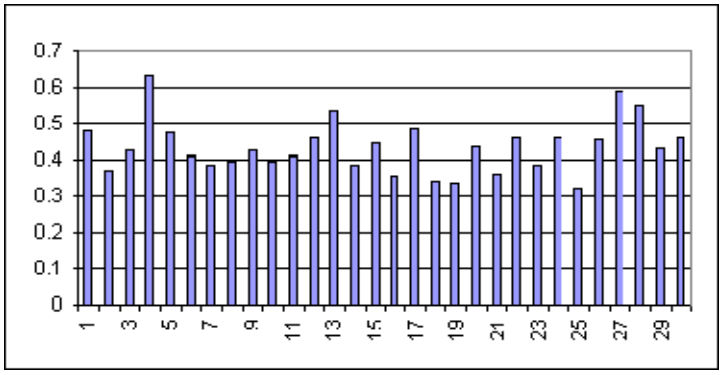

0.435095	S1 avg	
0.07285	S1 s.d	16.7

Fox St

0 degree	63 degree	S1
260	425	0.611765
267	428	0.623832
233	390	0.597436
220	371	0.592992
223	363	0.614325
218	348	0.626437
218	366	0.595628
212	360	0.588889
280	363	0.77135
216	367	0.588556
216	362	0.596685

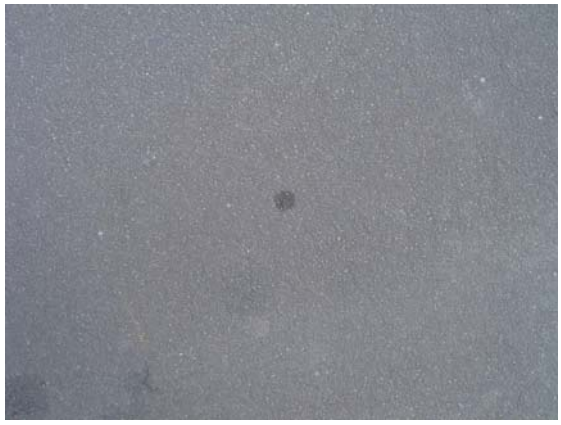

224	359	0.623955			
218	351	0.621083			
237	384	0.617188			
235	359	0.654596			
199	356	0.558989			
210	344	0.610465			
225	350	0.642857			
205	356	0.575843			
207	348	0.594828			
225	333	0.675676			
189	356	0.530899			
190	349	0.544413			
190	338	0.56213			
198	336	0.589286			
191	348	0.548851			
212	331	0.640483			
199	335	0.59403	0.606917	S1 avg	
224	360	0.622222			
203	343	0.591837	0.044876	S1 s.d	7.4

Wellington St

0 degree	63 degree	S1
141	431	0.327146
131	421	0.311164
144	400	0.36
161	371	0.433962
117	363	0.322314
106	381	0.278215
100	345	0.289855
115	393	0.292621
117	372	0.314516
100	359	0.278552
107	355	0.301408
135	406	0.332512
113	436	0.259174
134	356	0.376404
97	336	0.28869
161	428	0.376168
118	274	0.430657
122	338	0.360947
157	345	0.455072
104	278	0.374101
152	336	0.452381
130	397	0.327456
126	381	0.330709
109	346	0.315029
142	336	0.422619
168	343	0.489796
137	337	0.406528

141	429	0.328671	0.34798	S1 avg	
114	380	0.3			
122	403	0.30273	0.061122	S1 s.d	17.6

Firth St

0 degree	63 degree	S1
232	366	0.63388
298	320	0.93125
227	331	0.685801
322	367	0.877384
278	312	0.891026
235	299	0.785953
273	278	0.982014
263	320	0.821875
326	336	0.970238
257	334	0.769461
215	261	0.823755
220	291	0.756014
258	310	0.832258
244	274	0.890511
258	318	0.811321
286	268	1.067164
280	291	0.962199
222	265	0.837736
230	299	0.769231
240	267	0.898876
284	305	0.931148
244	323	0.755418
228	306	0.745098
342	293	1.167235
223	318	0.701258
217	305	0.711475
300	293	1.023891
250	305	0.819672
288	305	0.944262
247	305	0.809836
199	281	0.708185
270	288	0.9375

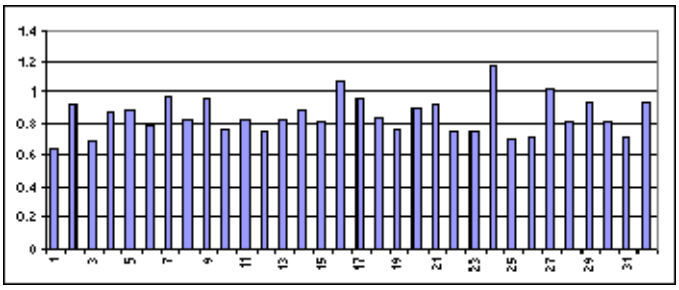

0.851654	S1 avg	
0.119889	S1 s.d	14.1

Clarence St

0 degree	63 degree	S1
78	360	0.216667
73	365	0.2
86	357	0.240896
104	383	0.27154
80	353	0.226629
110	291	0.378007
92	322	0.285714

109	285	0.382456			
69	357	0.193277			
92	285	0.322807			
77	295	0.261017			
83	320	0.259375			
78	333	0.234234			
111	376	0.295213			
85	332	0.256024			
87	281	0.309609			
111	325	0.341538			
74	231	0.320346			
77	317	0.242902			
66	298	0.221477			
111	305	0.363934			
85	255	0.333333			
91	251	0.36255			
128	284	0.450704			
90	305	0.295082			
96	325	0.295385			
65	328	0.198171			
180	343	0.524781	0.290474	S1 avg	
71	330	0.215152			
70	325	0.215385	0.078155	S1 s.d	26.9

QUEENS AVE

0 degree	63 degree	S1
94	356	0.264045
77	291	0.264605
63	373	0.168901
63	309	0.203883
63	306	0.205882
84	278	0.302158
60	342	0.175439
48	264	0.181818
53	325	0.163077
67	303	0.221122
58	262	0.221374
56	306	0.183007
83	347	0.239193
50	264	0.189394
54	302	0.178808
60	330	0.181818
86	317	0.271293
71	315	0.225397
91	289	0.314879
63	271	0.232472
66	310	0.212903
80	285	0.280702
53	292	0.181507
74	283	0.261484
57	335	0.170149

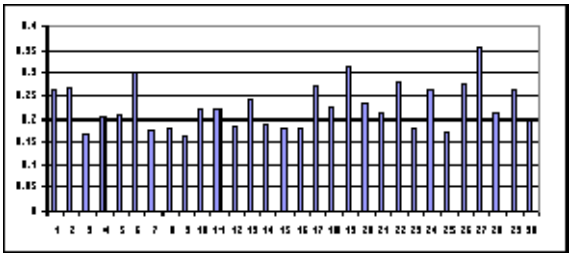

66	240	0.275				
97	273	0.355311				
68	322	0.21118	0.226546	S1 avg		
83	315	0.263492				
50	255	0.196078	0.049164	S1 s.d	21.7	Covarianc

Anglesea Phamacy Pharmacy lot1

0 degree	63 degree	S1
160	525	0.304762
156	536	0.291045
172	563	0.305506
185	566	0.326855
160	512	0.3125
148	523	0.282983
154	503	0.306163
160	497	0.321932
143	489	0.292434
152	490	0.310204
141	504	0.279762
140	479	0.292276
124	506	0.245059
150	438	0.342466
148	518	0.285714
175	470	0.37234
156	458	0.340611
153	488	0.313525
160	480	0.333333
158	513	0.307992
145	507	0.285996
155	510	0.303922
135	479	0.281837
128	526	0.243346
142	501	0.283433
135	479	0.281837
132	499	0.264529
140	472	0.29661
142	445	0.319101
138	456	0.302632
145	473	0.306554

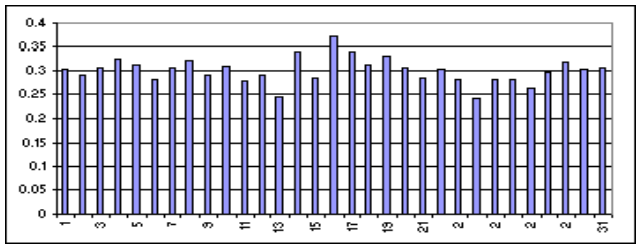

0.301202	S1 avg				
0.026902	S1 s.d				8.9

NAYLOR St (Irregular tar stains)

0 degree	63 degree	S1
237	253	0.936759
213	250	0.852
213	292	0.729452
210	267	0.786517

169	280	0.603571				
178	233	0.763948				
128	290	0.441379				
148	266	0.556391				
200	247	0.809717				
202	228	0.885965				
186	256	0.726563				
210	242	0.867769				
143	287	0.498258				
172	261	0.659004				
202	237	0.852321				
148	242	0.61157				
220	240	0.916667				
145	273	0.531136				
158	267	0.59176				
206	262	0.78626				
165	230	0.717391				
223	238	0.936975				
176	242	0.727273				
166	253	0.656126				
190	242	0.785124				
167	258	0.647287				
122	253	0.482213				
166	253	0.656126	0.729454	S1 avg		
272	278	0.978417				
250	281	0.88968	0.14831	S1 s.d	20.3	% C

PavnSave

0 degree	63 degree	S1
141	402	0.350746
141	341	0.41349
152	354	0.429379
160	369	0.433604
193	350	0.551429
186	342	0.54386
169	327	0.51682
164	308	0.532468
166	312	0.532051
184	301	0.611296
140	325	0.430769
162	323	0.501548
166	314	0.528662
120	337	0.356083
107	312	0.342949
121	346	0.349711
136	350	0.388571
136	349	0.389685
122	317	0.384858
147	332	0.442771
167	307	0.543974

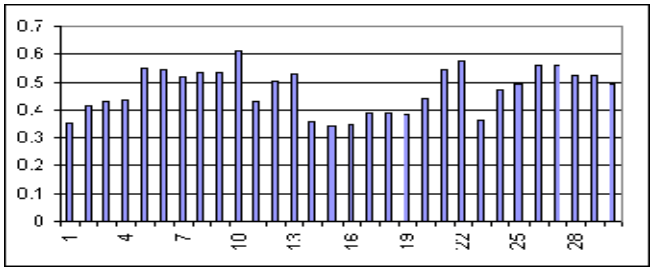

176	307	0.57329			
111	308	0.36039			
162	342	0.473684			
168	340	0.494118			
165	294	0.561224			
174	311	0.559486			
155	297	0.521886	0.471147	S1 avg	
155	295	0.525424			
150	306	0.490196	0.079705	S1 s.d	17

POWER HOUSE

0 degree	63 degree	S1
302	482	0.626556
303	504	0.60119
317	456	0.695175
323	465	0.694624
273	424	0.643868
280	453	0.618102
290	513	0.565302
293	467	0.627409
333	472	0.705508
300	455	0.659341
288	459	0.627451
287	469	0.61194
280	463	0.604752
269	477	0.563941
267	459	0.581699
258	472	0.54661
255	501	0.508982
289	475	0.608421
291	461	0.631236
315	465	0.677419
284	474	0.599156
275	464	0.592672
255	442	0.576923
301	424	0.709906
311	458	0.679039
294	441	0.666667
295	423	0.6974
304	445	0.683146
281	460	0.61087
286	463	0.617711

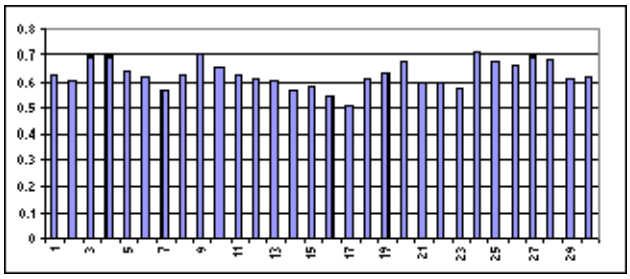

0.627767	S1 avg	
0.050979	S1 s.d	8.1

PATERSON ST

111	383	0.289817
104	366	0.284153

90	370	0.243243
84	370	0.227027
107	387	0.276486
93	435	0.213793
110	414	0.2657
118	385	0.306494
80	407	0.19656
93	407	0.228501
89	376	0.236702
83	423	0.196217
79	366	0.215847
82	381	0.215223
80	376	0.212766
81	325	0.249231
89	374	0.237968
91	415	0.219277
104	400	0.26
77	316	0.243671
81	323	0.250774
76	336	0.22619
104	341	0.304985
73	365	0.2
94	385	0.244156
103	395	0.260759
98	419	0.23389
111	373	0.297587
84	349	0.240688
83	373	0.22252
103	388	0.265464

0.244055 S1 avg

0.03104 S1 s.d 12 % C

Upper CLARENCE

0 degree	63 degree	S1
148	271	0.546125
115	242	0.475207
111	232	0.478448
125	230	0.543478
136	282	0.48227
121	252	0.480159
110	271	0.405904
158	242	0.652893
128	260	0.492308
121	245	0.493878
138	226	0.610619
135	239	0.564854
111	207	0.536232
100	237	0.421941
115	243	0.473251
107	221	0.484163
110	257	0.428016
85	230	0.369565
107	196	0.545918

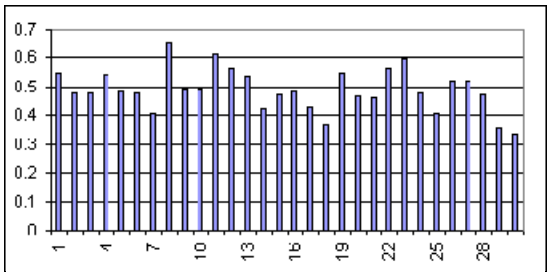

110	235	0.468085			
97	211	0.459716			
123	219	0.561644			
141	237	0.594937			
120	251	0.478088			
95	233	0.407725			
116	223	0.520179			
112	216	0.518519			
113	238	0.47479	0.488788	S1 avg	
85	237	0.35865			
82	244	0.336066	0.073383	S1 s.d	15

References

[1] Fuat Aktan, Thomas Schnel *Development of a Model to Calculate Roadway Luminance Induced By Fixed Roadway Lighting*, 2005

[2] J.Hill and R Loveless, *Streetlight Developments in High Speed Street Lighting Performance Measurement Techniques to Cover Main Roads*, 2004

[3] www.odyseey.co.nz

[4] J.Hill, *Reflectivity Measurement for Carriageway Lighting Luminance Performance Assessment*, MSc. Thesis, University of Waikato,2004

[5] A. Ryer, *Light Measurement Handbook,* 1997

[6] Internet reference

[7] *Australia/New Zealand Streetlight Standard*, AS/NZS 1158:1986.

[8] O.Cuvalci and B. Rrtas, *Roadway Lighting Desigh Methodology and Evaluation*, 2000

[9] Chapte 18

[10] W. Adrian and R. Jobanputra, Influence of Pavement Reflectance on Lighting for Parking Lots, 2005 Q Measurement…

[11] N.V. Vh Ets. F. VERDEYEN S.A, *General Information: Photometric Calculation*

[12] R. B. Gibbons, *Influence of Pavement Reflection on Target Visibility*, PhD. Thesis, University of Waterloo, 1997

[13] [a guide to integrating sphere app.pdf]

[14] internet Memphis website

[15] W. Jung, A. Kazakov, and A.I. Titishov, *Road Surface Reflectance Measurements in Ontario* , 1984

[16] [data sheet NORP12]

[17] *Road Reflection Properties, Wellington Area* by J. V. Nicolas and R. J. Stevens